Aus der

Abteilung für Klinische Pharmakologie

Klinikum der Ludwig-Maximilians-Universität München

Exploiting RIG-I-targeted therapy as a strategy to overcome CAR T cell therapy limitations in the treatment of solid tumors

Dissertation

zum Erwerb des Doctor of Philosophy (Ph.D.)

an der Medizinischen Fakultät der

Ludwig-Maximilians-Universität München

vorgelegt von

Anne Marie Senz Giusti

aus

Cali

Jahr

2023

Mit Genehmigung der Medizinischen Fakultät der
Ludwig-Maximilians-Universität München

Erstes Gutachten:	Priv. Doz. Dr. Lars König
Zweites Gutachten:	Prof. Dr. Wolfgang Zimmermann
Drittes Gutachten:	Priv. Doz. Dr. Andreas Moosmann
Viertes Gutachten:	Priv. Doz. Dr. Reinhard Obst

Dekan: Prof. Dr. med. Thomas Gudermann

Tag der mündlichen Prüfung: 10.11.2023

To my amazingly supportive family and friends:

¡Siempre gracias!

Table of Contents

Abstract

Attempts to treat solid tumors with chimeric antigen receptor (CAR) T cells often fail due to compromised trafficking of the CAR T cells into the tumor, and the dampening of cytotoxic immune responses, exerted by abundant immunosuppressive cells and factors present in the tumor microenvironment (TME). 5'-triphosphate double-stranded RNA (3p-RNA) – commonly produced during viral replication – is intracellularly sensed by retinoic acid-induced gene I (RIG-I). RIG-I is a pattern recognition receptor, which upon activation, unleashes a series of events that culminate in the expression of type I interferons (IFN), other pro-inflammatory cytokines and diverse chemokines, overall enhancing surveillance by immune cells.

We show that intra-tumoral 3p-RNA injections improve CAR T cell therapeutic efficacy in preclinical models of pancreatic cancer by enhancing each step of the cancer immunity cycle proposed by Chen and Mellman (Chen & Mellman, 2013). This starts with the induction of an immunogenic form of cell death in step (1), followed by the increase of antigen uptake and activation of antigen presenting cells (APC) (2). These APC process and present the acquired antigens to naïve T cells in the lymph nodes, priming and activating them (3). The newly primed T cells travel to the tumor site (4) and penetrate the tumoral mass (5). Once inside the tumor, T cells recognize the cancer cells, get activated (6) and unleash a cytotoxic response that contributes to increased cancer cell death and superior tumor growth control (7), re-starting the cycle (Figure 1).

Intra-tumoral administration of 3p-RNA remodeled the myeloid immune compartment in the TME by reducing the relative frequency of immunosuppressive populations i.e., macrophages and polymorphonuclear myeloid-derived suppressor cells (PMN-MDSC), while increasing Ly6C^{high} inflammatory monocytes. Furthermore, treating tumor cells with 3p-RNA induced cell death and the release of damage-associated molecular patterns (DAMP), prompting higher antigen uptake, activation, and cross-presentation by APC. Importantly, cytokine and chemokine secretion in response to 3p-RNA treatment

enhanced the infiltration of both CAR T cell and endogenous T cell into the tumors, and additionally increased CAR T cell persistence, proliferation, activation, and cytotoxicity. This culminated in better tumor growth control and prolonged survival of mice bearing pancreatic ductal adenocarcinoma (PDAC) tumors. The induction of immunogenic cell death by the combination treatment stimulated a *de novo* immune response leading to antigen spreading that can potentially prevent tumor relapse due to antigen loss.

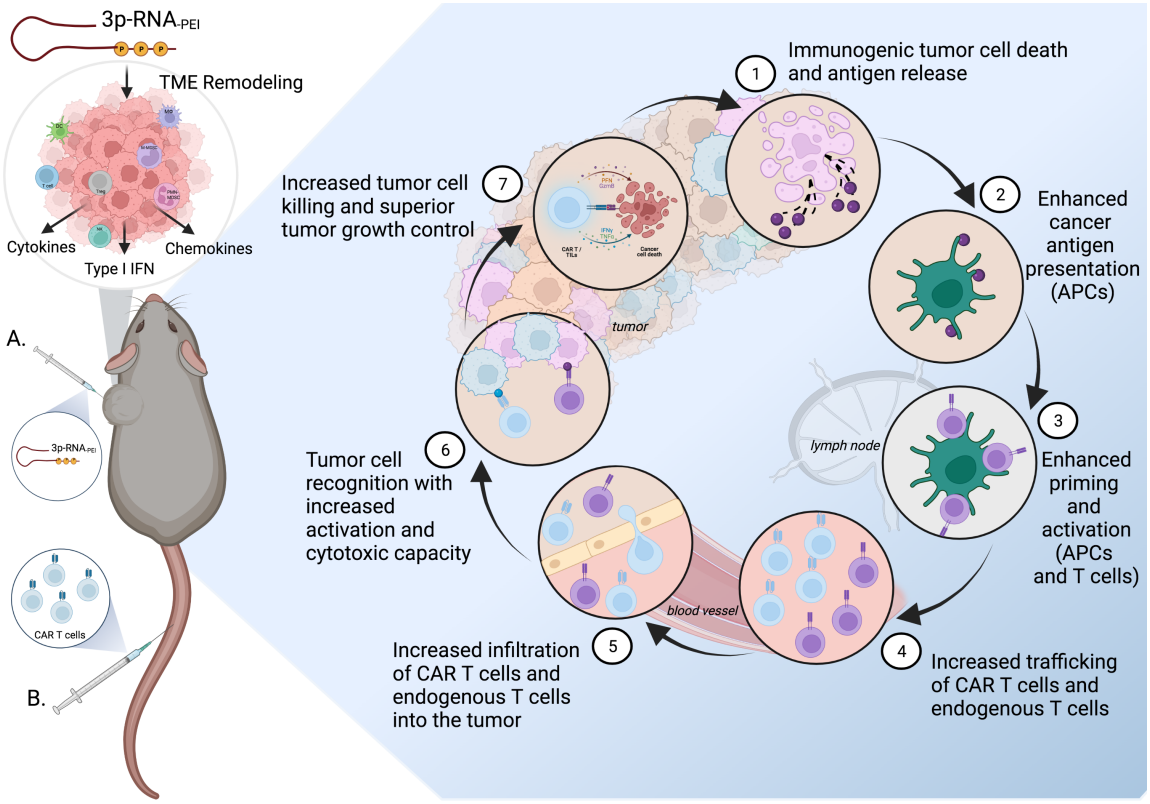

Figure 1. RIG-I targeted therapy improves CAR T cell efficacy in solid tumors by enhancing each step of the cancer immunity cycle.

The figure depicts how treating PDAC-bearing mice with the combination of PEI-complexed 3p-RNA injected intratumorally together with systemic injections of CAR T cells leads to remodeling of the TME inducing secretion of type I IFN, cytokines and chemokines. In parallel, this combination treatment leads to 1) cell death induction and release of DAMP and antigens. 2) Enhancement of cancer antigen uptake and presentation by APC. 3) Enhanced priming and activation of T cells. 4) Increased migration and 5) infiltration of both CAR T cells and endogenous T cells. 6) Improved tumor cell recognition with increased activation and cytotoxicity of T cells leading to 7) increased tumor cell killing and superior tumor growth control. Figure adapted from The "cancer-immunity cycle" proposed by Chen and Mellman in 2013 (Chen & Mellman, 2013).

List of figures

List of supplementary figures

List of tables

List of Abbreviations

3-MCA	carcinogen 3-methylcholanthrene
3p-RNA	5’-triphosphate double-stranded RNA
ACT	adoptive cell therapy
AE	adverse events
AGER	advanced glycosylation end-product-specific receptor
APC	antigen presenting cells.
aPSC	activated pancreatic stellate cells.
BCR	B cell receptor
BM	bone marrow
BMDC	bone marrow-derived dendritic cells
BRCA1	breast cancer 1
BRCA2	breast cancer 2
CAF	cancer-associated fibroblast
CAR	chimeric antigen receptor
CARDs	caspase activation and recruitment domains
CCL2	C-C ligand 2
CCL5	C-C ligand 5
CCR4	C-C chemokine receptor 4
CCR5	C-C chemokine receptor 5
CMP	common myeloid precursor
CTD	carboxy-terminal domain
CTL	cytotoxic T cell
CTLA4	cytotoxic T-lymphocyte-associated protein 4
CXCL10	C-X-C ligand 10
CXCL11	C-X-C ligand 11
CXCL12	C-X-C ligand 12
CXCL9	C-X-C ligand 9
CXCR2	C-X-C chemokine receptor 2
CXCR3	C-X-C chemokine receptor 3
DAMP	damage-associated molecular patterns
DC	dendritic cells
ECM	extracellular matrix
EDU	5-Ethynyl-2′-deoxyuridine
EGFR	epidermal growth factor receptor
EMT	epithelial-to-mesenchymal transition
ER	endoplasmic reticulum.
FcR	Fc-(immunoglobulin) receptors
FDA	Food and Drug Administration
FGF	fibroblast growth factor

FVD	Fixable Viability Dye
GMP	granulocyte macrophage precursor
GvHD	graft-versus-host disease
HMGB1	high-mobility group box 1
iCAF	inflammatory cancer-associated fibroblasts
ICD	immunogenic cell death
IFN	interferons
IFNAR	interferon-α/β receptor
IGF1	insulin-like growth factor 1
IL-10	interleukin 10
IL-1β	interleukin 1β
IL-2	interleukin 2
IL-6	interleukin 6
IRF 3/7	interferon regulatory factor 3 and 7
IRF9	interferon regulatory factor 9
ISG	interferon-stimulated genes
ISGF3	Interferon-stimulated gene factor 3
ISRE	IFN-stimulated response element
JAK-STAT	Janus kinase–signal transducer and activator of transcription pathway
KPC	murine model ($Ptf1a^{Cre+/-}$, $LSL\text{-}Kras^{G12D}$, $p53^{fl/R172H}$)
LGP2	laboratory of genetics and physiology 2
LN	lymph node
M-MDSC	monocytic myeloid-derived suppressor cells
MAVS	mitochondrial antiviral signaling protein.
MDA5	melanoma differentiation-associated protein 5
MDSC	myeloid-derived suppressor cells
MHC-I	major histocompatibility complex class I
MMPs	matrix metalloproteases
MSLN	mesothelin
myCAFs	myofibroblastic cancer-associated fibroblast
NF-κB	nuclear factor κB
NK	natural killer cells
NOXA	phorbol-12-myristate-13-acetate-induced protein 1
NSG	NOD scid gamma mouse
OAS	oligoadenylate synthetase
PAMPs	pathogen-associated molecular patterns
PD-L1	programmed cell death protein ligand 1.
PD1	programmed cell death protein 1.
PDAC	pancreatic ductal adenocarcinoma
PDGF	platelet-derived growth factor

PEI	polyethylenimine
PMN	polymorphonuclear neutrophils
PMN-MDSC	polymorphonuclear myeloid-derived suppressor cells
poly(I:C)	polyinosinic: polycytidylic acid
PRR	pattern recognition receptor
PSC	pancreatic stellate cells
PSCA	prostate stem cell antigen
RIG-I	retinoic acid-induced gene I
RLH	RIG-I-like helicases
RLR	RIG-I-like receptor
ROS	reactive oxygen species
scFv	single chain variable fragment
SD	standard deviation
SEM	standard error of the mean
TAA	tumor-associated antigens
TAM	tumor-associated macrophages
TBK1	TANK-binding kinase 1
TCR	T cell receptor
TGF-β	transforming growth factor-β.
T_h	helper T cell
TIL	tumor infiltrating lymphocytes
TIMP	tissue inhibitor of metalloproteases
TLR	toll-like receptors
TME	tumor microenvironment
TNF-α	tumor necrosis factor-α
TRAF	TNF receptor associated factors.
Treg	T regulatory cells
TRUCKs	T cells redirected for antigen-unrestricted cytokine-initiated killing.
UT	untransduced T cell
VEGF	vascular endothelial growth factor

1. Introduction

1.1 The immune system

The immune system is composed of a complex and interactive network of cells, organs, and molecules that collaborate to protect the organism from invading pathogens and damaged or mutated cells (Sarén, 2022). It is divided into innate and adaptive immune branches, which differ from one another in terms of cellular components, reaction speed and specificity. Yet, they work closely together to eliminate threats such as cancer (Parkin & Bryony, 2001).

1.1.2 Innate immunity

The term innate immunity is generally used to describe the first line protection against pathogens. Sometimes physical, chemical, and microbial barriers are included within the description of innate immunity. However, the cellular elements composing this type of immunity are monocytes/macrophages, granulocytes (neutrophils, basophils, and eosinophils), NK cells, dendritic cells (DC) and their soluble effector proteins called cytokines and those belonging to the complement system (Parkin & Bryony, 2001). Neutrophils, monocytes, and macrophages are professional phagocytic cells that rapidly infiltrate microbial-invaded or damaged tissue, phagocyte foreign particles and apoptotic debris and release anti-microbial peptides, reactive oxygen species and pro-inflammatory cytokines that attract other immune cells towards the inflammation site (Kantari et al., 2008). NK cells are part of the family of innate lymphocyte cells and contrary to B and T lymphocytes, they do not express specific antigen receptors. They recognize abnormal cells via binding of their immunoglobulin receptors (FcR) to antibody coated targets. Alternatively, they sense the membrane expression of major histocompatibility complex class I (MHC-I) in target cells and their cytotoxic capacity is unleashed when such expression is absent (Parkin & Bryony, 2001).

The communication between innate and adaptive branches of the immune system is performed by antigen presenting cells (APC). Both DC and macrophages are APC, however, DC are described to be the most skilled in antigen cross-presentation (Yatim & Lakkis, 2015). DC activation is induced upon pattern recognition receptor (PRR) sensing of damage-associated molecular patterns (DAMP) or pathogen-associated molecular patterns (PAMP). Once activated, DC take up cellular debris including antigen fragments that are processed and presented as peptides in one of the two types of major histocompatibility complexes MHC (Eisenbarth, 2019). Extracellular antigens are usually presented on MHC-II to prime and activate $CD4^+$ T cells. Specialized DC have the ability to cross-present antigens from extracellular sources – for example virus-infected cells or tumor cells – on MHC-I to prime and activate $CD8^+$ T cells, inducing a cytotoxic T cell response (Cruz et al., 2017).

DC1 are a subset of DC that have been described to have a particularly high capability of promoting IL-12-mediated Th1 responses and cross-present antigens on MHC-I to $CD8^+$ T cells (Collin & Bigley, 2018), playing an important role in anti-tumor immune defenses (Cance et al., 2019).

1.1.3 Adaptive immunity

B and T cell comprise the adaptive branch of the immune system. Both cell types mount an immune response upon antigen-specific recognition via the B cell receptor (BCR) or T cell receptor (TCR) (Alberts et al., 2002). Unique BCR and TCR receptors are expressed on each B and T cell and are the result of genetic rearrangements in the antigen-recognition domains of the receptors. This means that both cell types have the capacity to recognize millions of different antigens specifically (Janeway et al., 2001). Upon maturation, antigen-specific B cells develop into plasma cells (which produce antibodies) and memory B cells and can act as APC (Parkin & Bryony, 2001). T cells are mainly divided into helper T cell (T_h) and $CD8^+$ cytotoxic T cells (CTL). T_h cells induce and support antigen-specific B and $CD8^+$ T cell responses while CTL drive directed killing of target

cells expressing the TCR specific antigen (Parkin & Bryony, 2001) and are important effector cells of anti-tumoral immune responses.

1.1.4 Immunogenic cell death and the immune system

Cell death plays a key role in different processes such as embryonic development and removal of damaged cells. The perpetual decease of these cells is hardly recognized by the immune system which is important to prevent catastrophic autoimmune disorders (Fuchs & Steller, 2011). Contrariwise, if cell death is generated by pathogen infections or pathological conditions, an efficient immune response is necessary to fight and eliminate the threat, preserving the integrity of the organism and generating memory responses to overcome such challenges in case they would arise again (Zhou et al., 2019). The determination of whether cellular death will be acknowledged by the immune system and unleash a response is therefore explained by the conjunction of multiple factors leading to what is known as immunogenic cell death.

Immunogenic cell death (ICD) entails the release of DAMP by dying cells. These factors act as adjuvants that trigger innate immune responses through PRR sensing and signaling, communicating a state of danger (Fuchs & Steller, 2015). Key DAMP released or exposed during an immunogenic form of cell death include calreticulin, high-mobility group box1 (HMGB1), ATP, ANXA1 and type I IFN (Fucikova et al., 2020). Calreticulin is an endoplasmic reticulum (ER) chaperone that upon exposure in the membrane of dying cells serves as an “eat me” signal facilitating CD91-mediated engulfment by DC.

HMGB1 is a non-histone chromatin binding protein, normally localized in the nucleus of cells. Upon permeabilization of the nuclear lamina and cytoplasmic membrane HMGB1 is released. At this point it can be recognized by several PRR such as advanced glycosylation end-product-specific receptor (AGER) or Toll-like receptors (TLR), initiating an innate immune response in both DC and other myeloid cells (Fucikova et al., 2020). However, the generation of a *de novo*

immune response and induction of immunological memory requires the engagement of the adaptive immune system.

The bridging between the innate and adaptive immune system requires dying cells to not only release DAMP (adjuvanticity) but also to display foreign or mutated antigens (antigenicity). These means that the dying cells should also release novel neo-epitopes which can be encoded by either microbial genes or host genes that have mutated as a result of oncogenesis or tumor progression (van Kempen et al., 2015). The fact that tumors with high mutational load show a superior response to immunotherapy with immune-checkpoint blockade, and that this response relies on cells of the adaptive immune system, further supports this point. In parallel, it has also been shown that cancer cells with defects in pathways involved in the secretion of cell death associated DAMP fail to die in an immunogenic way (Krysko et al., 2012). However, it has been shown that artificial boosting of DAMP release can rescue cell death immunogenicity (Bezu et al., 2015). Overall, both antigenicity provided by neo-epitopes, and adjuvanticity provided by the release of DAMP or PAMP, are of paramount importance to induce ICD and mount an effective and long-lasting immune response against a threat like cancer cells (Galluzzi et al., 2017, Kroemer et al., 2022).

1.1.5 RIG-I-like receptors and their physiological role

RIG-I-like receptors (RLR) are a group of three intracellular PRR located in the cytosol of cells: retinoic acid-inducible gene I (RIG-I), melanoma differentiation-associated protein 5 (MDA5) and laboratory of genetics and physiology 2 (LGP2) (Rehwinkel & Gack, 2020). All of them possess a carboxy-terminal domain (CTD) and a central helicase domain which allow the sensing of DAMP and PAMP in the form of non-modified double-strand RNA (dsRNA), derived for example from viral infections (Loo & Gale, 2011)or from endogenous sources as a result of pathophysiological stress (Chen & Hur, 2022). In contrast to RIG-I and MDA5, LGP2 doesn’t mediate downstream signaling.

MDA5 senses RNA length and secondary structure (Dias Junior et al., 2019). Meanwhile, RIG-I recognizes short dsRNA that harbor 5'-tri- or di-phosphate moieties (Schlee et al., 2009). 5'-triphospate moieties are present in all forms of endogenous nascent RNA transcripts but are quickly removed after 5' processing and RNA maturation (Gesteland RF et al., 1999). However, viral derived RNA doesn't usually undergo extensive post-transcriptional processing and therefore retains an exposed 5'-triphosphate RNA (3p-RNA) making it a target for RIG-I sensing (Hornung et al., 2006).

Both RIG-I and MDA5 have two caspase activation and recruitment domains (CARD), that mediate the interaction with the adapter protein mitochondrial antiviral-signaling protein (MAVS). The interaction between RIG-I/MDA5 and MAVS leads to the recruitment of TNF receptor associated factors (TRAF) and TANK-binding kinase 1 (TBK1), which in turn promote activation and nuclear translocation of interferon regulatory factors (IRF3/7) and nuclear factor-κB (NF-κB), ultimately leading to the initiation of an antiviral immune response mediated by the expression of type I IFN and other pro-inflammatory cytokines and chemokines (Onomoto et al., 2021).

The release of these pro-inflammatory cytokines and chemokines, derived from immunostimulatory sensing by PRR, alerts, attracts, and activates immune cells to combat viral infection. Paracrine and autocrine sensing of type I IFN by type I interferon receptor (interferon- α/β receptor (IFNAR)), triggers the activation of the intracellular Janus kinase–signal transducer and activator of transcription (JAK–STAT) pathway (Rehwinkel & Gack, 2020). The activation of this pathway facilitates the formation of a tripartite complex called IFN-stimulated gene factor 3 (ISGF3). ISGF3 is composed of phosphorylated STAT1 and STAT2 combined with interferon regulatory factor 9 (IRF9). This complex recognizes IFN-stimulated response elements (ISRE) on the promoters of IFN-inducible genes (ISG) and modulate their transcription (Onomoto et al., 2021).

Up to a thousand ISG have been described depending on the cell type, IFN dose and stimulation time (Schoggins & Rice, 2011). The proteins encoded by ISG have a wide variety of functions. Some ISG encode proteins that recruit immune

cells and induce strong anti-viral innate immunity. Others encode proteins that interfere with different steps in the pathogen's lifecycle, such as inhibition of virus replication, translation, and cell death induction (Schneider et al., 2014).

The 3p-RNA-mediated induction of cell death was originally attributed to be a result of RIG-I downstream signaling pathway (Besch et al., 2009). However, members of our working group recently showed that cell death observed upon 3p-RNA treatment is not a direct result of the RIG-I downstream signaling pathway. It is rather a separate event and the consequence of a two-step process consisting of a priming and effector phase (Figure 2). In the priming phase, cytokine release as a result of RIG-I signaling leads to upregulation of proteins involved in translational arrest such as oligoadenylate synthetase (OAS) and RNaseL. The execution of cell death in the effector phase is the result of translational arrest, exerted by the OAS/RNaseL pathway, and the induction of proapoptotic mitochondrial proteins like phorbol-12-myristate-13-acetate-induced protein 1 (NOXA) (Boehmer et al., 2021) that both lead to the rapid depletion of the anti-apoptotic protein MCL1. At the end, the concerted action of type I IFN, pro-inflammatory cytokines, chemokines and ISG-encoded proteins that work together to fight the infection.

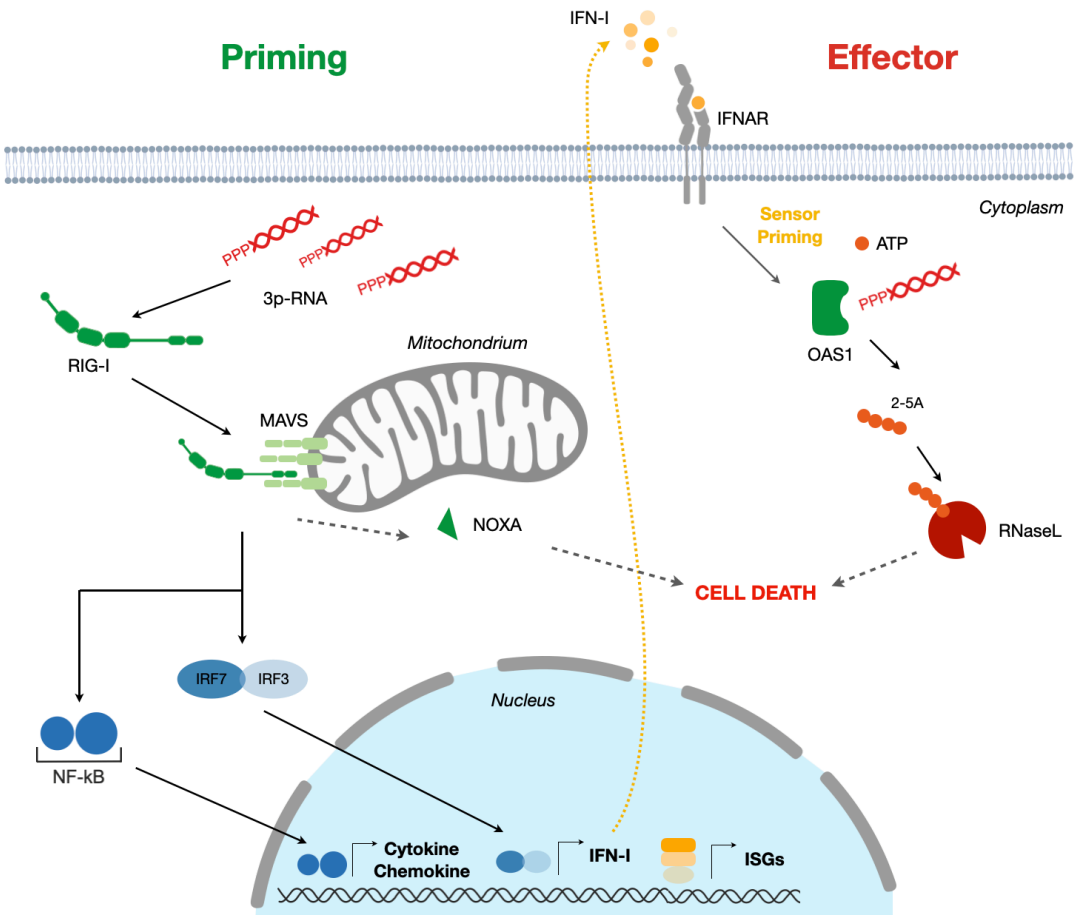

Figure 2. Two phases of 3p-RNA mediated cell death.

Schematic representation of 3p-RNA-mediated cell death as a two-phase process proposed by Boehmer et al. RIG-I cytoplasmic sensing of 3p-RNA and its interaction with MAVS endorses the activation and nuclear translocation of IRF3/7 and NF-κB. In the nucleus, they drive the expression of type I IFN and other pro-inflamatory cytokines and chemokines. Type I IFN drives the expression of ISG and sensor priming of the OAS/RNaseL pathway which executes cell death in conjunction with NOXA in the effector phase (Boehmer et al., 2021).

1.2 The immune system and cancer

1.2.1 Immunotherapy and the cancer immunity cycle

The first reports hinting that the immune system had the capability to identify and control tumor growth date back almost 250 years. One of the earliest records in 1777 shows how doctors and surgeons back at that time were experimenting with early vaccination strategies using cancer cells or malignant tumors to prevent or treat neoplasia's (Ichim, 2005). In the late 19th century William Coley was able to demonstrate a 10% cure rate in soft tissue sarcomas using attenuated bacteria (Previdi, 1968). Moreover in 1909 and 1950, studies from Paul Ehrlich, Lewis Thomas and Sir Macfarlane Burnet contributed to the postulation of the theory of immunosurveillance. This theory states that cancer cells can appear spontaneously in the body and the immune system is constantly monitoring, recognizing, and attacking them (Ehrlich, 1909). The immunosurveillance theory has been subject of debate for several decades. Nevertheless, as more knowledge had been accumulated describing the different effector cells and cytokine networks that compose the immune system, immunotherapy for cancer gained great importance in the treatment of several malignancies (Ichim, 2005) and is today the most promising approach to achieve a curative therapeutic response.

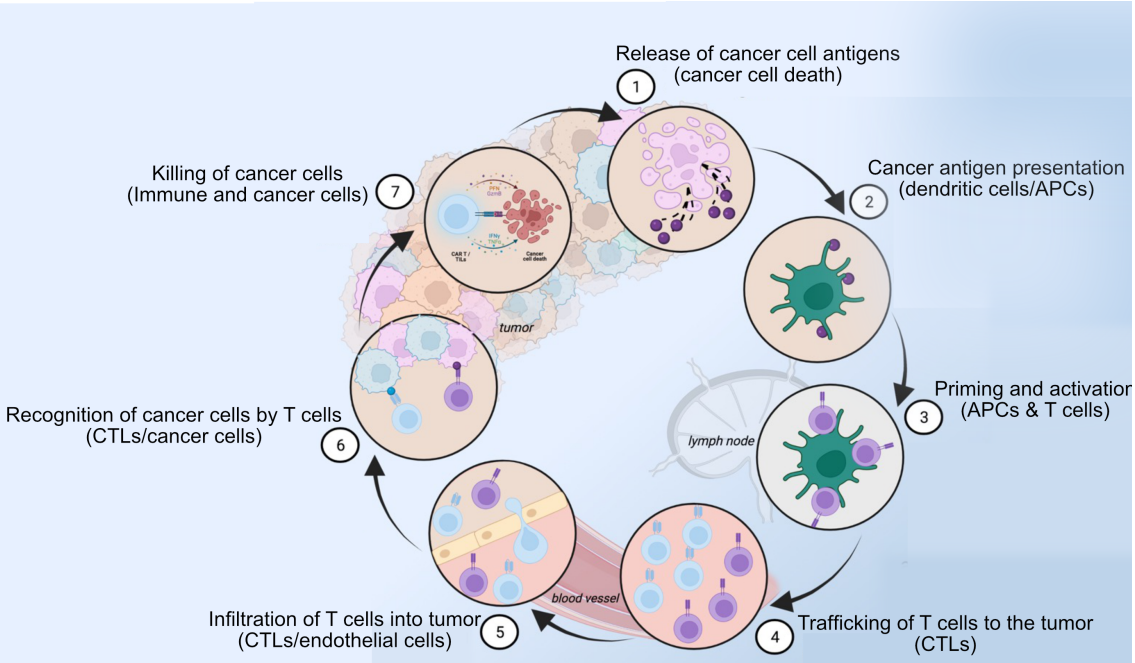

Figure 3. The Cancer-Immunity Cycle.
Figure adapted from The "cancer-immunity cycle" proposed by Chen and Mellman (Chen & Mellman, 2013). Depicting the generation of anti-cancer immunity as a cyclic process that starts with the liberation of neo-antigens upon tumor cell death (1) that are taken up by APC (2) and presented to T cells in the lymph nodes (3). T cells travel to (4) and penetrate (5) into the tumor mass where they can recognize the tumor cells (6) and kill them (7), re-starting the cycle.

In 2013 Chen and Mellman described a concept of how the immune system recognizes and fights cancer cells in a process termed the "cancer-immunity cycle" (Figure 3) (D. S. Chen & Mellman, 2013). During malignant transformation, cancer cells accumulate mutations and genetic alterations that lead to protein overexpression or the generation of new proteins that can be identified as neo-antigens by the immune system (Aldous & Dong, 2018). When cancer cells die in an immunogenic way (step 1), neo-antigens are released together with DAMP and can be sensed and processed by antigen presenting cells (APC) in the tumor microenvironment (step 2). APC, especially DC, get activated and can migrate to the lymph nodes and subsequently prime and activate effector lymphocytes against the tumor (step 3). The primed cytotoxic lymphocytes travel through the blood stream and infiltrate into the tumor (step 4 and 5), where they can now recognize the tumor cells (step 6) and eliminate them (step 7), generating a new release of antigens and DAMP that re-starts the cycle (D. S. Chen & Mellman, 2013).

This previously explained cycle describes a perfect immunological response scenario. In cancer patients the immunological response is dampened due to several reasons: for one, tumors such as pancreatic cancer are classified as “cold” immunological tumors which are characterized by having a low presence of cytotoxic effector cells and presenting a low mutational burden which translates in limited antigen availability (Bonaventura et al., 2019). Additionally, many “cold” tumors present defects in antigen presentation and/or T cell activation that can be exacerbated by the modified production of chemokines and cytokines by tumor cells and immunosuppressive cells (Motz & Coukos, 2013). Moreover, cancer cells can express proteins that inhibit the immune system’s cytotoxic response (Maleki Vareki, 2018). Over the years, several approaches have been explored to counteract these conditions and unleash the fighting power of the immune system against cancer, in this work we have focused on a combinatorial approach described in the following section.

1.3 Immunotherapy strategies explored in this work

1.3.1 RIG-I-targeted tumor immunotherapy

Activation of PRR such as RIG-I is an interesting therapeutic option in cancer immunotherapy due to their potential to initiate an innate immune response and promote the formation of a specific adaptive immune response against tumor antigens (Yang et al., 2022). It has been convincingly shown that activation of RIG-I signaling induces strong therapeutic responses in several pre-clinical models of solid tumors, as highlighted in a recent review by Lurescia *et al.* (Lurescia et al., 2020). Some of the mechanisms behind the therapeutic efficacy of RIG-I activation are linked to the expression of type I IFN, other pro-inflammatory cytokines and chemokines which enhances surveillance by immune cells and remodels the immunosuppressive TME, while inducing immunogenic cell death of tumor cells (Zitvogel et al., 2015).

Therapeutic activation of RIG-I can be achieved using intracellularly delivered *in vitro*-transcribed 3p-RNA and is associated with increased recruitment and activation of different cytotoxic immune cells. Recently, Dassler-Plenker et al. demonstrated NK cell activation upon 3p-RNA transfection, resulting in enhanced expression of membrane-bound TRAIL, capable of initiating apoptosis in melanoma cells (Daßler-Plenker et al., 2019).

Furthermore, experiments with length and structure modified versions of 3p-RNA have further confirmed efficient anti-tumor responses in immunogenic and poorly immunogenic mouse tumor models like B16F10 melanoma. Studies showed not only an increase of infiltrating $CD8^+$ T cells and NK cells, but also a TME reprograming with marked reduction of immunosuppressive populations like $CD4^+$ $FoxP3^+$ Treg (Jiang et al., 2019).

Moreover, synergistic anti-tumor effects have been observed when combining 3p-RNA treatments with checkpoint blockade using anti-PD1 against melanoma, breast, and colon cancer tumor models (Elion et al., 2018). Studies by Heidegger et al. established that combining RIG-I targeted therapy with CTLA4 blockade improved expansion of $CD8^+$ T-cells that were antigen-specific. This induced not only better tumor control but also a reduction of metastatic tumor burden (Heidegger et al., 2019). Ruzicka and colleagues further showed that RIG-I-targeted therapy sensitizes mice in preclinical AML models to checkpoint blockade and induces an immunological memory that can defend the mice upon tumor rechallenge (Ruzicka et al., 2020).

Importantly, the cell death induced by 3p-RNA treatment prompts the release of DAMP and markers of immunogenic cell death which stimulate the phagocytic potential of DC, promoting increased HLA and co-stimulatory molecule expression (Duewell et al., 2015). The IFN-enriched environment upregulates membrane expression of MHC-I also in naïve $CD8^+$ T cells, promoting antigen-cross presentation and effective anti-tumor responses in different types of cancer (Castiello et al., 2019).

Many of the above-mentioned anti-tumoral effects of RIG-I targeted therapies are directly linked with the release of type I IFN and pro-inflammatory cytokines and chemokines. Type I IFN such as IFN-α and IFN-β, as well as other pro-inflammatory cytokines, have been described to play a pleiotropic immunomodulatory function with both pro- and anti-tumoral effects (Dinarello, 2006). For example, chronic exposure to type I IFN contributes to increased IL-10 production by macrophages. This together with tryptophan starvation and increased expression of programmed cell death protein ligand 1 (PD-L1) by cancer cells, leads to exhaustion of cytotoxic T cell and proliferation and maintained expression of Foxp3 in Treg (Medrano et al., 2017). This combination of effects can ultimately contribute to tumor progression.

However, type I IFN are also widely known for their anti-tumoral role. Cancer cells upregulate surface expression of MHC-I and antigen presentation in response to type I IFN, making them more susceptible to recognition by NK cells. Both $CD8^+$ and $CD4^+$ T cells are known to augment their cytokine secretion, proliferation, and effector functions upon type I IFN stimulation. DC are described to have enhanced antigen cross-presentation and maturation while, suppressive cells like Treg, MDSC and TAM are decreased in their suppressive capacity in response to type I IFN (Medrano et al., 2017).

1.3.2 CAR T cell therapy

Chimeric antigen receptor (CAR) T cell therapy is a kind of adoptive cell therapy (ACT) pioneered by Gideon Gross and colleagues in 1989 (Gross et al., 1989). It involves T cell isolation from the blood of patients, followed by genetic engineering *in vitro* to induce expression of a synthetic tumor-targeting receptor. The engineered cells are expanded in controlled culture conditions and infused back into the patient (Rosenberg & Restifo, 2015). In its most basic form, CAR are composed of an extracellular domain, classically a single chain variable fragment (scFv) derivative from a monoclonal antibody, that specifically recognizes surface antigens expressed on tumor cells. The scFv is connected to a hinge and

transmembrane region, which in turn is connected to an intracellular part that triggers downstream activatory signaling upon antigen recognition (Eshhar et al., 1993).

To date, five generations of CAR are described and are summarized in figure 4. The first generation mentioned above entails the simple coupling of the extracellular scFv with an intracellular CD3ζ chain. Second and third generation CAR T cells include either one or two co-stimulatory domains, respectively. The addition of these domains aims to augment T cell activation while also promoting proliferation, cytokine production and cell persistence (Smith et al., 2016). Currently, five CAR T cell products are approved for therapeutic treatment of B cell-associated neoplasms and all products are second generation CAR T cells harboring either 4-1BB or CD28 as co-stimulatory domains (Yeo et al., 2022).

Research aiming to improve CAR T cell efficacy resulted in the proposal of a fourth and fifth generation of CAR T cells. The fourth generation CAR T cells, termed TRUCKs, can unleash antigen-unrestricted cytokine-initiated killing (Chang & Chen, 2017). These constructs encode additional cytokine secretion to enhance not only T cell function but also engage innate immune responses. Finally, a fifth generation of CAR T cell construct was proposed recently, in which antigen-dependent CAR activation leads to initiation of the JAK-STAT pathway, positively influencing T cell proliferation and anti-tumor response (Kagoya et al., 2018).

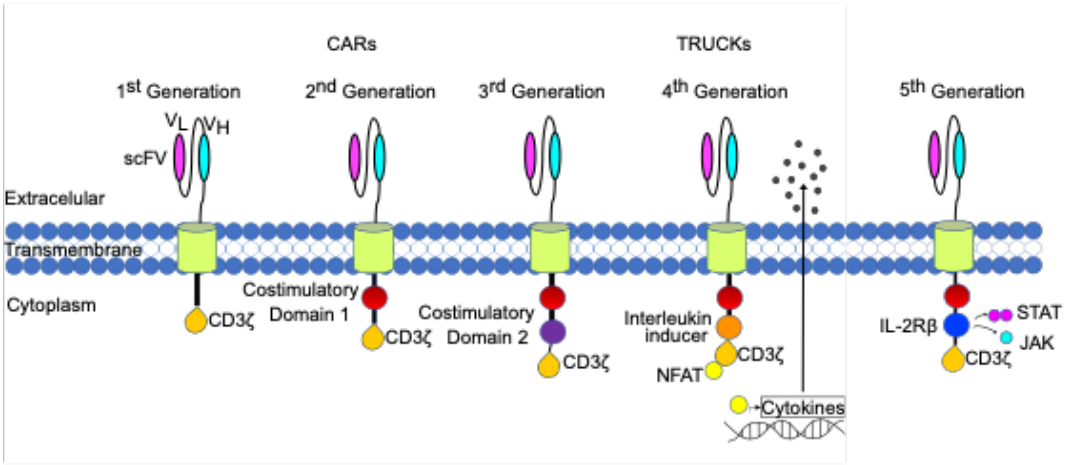

Figure 4. Representation of the different CAR T cell construct generations.

Chimeric antigen receptors (CAR) are comprised of extracellular single chain variable fragments (scFv) of monoclonal antibodies (VL and VH) fused with transmembrane and intracellular domains. First generation CAR harbor only a CD3ζ intracellularly. Second and third generation CAR include one or two costimulatory domains in addition to CD3ζ. Fourth generation CAR include interleukin inducer domain coupled with CD3ζ inducing cytokine secretion through NFAT transcription factor. Fifth generation CAR include IL-2Rβ domain inducing JAK-STAT signaling upon activation. Figure adapted from (Yeo et al., 2022).

1.3.3 Challenges of CAR T cell therapy in solid tumors

The fact that solid tumors have remained utterly unresponsive to CAR T cell therapy so far has been attributed to both intrinsic and extrinsic characteristics of the TME (Bellone & Calcinotto, 2013). For one, solid tumors are masses of disorganized tissue, which are irrigated by abnormal blood vessels. This represents a physical barrier, where the defective blood supply and vessel leakiness contributes to an overall hypoxic microenvironment unfavorable for CTL extravasation and survival (Lim & June, 2017).

In parallel, incompatibility between tumor secreted chemokines and chemokine receptors expressed by effector T cells, including CAR T cells, have been linked to suboptimal trafficking and infiltration into the tumors. Importantly, higher numbers of infiltrating T cells in the tumor correlate positively with therapeutic outcome (Slaney et al., 2014). Furthermore, even if an appropriate infiltration of the tumor site is achieved, interactions between CAR T cells and immunosuppressive cells and soluble factors can lead to immunosuppression and exhaustion, dampening proliferation, and overall cytotoxic anti-tumor immune response (Srivastava & Riddell, 2018).

In solid tumors, CAR T cell expansion and long-term persistence are strongly hindered due to the TME. Contrary to hematological malignancies, solid tumors provide a space restriction to antigen availability (Pant & Jackson, 2022). This combined with the difficulties that CAR T cells face to traffic and infiltrate into the tumor mass translate into decreased CAR T cell survival and anti-tumoral activity (Pietrobon et al., 2021a). Vaccination strategies that promote antigen

presentation on the surface of DC with the aim to expand the CAR T cells and improve their persistence and anti-tumoral effect in solid tumors are currently being tested in the clinic and initial results are promising (NCT04503278), showcasing that the improvement of CAR T cell persistence can be indeed beneficial to improve solid tumor response to therapy.

Additional strategies have been explored that focus on improvement of T cell infiltration into tumors. Normalization of the tumor vasculature, the use of antibodies to target VEGF and its receptors (Shrimali et al., 2010), induction of an inflammatory environment by irradiation (Ganss et al., 2002), or direct targeting of TNF to the blood vessels (Johansson et al., 2012) have shown improvements in T cell trafficking. However, tumor cells themselves also induce exclusion of effector T cells from their vicinity through increased expression or downregulation of chemokines (Harlin et al., 2009).

Chemokine gradients can modulate T cell movements through chemotaxis. Therefore, it has been suggested that both the induction of chemokine expression patterns by therapies like chemotherapy (Hong et al., 2011), and the screening of tumors for their chemokine receptor and ligand expression profiles can help modulate effector T cell infiltration capacities (Cadilha et al., 2017). Approaches including overexpression of chemokine receptors such as C-C chemokine receptor 4 (CCR4) and C-X-C chemokine receptor 2 (CXCR2) in T cells have shown promising results in increasing leukocyte recruitment during ACT and improving therapeutic outcome in preclinical models of different types of cancer including pancreatic tumors (Rapp et al., 2016). Overall, the findings hint towards modulation of chemokine receptors and their ligands as interesting strategies for improving CAR T cell therapy against solid tumors.

Many chemokine receptors and their ligands are known to be involved in T cell recruitment, two examples are CXCR3 and CCR5 ligands. They are described to be highly upregulated in biopsies of different types of solid tumors, correlating with high T cell infiltrations, improved therapeutic response and prolonged survival (Strazza & Mor, 2020). CXCR3 is rapidly upregulated upon activation of

naïve T cells and remains highly expressed on both Th1 $CD4^+$ and effector $CD8^+$ T cells (Karin, 2020). The main ligands for CXCR3 are the interferon-inducible chemokine ligands like CXCL9, CXCL10 and CXCL11 (Loetscher et al., 1998). CCR5 is also expressed by activated T cells and directs their migration towards gradients of CCL3, CCL4 and CCL5 (Contento et al., 2008). The CXCR3 axis is thought to mediate T cell recruitment towards inflammation sites in a chain of events that starts with innate immune cells sensing danger through PRR and inducing the secretion of type I IFN that promotes the expression of CXCL10. CXCL10 recruits $CXCR3^+$ $CD4^+$ Th1 T cells that are activated on site by DC and secrete IFNγ, further promoting the expression of CXCL9, CXCL10 and CXCL11, thereby inducing migration of $CXCR3^+$ $CD8^+$ CTL (Groom & Luster, 2011).

The CCR5/CCL5 axis has been recently described to drive increased infiltration of anti-tumor $CD4^+$ T cells in a pancreatic mouse model when treated with CD40 agonists (Huffman et al., 2020). Nonetheless, tumor derived CCL5 can also recruit Treg, promoting tumor progression (Tan et al., 2009). The high degree of promiscuity between chemokine receptors and their ligands translates in many cases into an increased recruitment of immunosuppressive cells to the TME. Therefore, solely increasing T cell infiltration into the tumors is not sufficient to unleash long lasting anti-tumor responses but there is a strong need to combine the increased infiltration with methods that can reduce immunosuppression and promote T cell activation and persistence.

Persistent antigen stimulation and upregulation of inhibitory receptors in the context of an immunosuppressive tumor microenvironment can lead to CAR T cell exhaustion and the consequent inhibition of their proliferation and effector functions (Gumber & Wang, 2022). To overcome these challenges, strategies have been explored on the T cell side to optimize the CAR construct design and reprogram the cells epigenetic footprint prolonging or restoring their effector function (Luo et al., 2022). However, the immunosuppressive cells and molecules in the TME can still induce T cell exhaustion. Therefore, TME modulation is of vital importance to potentiate anti-tumor cytotoxic responses.

Additionally, there is the issue of antigen specificity. It is rare to encounter a membrane expressed antigen uniquely present in tumor cells and not in healthy tissue. Therefore, most CAR T cells are engineered to recognize tumor-associated antigens (TAA) that have higher expression levels in tumor cells than in normal tissue but are still present in the latter. CAR T cell recognition of their target antigen in healthy tissue leads to on-target off-tumor toxicities that have proven to be fatal in some cases (Morgan et al., 2010). Moreover, tumor cells present highly heterogeneous expression levels of the target antigens, and it has been commonly observed that patients with initially responsive disease relapse due to antigen downregulation or loss (Lemoine et al., 2021). To prevent disease relapse due to antigen loss, it would be necessary for the immune system to generate a response against neo-antigens found in the tumor. For the efficient mounting of a *de novo* immune response against neo-antigens, tumor cells need to go through immunogenic forms of cell death that are capable of alerting and engaging APC (Fucikova et al., 2020).

1.4 Pancreatic cancer and its treatment options

1.4.1 Pancreatic cancer

The pancreas is a key organ of the digestive and endocrine systems performing a dual exocrine and endocrine function. It aids in the process of breaking down sugars, fats, and starches through the secretion of digestive enzymes such as proteases, amylase, and lipase. On the other hand, it produces hormones like glucagon and insulin that assist sugar level control in the blood (Busnardo et al., 1983). The majority of tumors in the pancreas arise from ductal or acinar cells and are therefore termed as pancreatic ductal adenocarcinoma (PDAC). PDAC is one of the world's most lethal types of cancer. Around 90% of cases arise because epithelial cells in the pancreatic ducts accumulate mutations on the KRAS oncogene, and/or CDKN2A, TP53 and SMAD4 tumor suppressor genes (Wood & Hruban, 2012). The presence of these mutations, among other genetic

alterations and environmental factors, lead to uncontrolled cellular proliferation and neoplasm formation (Hruban et al., 2001).

According to statistics from the American Cancer Society, the incidence of PDAC is rising, and in 2020 was already predicted to be the top fourth cause of cancer associated deaths in the U.S. The 5-year survival rate for PDAC does not exceed 11% (Siegel et al., 2022). One of the central reasons for the poor prognosis and high mortality rate of PDAC is its late diagnosis. Most patients with early stage PDAC remain asymptomatic or present mild, non-specific symptoms. Therefore, when the cancer is diagnosed, only 20% of the patients are still eligible for surgery (Kamisawa et al., 2016). The rest of the patients present with either locally advanced disease, which is treated with neoadjuvant therapies aiming to achieve a potential tumor down-staging for subsequent surgery, or with advanced metastatic disease. In the latter case palliative chemotherapy is usually the only option (Gillen et al., 2010).

1.4.2 Tumor microenvironment in PDAC

The tumor microenvironment (TME) in PDAC is a complex structure composed of cancer cells, stromal cells, and extracellular components. These components interact with each other playing a critical role in disease progression, invasion, metastasis, and treatment response (Provenzano et al., 2012). The stroma in PDAC can make up to 80% of the tumor volume (Erkan et al., 2008). It comprises among others, cancer-associated fibroblasts (CAF), endothelial cells, and immune cells. These cells together with the cancer cells, contribute to the secretion of extracellular components like a dense extracellular matrix (ECM), growth factors, cytokines and chemokines that maintain the complex TME (Zhang et al., 2022).

CAF are derived from diverse types of progenitor cells, which upon exposure to environmental stress and/or different cytokines and secretory factors get pathologically activated. This leads to their differentiation into activated pancreatic stellate cells (aPSC), myofibroblastic CAFs (myCAF) and inflammatory CAFs

(iCAF) (Öhlund et al., 2017). These CAF contribute to tumor desmoplasia by producing several components of a dense ECM that constitutes a physical barrier for drug penetration (Neesse et al., 2019). Additionally, CAF secretion of various factors contributes to epithelial-to-mesenchymal transition (EMT), cancer-cell migration and invasion, angiogenesis, metastasis as well as recruitment of immunosuppressive cells (Murakami et al., 2019). Furthermore, CAF can modulate chemokine receptors expression to prevent T cell recruitment and favor their exclusion (Gorchs et al., 2022). Disruption of the desmoplastic stroma in pre-clinical models of PDAC improved drug delivery and chemotherapy response (Provenzano et al., 2012). However, clinical studies testing several therapeutic strategies to target aPSC and CAF have shown high level of adverse events (AE) and no clinical benefit or even induced higher mortality (Schnittert et al., 2019).

The TME of PDAC is highly immunosuppressive as it is characterized by the elevated occurrence of myeloid-derived suppressor cells (MDSC), M2-polarized tumor-associated macrophages (TAM) and T regulatory cells (Treg), in contrast to very little infiltration of cytotoxic $CD8^+$ T cells and NK cells (Zhang et al., 2022). Tumor cells and the stroma secrete a variety of factors that affect myelopoiesis, differentiation, and polarization of MDSC and macrophages (Gabrilovich, 2017). GM-CSF, G-CSF, and IL-6 promotes the development of myeloid cells and their release from the BM into the circulation, while IFNγ, tumor necrosis factor (TNF), IL-1b, and IL-6 contribute to the pathological activation of these cells (Condamine et al., 2015). Moreover, GM-CSF, CXCR2 ligands and CSF-3, together with CCL2 and CSF1 are some of the tumor-secreted factors that drive the recruitment of MDSC and macrophages into the tumor (Vonderheide & Bear, 2020).

Two subtypes of MDSC have been described in mouse and humans. MDSC derived from granulocyte precursor are termed polymorphonuclear MDSC (PMN-MDSC) and those derived from monocytic precursors are referred to as monocytic MDSC (M-MDSC). The distinction of the pathologically activated PMN-MDSC from human granulocytes is facilitated by the expression of lectin-type oxidized LDL receptor-1 (LOX1) (Bronte et al., 2016). However, in mice no specific receptors have been identified to date to differentiate pathologically activated

PMN-MDSC and M-MDSC from granulocyte and monocytes. Therefore, the same markers used to identify granulocytes and monocytes apply for PMN-MDSC and M-MDSC, the distinction comes based on their expansion in the tumor setting and their capacity to suppress T cells (Bronte et al., 2016).

MDSC induce immunosuppression either directly or indirectly through the emission of immunosuppressive factors and upregulation of checkpoint proteins as well as through the depletion of essential amino acids in TME (Zhang et al., 2022). Moreover, immunosuppressive cytokines produced by MDSC induce Treg differentiation, inhibit NK cell cytotoxicity and promote M2 polarization of TAM (Kim et al., 2018). M2-polarized macrophages play a pro-tumorigenic role in PDAC, and overall survival of patients was shown to correlate inversely with the density of M2 macrophage infiltration (Hu et al., 2016). These cells have a described involvement in facilitating cancer stemness, angiogenesis, desmoplasia, tumor invasion, and metastasis through EMT induction. Moreover, they also play an active role in excluding and suppressing adaptive immune cells (Poh & Ernst, 2021).

PDAC cells can directly recruit Treg and secretion of cytokines and molecules like IL-10 and TGF-β by Tregs can induce direct lysis and inactivation of effector T cells (Beyer et al., 2016). Furthermore, competition for IL-2 in the TME limits its availability, hampering effector T cell proliferation (Pandiyan et al., 2007). Moreover, CTLA4-mediated interaction between Tregs and DC initiates tryptophan catabolism, depleting this essential amino acid and promoting the accumulation of immunosuppressive kynurenines (Fallarino et al., 2003).

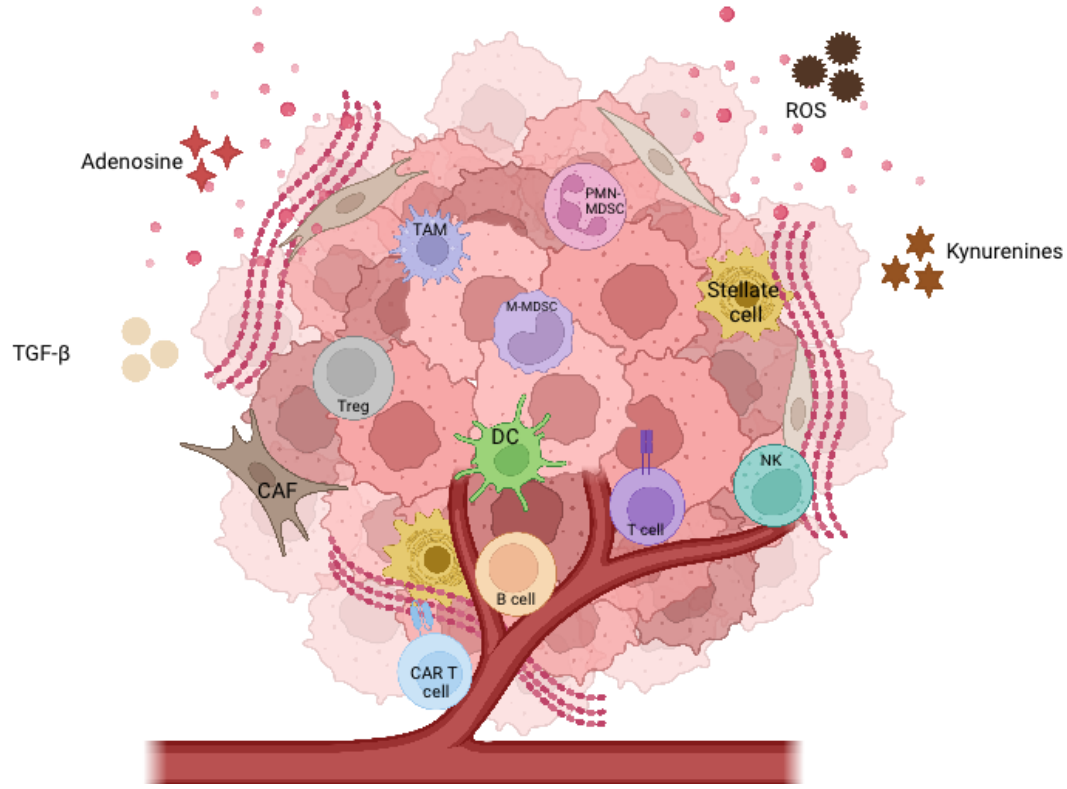

Figure 5. Tumor microenvironment in PDAC.

Schematic representation of the TME in PDAC tumors, composed of tumor cells, cancer-associated fibroblasts (CAF), and activated stellate cells which induce a dense extracellular matrix. The TME depicts an enriched presence of immune suppressive cells such as polymorphonuclear myeloid-derived suppressor cells (PMN-MDSC) and monocytic myeloid-derived suppressor cells (M-MDSC), T regulatory cells (Treg) and tumor-associated macrophages (TAM) as well as immunosuppressive factors like TGF-β, reactive oxygen species (ROS), kynurenins and adenosine. Peripheral location of dendritic cells (DC), B cells, T cells, NK cells and CAR T cells.

Clearly, the immunosuppressive nature of the TME in PDAC strongly contributes to its aggressiveness. Therefore, several strategies have been devised to target immunosuppressive cells in PDAC in an attempt to modulate the TME and improve therapeutic outcomes. Ho *et al.* recently published a comprehensive compendium of clinically explored combination strategies that modulate the TME in PDAC. These include chemokine receptor inhibition to prevent recruitment of MDSC and TAM, or depletion of these cell types by CSF-1 receptor (CSF-1R) inhibition, as well as incorporation of low-dose cyclophosphamide treatment regimens to selectively eliminate Tregs (Ho et al., 2020). Results from many of these clinical trials showed that these therapies can be well tolerated by patients and display encouraging initial therapeutic responses. Further supporting the notion that the TME has critical role in PDAC disease and its treatment response.

1.4.3 Current therapeutic options in PDAC

Currently, the first treatment attempt for patients diagnosed with resectable PDAC is surgery, followed by chemotherapy. Chemotherapy alone or in combination with radiotherapy are the only alternatives for most of PDAC patients, that have locally advanced and/or metastatic disease (Neoptolemos et al., 2018). Moreover, despite using very aggressive combinations of chemotherapeutic regimens, such as gemcitabine together with nab-paclitaxel, or folinic acid, fluorouracil, irinotecan with oxaliplatin (FOLFIRINOX), the overall survival of patients has not improved more than a few months, and dose limiting toxicities are commonly observed (Conroy et al., 2011).

Efforts to develop targeted therapy options to treat PDAC have shown little success in clinical trials, and the few responsive examples are limited to patients presenting with rare and unique genetic signatures. One of these examples is that of patients presenting with mutations in Breast Cancer 1 (BRCA1) and BRCA2 genes (25% PDAC patients). These patients are responsive to treatment with PARP inhibitors and platinum-based chemotherapy (Golan et al., 2019). Similarly, epidermal growth factor receptor 1 (EGFR) inhibitors have shown minor improvements in the treatment of metastatic PDAC patients and have therefore been approved by the US Food and Drug Administration (FDA) (Moore et al., 2007).

1.4.4 Immunotherapy approaches in PDAC

Despite the success of immunotherapy in treating other tumor entities, PDAC remains largely unresponsive. Several trials have explored the use of checkpoint inhibitors, cancer vaccines, agonistic therapy, oncolytic viruses, and ACT as monotherapies or in different combinations without much success. Low mutational burden, together with the described immunosuppressive TME, are thought to be two main reasons behind the lack of therapeutic benefit of immunotherapies in PDAC (Connor et al., 2017).

Monotherapies with immune checkpoint inhibitors, like anti-programmed cell death protein 1 (PD1), or anti-cytotoxic T-lymphocyte-associated protein 4 (CTLA4), have shown little benefit in PDAC patients, likely due to the low cytotoxic T cell presence and dysfunction in the tumor (Royal et al., 2010). Only patients presenting with microsatellite instability (1-2% of PDAC patients) have shown favorable responses to anti-PD1 blockade, presumably due to a higher neo-antigen load (Le et al., 2017).

Efforts to induce endogenous anti-tumor immune responses with cancer vaccines or agonistic therapies like CD40, TLR or STING, aim to activate and polarize APC. Early trials testing these agents as monotherapies evidenced the induction of tumor-specific immune responses but failed to translate into improved patient survival in several clinical trials (Morrison et al., 2018). Recent reports from the randomized phase II PRINCE trial (NCT03214250) showed that only the combination of chemotherapy with gemcitabine/nab-paclitaxel together with anti-PD1 (nivolumab) increased the 1-year overall survival (OS) while the effect of combining chemotherapy with CD40 agonist (Sotigalimab) had only modest effects on OS (Padrón et al., 2022). Furthermore, data from a phase I clinical trial (NCT04161755) using a mRNA-based neoantigen vaccine, in combination with anti-PD-L1 blockade, and a modified version of FOLFIRINOX showed a substantial induction of neo-antigen specific T cells, that persisted up to two years and correlated with delayed tumor recurrence in patients with resected PDAC (Rojas et al., 2023). Oncolytic viruses, as monotherapies, or in combination with checkpoint inhibitors, have been tested in several phase I or II clinical trials. So far, the efficacy has been limited. Most of the treated patients showed disease progression, and only a small proportion exhibited minor responses or stable disease (Brouwer et al., 2021).

ACT in the form of tumor infiltrating lymphocytes (TIL) and engineered NK cells and CAR T cells, are actively explored for the treatment of PDAC. Preclinical studies evaluating efficacy of TIL and engineered CAR NK and T cells have shown promising results in murine models and several clinical trials are being carried out, testing safety and efficacy in patients (Yeo et al., 2022). Isolation, selection,

expansion, and re-infusion of TIL has shown promising results in phase I-II clinical trials against melanoma, non-small cell lung cancer and metastatic cervical cancer. However, several adverse events (AE) have been recorded as a result of the elevated IL-2 dose infusions required to support the treatment (Nguyen et al., 2019). Results for phase I-II clinical trials using TIL to target PDAC are yet to be published (NCT05098197, NCT03935893, NCT03610490).

NK cells have the benefit that they do not necessarily require antigen specificity to elicit anti-tumor cytotoxicity, yet they can be engineered towards specific targets. Furthermore, in the allogeneic setting, they induce little to none graft-versus-host disease (GvHD), opening the possibility of generating off-the-shelf products (Mehta et al., 2018). In a humanized mouse model of metastatic pancreatic cancer, NK cells isolated from umbilical cord and engineered to target prostate stem cell antigen (PSCA), and co-express soluble IL-15, showed increase cytotoxicity leading to tumor growth control, increase in survival and persistence of the therapeutic cells in the TME at day 48 after treatment (Froelich, 2021). So far, clinical trials testing infusions of allogeneic CAR NK cells engineered to target MUC1 (NCT02839954) and ROBO1 (NCT03941457) in PDAC have been initiated. The first reports show the therapies are well tolerated and did not show serious toxicities (C. Li et al., 2020). Similarly, clinical trials testing activated NK-92 cells targeting MUC1 and PD1 have been tested in a range of different cancers showing no severe AE and stable disease in 9/13 patients (Q. Li et al., 2019).

When it comes to CAR T cells, clinical studies with therapies directed against different antigens in PDAC display good toxicity profiles, but with little to no therapeutic benefit (Beatty et al., 2018). Recently published data show that the majority of PDAC patients enrolled in CAR T cell clinical trials exhibited only short-term responses, or even disease progression (Yeo et al., 2022).

1.4.5 Clinical outcomes of CAR T cell therapy trials in PDAC

Clinically approved CAR T cell therapies against hematological malignancies have shown remarkable results, with studies reporting remission in up to 90% of the treated individuals (Park et al., 2018). However, attempts to treat solid tumors with CAR T cells have not been so successful. More than 30 clinical trials are registered at clinicaltrials.gov that explore CAR T cell treatment in pancreatic tumors. These studies explore different targeting antigens of which the most common are CD133, EGFR, HER2 and mesothelin (MSLN) (Schaft, 2020). In a phase I clinical trial using CAR T cells against CD133 (NCT02541370), Wang and colleagues reported that from the seven pancreatic cancer patients included in the cohort, three achieved stable disease, two had partial remission and two showed disease progression after receiving two to four cycles of CAR T cell therapy (Wang et al., 2018). Similar results were obtained by Liu and colleagues upon attempting to treat 16 PDAC patients with CAR T cells targeting EGFR in a phase I clinical trial (NCT01869166). The results of this trial showed a partial response in four of the patients for 2-4 months, while eight remained with stable disease, two showed disease progression and two individuals died during follow-up (Liu et al., 2020). Following the same line, phase I clinical trials testing CAR T cell therapy against HER2 (NCT01935843) and MSLN (NCT01897415, NCT02159716) in several patients with solid tumors including PDAC reported patients achieving only stable disease or progressive disease (Yeo et al., 2022). The results of these clinical trials are a small set of examples showcasing the decreased efficiency of CAR T cell therapy in solid tumors in comparison to hematological malignancies and the great need for improvement (Patel et al., 2021).

1.5 Previous work of the group

Strategies that exploit intracellular viral sensing pathways as a therapeutic option in pre-clinical models of cancer, such as PDAC, have been widely studied in our group. In a murine PDAC model Ellermeier et al. showed that concomitant silencing of TGF-b1 and RIG-I activation induced systemic immune cell activation and increased mice survival in a $CD8^+$ T cell dependent manner (Ellermeier et al., 2013). Additionally, Metzger et al. showed that treatment with immunostimulatory RNAs of orthotopically induced tumors leads to increase infiltration of $CD8^+$ T cells and a functional reprograming of the myeloid compartment in the TME, reducing immunosuppression in a type I IFN dependent manner (Metzger et al., 2019). Furthermore, ligands for cytosolic RNA sensors, such as polyinosinic:polycytidylic acid (poly(I:C) or 3p-RNA, were shown to induce an immunogenic form of cell death of PDAC tumor cell lines, promoting antigen uptake, presentation, and activation by DC, and ultimately sensitizing tumors towards $CD8^+$ T cell-mediated killing (Duewell et al., 2014).

1.6 Objectives

The primary objective of the present work was to evaluate whether 3p-RNA treatment can enhance the efficacy of CAR T cell therapy in PDAC models and assess what are the mechanisms behind the observations. Our hypotheses are:

1. 3p-RNA treatment primes the TME for an effective immune response
2. Cytokine and chemokine secretion in response to 3p-RNA treatment improves CAR T cell infiltration and efficacy
3. 3p-RNA induces immunogenic cell death promoting antigen spreading

2 Materials and Methods

2.1 Materials

2.1.1 Technical Equipment

Equipment	Company
Cell culture CO2 incubator (BD 6220)	Heraeus, Germany
Cell culture Laminar Flow	Thermo Scientific, Germany
Centrifuge (5424 and 5415R)	Eppendorf, Germany
Centrifuge (Multifuge 3L-R)	Thermo Scientific, Germany
Gentle MACS Dissociator	Miltenyi Biotec, Germany
Biotech ELISA reader (Mithras LB940)	Berthold Technologies, Germany
Biotech ELISA reader (Tristar 3)	Montreal Biotech, Germany
FACSCanto II	BD Bioscience, Germany
FACS Fortessa	BD Bioscience, Germany
FACS Aria III	BD Bioscience, Germany
Fine scale, MC1 Analytic AC 210 S	Sartorius, Germany
Lightcycler® 480 II	Roche, Germany
Microscope Axiovert25 and Axiovert200M	Zeiss, Germany
NanoDrop® 2000c	Thermo Scientific, Germany
Thermocycler T3	Biometra, Germany
Vortex Genie 2	Scientific Industries, Germany
Vortex, Galxy Mini	Merck Eurolab, Germany
Water bath	Köttermann, Germany
xCellingence	ACEA Bioscience, USA

2.1.2 Chemicals and reagents

Name	Company
Albumin fraction V (BSA)	Sigma-Aldrich, Germany
BD Pharm lyse lysing buffer (10x)	BD Biosciences, USA
Brefeldin A, Ready Made Solution 10 mg/ml in DMSO	Sigma-Aldrich, Germany
CellTiter-Blue (CTB) Cell Viability Assay	Promega, USA
Count Bright, counting beads	Life technologies, Germany
Deoxyribonucleotide triphosphate (dNTP)-Mix	Invitrogen, Germany
DNase I	Roche, Germany
dNTP-Mix, 10 mM each	Thermo Scientific, Germany
Dulbecco's PBS (1x)	Lonza, Belgium
Ethylenediaminetetraacetic acid (EDTA)	Sigma-Aldrich, Germany
FACSFlow, FACSClean	BD Biosciences
Fixable Viability Dye (FVD)	Life technologies, Germany
Ionomycin calcium salt	Sigma-Aldrich, Germany

Isoflurane-CP®	CP-Pharma, Germany
Isopropanol	Apotheke Uni Munich, Germany
Lipofectamine RNAiMax	Life technologies, Germany
Methanol	Merck, Germany
Oligo-dT 18 Primer	Eurofins, Germany
Paraformaldehyde (PFA)	Merck, Germany
Phorbol 12-myristate 13-acetate (PMA)	Sigma-Aldrich, Germany
Revert Aid H Minus RT (Reverse Transcriptase)	Thermo Scientific, Germany
RiboLock RI (RNAse Inhibitor)	Thermo Scientific, Germany
Trypan blue	Sigma-Aldrich, Germany
Trypsin-EDTA (10x)	PAA, Austria
UltraComp eBeads® eBioscience	Affymetrix , USA

2.1.3 Cell culture reagents and supplements

Name	Company
β-mercaptoethanol	Sigma-Aldrich, Germany
Murine anti-CD3 clones 145-2C11	eBioscience, Germany
Murine anti-CD28 clone 37.51	eBioscience, Germany
Dulbecco's modified Eagls's medium (DMEM) high glucose	Sigma-Aldrich, Germany
Dulbecco´s PBS (1x) without Ca^{2+} and Mg^{2+}	Sigma-Aldrich, Germany
Dynabeads® Mouse T activator CD3/CD28	Gibco,Germany
Dynabeads® Human T activator CD3/CD28	Gibco,Germany
Fetal bovine serum (FBS)	Life technologies,Germany
HEPES buffer 1 M	Sigma-Aldrich, Germany
Human Serum	Sigma-Aldrich, Germany
L-glutamine (200 mM)	PAA, Austria
MEM-NEAA (non-essential amino acids)	life technologies, Germany
Opti-MEM	life technologies, Germany
Penicillin/Streptomycin (100X)	Lonza, Germany
Sodium pyruvate	Biochrome, Germany
Trypsin-EDTA (10X)	PAA, Austria
VLE RPMI 1640 (very low endotoxin)	Biochrome, Germany

2.1.4 Recombinant cytokines and peptides

Name	Catalog	Company
OVA257-264 peptide (SIINFEKL)		InvivoGen, USA
Recombinant murine FLT3L	Cat. #250-31L	Peprotech, Germany
Recombinant murine GM-CSF	Cat. #315-03	Peprotech, Germany
Recombinant human/murine IL-15	Cat. #200-15	Peprotech, Germany
Recombinant human/murine IL-2	Cat. #200-02	Peprotech, Germany
Recombinant murine IFNγ	Cat. #315-05	Peprotech, Germany
Recombinant murine IFN-α	Cat. #752806	Biolegend, Germany
Recombinant Human IFN-α2α	Cat. #130-093-874	Miltenyi Biotec, Germany
Recombinant Human Fibronectin Fragmer	Cat. #T100B	Takara, Japan

2.1.5 Buffer and Media

Name	Components
Flow cytometry buffer (FACS buffer)	2 mM EDTA 2% FBS 0.1% NaN3 in PBS
MACS-buffer	0.2% FBS 2 mM EDTA in PBS
Blocking Buffer (Viral transduction)	2% BSA in PBS

2.1.6 Cell culture medium

Name	Components
Adherent tumor cell medium	10% FBS 2 mM L-glutamine 100 IU/ml penicillin 100 µg/ml streptomycin in DMEM
Murine T cell medium	10% FBS 2 mM L-glutamine 100 IU/ml penicillin 100 µg/ml streptomycin 1 mM sodium pyruvate 1 mM HEPES 1% MEM-NEAA 50 µM β-mercaptoethanol in RPMI 1640
Producer cell line medium	10% FBS 4 mM L-glutamine 100 IU/ml penicillin 100 µg/ml streptomycin in DMEM
DC medium	2 mM L-glutamine 100 IU/ml penicillin 100 µg/ml streptomycin 1 mM sodium pyruvate 1% MEM-NEAA 50 µM β-mercaptoethanol in RPMI 1640
Human T cell medium	2% human serum 2 mM L-glutamine 100 IU/ml penicillin 100 µg/ml streptomycin 1 mM sodium pyruvate 1% MEM-NEAA 50 µM β-mercaptoethanol in VLE RPMI

2.1.7 Cell lines

2.1.7.1 Tumor cell lines

The KPC-derived T110299 PDAC tumor cell line (Metzger et al. 2019) was modified using pMXs retroviral vectors to express either the murine EpCAM protein (UNIPROT entry Q99JW5) as CAR T cell target antigen (T110299-EpCAM) alone or in combination with chicken-derived ovalbumin model antigen (UNIPROT entry P01012) (T110299-EpCAM-OVA). The Panc02-OVA-EpCAM and SUIT-2-MSLN cell lines were a kind gift from Prof. Dr. Sebastian Kobold and engineered as described by Karches et al. (Karches et al., 2019). Surface expression of EpCAM or human mesothelin (MSLN) in the tumor cells lines was tested by flow cytometry using anti-mouse CD326 or anti-human mesothelin respectively. Modified tumor cell lines were also tested against antigen-specific T cells and the cytotoxic response and IFNγ secretion was evaluated as an indicator of antigen expression.

2.1.7.2 Virus producer cell lines

Virus-producing cell lines used for retroviral transduction of T cells were generated and kindly provided by Prof. Dr. Sebastian Kobold. In short, 293Vec_Eco packaging producer cell lines were previously engineered with retroviral pMP71 vectors encoding:

a) anti-EpCAM CAR_mCherry$^+$
b) anti-EpCAM CAR_eGFP$^+$
c) anti-hMSLN CAR_myc$^+$
d) Eco_mCherry$^+$
e) Eco_GFP$^+$
f) Chemokine receptors (CCR1-11, CXCR1-7, 3CX3CR1 and XCR1)_eGFP$^+$

2.1.8 Assay kits

Kit	Company
Mouse IFNγ T cell ELISPOT kit	U-CyTech biosciences, Netherlands
Cell Proliferation Dye eFluor™ 450	Invitrogen, USA
Cell TraceTM CFSE Cell Proliferation kit	Biolegend, Germany
CD8a+ T cell isolation kit, mouse	Miltenyi Biotec, Germany
Click-iT™ EdU Pacific Blue™ Flow Cytometry Assay	Invitrogen, USA
Fixation/Permeabilization kit (RUO)	BD Bioscience, Germany
HiScribe™ T7 Quick High Yield RNA Synthesis Kit	New England Biolabs, Germany
HMGB1 Elisa	Arigo, Germany
HMGB1 Elisa	Tecan, Switzerland
Human Granzyme B DuoSet ELISA	R&D Systems, USA
Human IFN-gamma DuoSet ELISA	R&D Systems, USA
Human IL-2 ELISA Set	BD Bioscience, Germany
KAPA PROBE FAST Universal 2X qPCR Master Mix	peqlab, Germany
Mouse IFN-gamma DuoSet ELISA	R&D Systems, USA
Mouse IFN-gamma ELISPOT	U-Cytech Biosciences, Ntherlands
Mouse Granzyme B DuoSet ELISA	R&D Systems, USA
Mouse IL-2 ELISA Set	BD Bioscience, Germany
Pan T cell isolation kit. human	Miltenyi Biotec, Germany
RevertAid™ First strand cDNA Synthesis kit	Thermo Scientific, USA
RNA clean up and concentration kit	Norgen, Canada
RNeasy Kit	QIAGEN, Germany
Tumor Dissociation Kit	Miltenyi Biotec, Germany

2.1.9 Antibodies

Primary conjugated antibodies

Specificity	Fluorophore	Clone	Host	Company	Catalog
CD3	FITC	17A2	rat	Biolegend	100204
CD3	PE	145-2C11	hamster	Biolegend	100308/200 µg
CD3	PE/Cy7	145-2C11	hamster	Biolegend	100320/100 µg
CD3	APC	17A2	rat	Biolegend	100236
CD3	PB	17A2	rat	Biolegend	100214/100 µg
CD3	BV785	17A2	rat	Biolegend	100232
CD3	BV605	145-2C11	hamster	Biolegend	100351/100 µg
CD3	PE/Dazzle	17A2	rat	Biolegend	100246
CD4	AF700	GK1.5	rat	Biolegend	100430
CD4	FITC	RM4-4	rat	Biolegend	116004
CD4	PE	GK1.5	rat	Biolegend	100408
CD4	PerCP	GK1.5	rat	Biolegend	100432
CD4	PerCP/Cy5.5	RM4-5	rat	Biolegend	100540
CD4	PE/Cy7	GK1.5	rat	Biolegend	100422
CD4	APC	GK1.5	rat	Biolegend	100412
CD4	PB	GK1.5	rat	Biolegend	100428
CD4	BV421	RM4-5	rat	Biolegend	100563
CD4	BV510	RM4-5	rat	Biolegend	100559
CD4	BV605	RM4-5	rat	Biolegend	100548

CD8	FITC	53-6.7	rat	BD Bioscience	553030
CD8	PerCP	53-6.7	rat	BD Bioscience	553036
CD8	APC	53-6.7	rat	Biolegend	100712/100 μg
CD8	PB	53-6.7	rat	Biolegend	100725/100 μg
CD8a	BV785	53-6.7	rat	Biolegend	100750
CD8a	BV711	53-6.7	rat	Biolegend	100748
CD8a	Percp-cy5.5	53-6.7	rat	BD Bioscience	1076177
CD8a	PE/Dazzle	53-6.7	rat	Biolegend	100762
CD11b	FITC	M1/70	rat	Biolegend	101206
CD11b	PerCP/Cy5.5	M1/70	rat	Biolegend	101228/100 μg
CD11b	PE-Cy7	M1/70	rat	BD Bioscience	552850
CD11b	APC	M1/70	rat	Biolegend	100212
CD11b	PB	M1/70	rat	Biolegend	101224/100 μg
CD11b	BV421	M1/70	rat	Biolegend	101251
CD11b	PE/Cy5.5	M1/70	rat	Biolegend	101210
CD11b	BV785	M1/70	rat	Biolegend	101243
CD11c	AF488		mouse	Antibody Directory	MCA1441A488
CD11c	PE	N418	hamster	Biolegend	117308
CD11c	PerCP_Cy5.5	N418	hamster	Biolegend	117328
CD11c	APC	HL3	hamster	BD Bioscience	550261
CD11c	APC	N418	hamster	Biolegend	117310/100 μg
CD11c	PB	N418	hamster	Biolegend	117322/100 μg
CD11c	BV605	N418	hamster	Biolegend	117334
CD19	FITC	1D3	rat	BD Bioscience	553785
CD19	FITC	1D3	rat	Biolegend	152404
CD19	PE	6D5	rat	Biolegend	115508/200 μg
CD19	PE/Cy7	6D5	rat	Biolegend	115520
CD19	BV711	6D5	rat	Biolegend	115555
CD19	APC	1D3	rat	Biolegend	152410
CD44	FITC	IM7	rat	Biolegend	103022
CD44	PE	IM7	rat	BD Bioscience	553134
CD44	PacBlue	im7	rat	Biolegend	103040
CD45	PE	30-F11	rat	Biolegend	103106
CD45	PerCP	30-F11	rat	Biolegend	103130
CD45	PE/Cy7	30-F11	rat	Biolegend	103114
CD45	APC	13 2 3	rat	Biolegend	147708
CD45	PB	30-F11	rat	Biolegend	103126
CD45	PE/Dazzle	30-F11	rat	Biolegend	103146
CD45	AF700	30-F11	rat	Biolegend	103128
CD62L	BV605	MEL-14	rat	Biolegend	104438
CD62L	PE	MEL-14	rat	Biolegend	104407
CD62L	APC/Cy7	MEL-14	rat	Biolegend	104428
CD62L	APC	MEL-14	rat	BD Bioscience	553152
CD62L	APC	MEL-14	rat	Biolegend	104412
CD62L	AF700	MEL-14	rat	Biolegend	104426
CD62L	PB	MEL-14	rat	Biolegend	104424
CD69	FITC	H1.2F3	hamster	Biolegend	104506
CD69	PE	H1.2F3	hamster	Biolegend	104508/200 μg

CD69	PerCP-CyTM5.5	H1.2F3	hamster	BD Bioscience	551113
CD69	APC	H1.2F3	hamster	Biolegend	104514
CD69	AF 700	H1.2F3	hamster	Biolegend	104539
CD80	PE	16-10A1	hamster	Biolegend	104708/200 μg
CD80	APC	16-10A1	hamster	Biolegend	104714
CD86	FITC	GL-1	rat	BD Bioscience	553691
CD86	PE	PO3	rat	Biolegend	105106
CD86	PE/Cy7	GL-1	rat	Biolegend	105014/100 μg
CD86	APC	GL-1	rat	eBioscience	17-0862-82
CD86	BV785	GL-1	rat	Biolegend	105043
CD95	FITC	Jo2	hamster	BD Bioscience	561979
CD95	PE	2 E7	hamster	BD Bioscience	554258
CD95	PE/Cy7	Jo2	hamster	BD Bioscience	557653
CD103	FITC	2 E7	hamster	Biolegend	121420
CD103	AF488	2 E7	hamster	Biolegend	121408
CD103	APC	2 E7	hamster	Biolegend	121414
PD-L1	PE	10F.9G2	rat	Biolegend	124308
PD-L1	PE-Cy7	10F.9G2	rat	Biolegend	124314
PD-L1	APC	10F.9G2	rat	Biolegend	124312
PD-L1	BV650			Biolegend	124336
CD279	PE	29F.1A12	rat	Biolegend	135206
CD279	APC	29F.1A12	rat	Biolegend	135210
CD279	PerCP/Cy5.5	29F.1A12	rat	Biolegend	135208
CD279	BV711	29F.1A12	rat	Biolegend	135231
F4/80	PE	BM8	rat	Biolegend	123110
F4/80	APC	BM8	rat	Biolegend	123116
F4/80	AF700	BM8	rat	Biolegend	123130
F4/80	PB	BM8	rat	Biolegend	123124
F4/80	BV605	BM8	rat	Biolegend	123133
F4/80	BV711	BM8	rat	Biolegend	123147
Foxp3	PE	FJK-16s	rat	eBioscience	12-5773-80
Granzym B	PE/Cy7	NGZB	rat	eBioscience	25-8898
H-2Kb	FITC	AF6-88.5	mouse	Biolegend	116506/500 μg
H-2Kb	APC	AF6-88.5	mouse	Biolegend	116518
IFNγ	FITC	XMG1.2	rat	Biolegend	505806
IFNγ	APC	XMG1.2	rat	Biolegend	505810/100 μg
Ly-6C	FITC	HK1.4	rat	Biolegend	128005
Ly-6C	PerCP-Cy5	HK1.4	rat	BD Bioscience	128012/50 μg
Ly-6C	PE-Cy7	HK1.4	rat	Biolegend	128018
Ly-6C	APC	HK1.4	rat	Biolegend	128016
Ly-6C	AF700	HK1.4	rat	Biolegend	128024
Ly6-C	PB	HK1.4	rat	Biolegend	128014
Ly6-C	BV421	HK1.5	rat	Biolegend	128031
Ly6-C	BV785	HK1.4	rat	Biolegend	128041
Ly6-C	BV711	HK1.4	rat	Biolegend	128037
Ly-6G	FITC	1A8	rat	Biolegend	127606/500 μg
Ly-6G	PE	1A8	rat	Biolegend	127608
Ly-6G	PE/Cy7	1A8	rat	Biolegend	127618

Ly-6G	BV785	1A8	rat	Biolegend	127645
MHC-II	FITC	AF6-120.01	mouse	BD Bioscience	553551
MHC-II	PE	AF6-120.01	mouse	Biolegend	116407/50 μg
MHC-II	PerCP Cy5.5	AF6-120.01	mouse	Biolegend	116416
MHC-II (I-A/I-E)	PB	M5/114.15.2	rat	Biolegend	107620
MHC-II (I-A/I E)	BV711	M5/114.15.2	rat	Biolegend	107643
NK-1.1	FITC	PK136	mouse	Biolegend	108706
NK-1.1	PE	PK136	mouse	Biolegend	108708
NK-1.1	PerCP Cy5.5	PK136	mouse	BD Bioscience	551114
NK-1.1	APC	PK136	mouse	Biolegend	108710
NK-1.1	PacBlue	PK136	mouse	Biolegend	108722
NK-1.1	BV421	PK136	mouse	Biolegend	108731
NK-1.1	BV605	PK136	mouse	Biolegend	108740
CD195	BV510	C34-3448	rat	BD	743696
CD195	BV421	C34-3448	rat	BD	743695
CD195	AF488	HM-CCR5	hamster	Biolegend	107008
CXCR3	APC	220803	rat	R&D	FAB1685A
CXCR3	BV241	CXCR3-173	hamser	Biolegend	126529

Primary unconjugated antibodies

Specificity	Host	Clone	Reactivity	Working Dilution	Company
phospho-eIF2alpha (Ser51)	Rabbit	Polyclonal	mouse/human	1:100	CST
Anti-Calreticulin antibody	Rabbit	Polyclonal	mouse/human	1:100	Abcam

Secondary conjugated antibodies

Specificity	Fluorophore	Host	Reactivity	Working Dilution	Company
IgG (H+L)	AF488	Goat	Rabbit	1:200	Invitrogen

2.1.10 Primers for qPCR

Gene	Sequence 5'->3'	Accession code	Position	Probe #
CCL2 murine	F: catccacgtgttggctca R: gatcatcttgctggtgaatgagt	NM_011333.3	F: 139 – 156 R: 192 - 214	# 62
CCL4 murine	F: gccctctctctcctcttgct R: ggagggtcagagcccatt	NM_013652.2	F: 98 – 117 R: 154 - 171	# 1
CCL5 murine	F: tgcagaggactctgagacagc R: gagtggtgtccgagccata	NM_013653.3	F: 3 – 23 R: 133 - 151	# 110
CCL6 murine	F: tctttatccttgtggctgtcc R: tggagggttatagcgacgat	NM_009139.3	F: 175 – 195 R: 238 - 257	# 64
CCL7 murine	F: ttctgtgcctgctgctcata R: ttgacatagcagcatgtggat	NM_013654.3	F: 92 – 111 R: 162 - 182	#12
CCL9 murine	F: tgggcccagatcacacat R: cccatgtgaaacatttcaatttc	NM_011338.2	F: 230 – 247 R: 299 - 321	# 98
CCL13 murine	F: gcacttctcttgccttctgg R: atgtaagggcgagaatgtgg	NM_010779.2	F: 61 – 80 R: 121 - 140	# 73
CCL17 murine	F: tgcttctggggacttttctg R: gaatggccccttttgaagtaa	NM_011332.3	F: 84 - 103 60 R: 157 - 176	# 27
CCL20 murine	F: aactgggtgaaaagggctgt R: gtccaattccatcccaaaaa	NM_016960.2	F: 299 – 318 R: 299 - 318	# 73
CCL25 murine	F: gagtgccaccctaggtcatc R: ccagctggtgcttactctga	NM_009138.3	F: 496 – 515 R: 563 - 582	# 9
CCL27a murine	F: ggaagcggaggaggagat R: cttgttggagacatcggactc	NM_001048179.1	F: 89 – 106 R: 161 - 181	# 45
CCL28 murine	F: cagagagctgacggggact R: gggctgatgcagattcttcta	NM_020279.3	F: 208 – 226 R: 261 - 281	# 71
CXCL2 murine	F: aaaatcatccaaaagatactgaacaa R: ctttggttcttccgttgagg	NM_009140.2	F: 308 – 333 R: 379 - 398	# 26
CXCL3 murine	F: ccccaggcttcagataatca R: tctgatttagaatgcaggtcctt	NM_203320.2	F: 317 – 336 R: 404 - 426	# 69
CXCL4 murine	F: tgggatccatcttaagcaca R: ccattcttcagggtggctat	NM_019932.4	F: 303 – 322 R: 376 - 395	# 64
CXCL5 murine	F: agagccccaatctccacac R: gagctggaggctcattgtg	NM_009141.2	F: 73 – 92 R: 141 - 159	# 67
CXCL7 murine	F: gcccacttcataacctccag R: gggtccatgccatcagatt	NM_023785.2	F: 129 – 148 R: 204 - 222	# 3
CXCL 9 murine	F: cttttcctcttgggcatcat R: gcatcgtgcattccttatca	NM_008599.4	F: 72 – 91 R: 127 - 146	# 1
CXCL10 murine	F: gctgccgtcattttctgc R: tctcactggcccgtcatc	NM_021274.1	F: 53 – 70 R: 146 - 163	# 3

CXCL11 murine	F: gctgctgagatgaacaggaa R: ccctgtttgaacataaggaagc	NM_019494.1	F: 55 – 74 R: 125 - 146	# 76
CXCL13 murine	F: tgaggctcagcacagcaa R: atgggcttccagaataccg	NM_018866.2	F: 34 – 51 R: 92 - 110	# 63
CXCL14 murine	F: gacagacggcaggagcac R: tttcaagcacgcctctctc	NM_019568.2	F: 209 – 226 R: 265 - 283	# 78
CXCL15 murine	F: tgctcaaggctggtccat R: gacatcgtagctcttgagtgtca	NM_011339.2	F: 43 – 60 R: 106 - 128	# 18
CXCL17 murine	F: tgttgcttccagtgatgctc R: ctaggagccaggtgttggtc	NM_153576.2	F: 135 – 154 R: 206 - 225	# 66
CX3CL1 murine	F: catccgctatcagctaaacca R: cagaagcgtctgtgctgtgt	NM_009142.3	F: 229 – 249 R: 287 - 306	# 80
HPRT murine	F: cctcctcagaccgcttttt R: aacctggttcatcatcgctaa	NM_013556.2	F: 105 – 123 R: 175 - 195	# 95

2.1.11 Oligonucleotide sequences

Name	Sequence
3p-RNA IVT DNA template	5'-GCGCTATCCAGCTTACGTAGAGCTCTACGTAAGCTGGATAGCGCTATAGTGAGTC GTATTA-3'
OH-RNA	5'- GCG CUA UCC AGC UUA CGU A -3

2.1.12 Consumables

Name	Company
1.5 ml reaction tubes	Eppendorf, Germany
2 ml reaction tubes	Eppendorf, Germany
1 ml disposable syringe Norm-Ject	Henke Sass Wolf, Germany
100 unit insulin syringe with orange cap	Henke Sass Wolf, Germany
Injection needle (27 G 3/4 0.4x19 mm)	Becton Dickinson, USA
6-well cell culture plate	Becton Dickinson, USA
24-well cell culture plate	Becton Dickinson, USA
24-well non-tissue culture plate	Becton Dickinson, USA
96-well cell culture plate round bottom	Greiner, Germany
96-well cell culture plate flat bottom	Greiner, Germany
96-well cell culture white plate	ThermoFisher, USA
96-well transwell plates	Corning, Germany
Cell culture flasks (175 cm^3, 75 cm^3)	Greiner, Germany
Cell culture dish	Greiner, Germany
Cell scraper	Sarstedt, Germany
15 ml, 50 ml Falcons	Sarstedt, Germany
Cryo`sTM Greiner	Frickenhausen, Germany
MACS® SmartStrainers (30 μm, 70 μm, 100 μm)	Miltenyi Biotec, Germany

LS Columns	Miltenyi Biotec, Germany
PCR-Tubes Biozym	Hess, Germany
Polystyrene round-bottom tubes	Dickinson, San Jose, USA

2.1.13 Material for animal experiments

Name	Company
Alzane (Atipamezol)	Pfizer, USA
Bepanthen (Augen und Nasensalbe)	Bayer, Germany
Buprenovet (Buprenorphin)	Bayer, Germany
Capillary tube, heparinized	Hirschmann, Germany
Dorbene vet (Medetomidin)	Zoetis, Germany
Flumazenil Hikma (Benzodiazepin-Antagonist)	Hikma, Germany
In vivo-JetPEI	Polyplus transfection, USA
Isoflurane-CP	CP-Pharma, Germany
Midazolam-hameln (Benzodiazepin)	Hameln, Germany
Scalpel (No. 22)	Feather, Japan
Sodium chloride, pyrogen-free (NaCl 0.9%)	Baxter, UK
Surgery and dissecting set, autoclaved	RSG, Germany
SurgiproTM II P-13 5-0	Covidien, Ireland

Anesthesia: 150 µl per-mouse

Compound	Stock [mg/ml]	Amount master mix	Volume required
Dorbene	1	0.5 mg	500 ml
Midazolam	5	5 mg	1 ml
NaCl (0.9%)	-	-	1 ml
Buprenorphin	0.324 mg in 6 ml	0.0675 mg	1.25 ml

Antidote: 110 µl per mouse

Compound	Stock [mg/ml]	Amount master mix	Volume required
Flumazenil	0.1	0.5 mg	5 ml
Alzane	5	2.5 mg	500 µl

2.1.14 Software

Name	Company
Affinity Designer	Serif (Europe) Ltd., UK
FACSDiva	BD Bioscience, Germany
FlowJo	Tree Star, USA
Graphpad Prism	Graphpad Software, USA
Image J	Image J Software, USA
Lightcycler 480 SW 1.5	Roche, Germany

2.2 Methods

2.2.1 Cell culture

Both tumor and primary cells were cultured in an incubator at 95% humidity, 37°C and with 5% CO_2. Mycoplasma contamination was excluded every second week by PCR.

2.2.2 Immunological methods

2.2.2.1 Enzyme-linked immunosorbent assay (ELISA)

The concentration of IFNγ, IL-2, Granzyme B and HMGB1 in the supernatant of tumor and T cell co-cultures was assessed by ELISA, following the manufacturer's protocol.

2.2.2.2 Enzyme-linked ImmunoSpot Assay (ELISpot)

Detection of OVA specific T cells was measured by IFNγ spot forming units (SFU) of murine cells isolated from the spleen and blood upon 24 hours of stimulation with 1 μg/ml SIINFEKL peptide. The assay was performed following the manufacturer's protocol, plating 2 x 10^5 cells/ well in 96 well PVDF membrane plates and including three technical replicates per sample.

2.2.3 Molecular biology methods

2.2.3.1 3p-RNA *in vitro*-transcription, clean-up, and concentration

The HiScribe™ T7 Quick High Yield RNA Synthesis Kit was used to generate double stranded 3p-RNA from the DNA template described in section 2.1.11 of Materials and Methods according to the manufacturer's protocol for short transcripts. Template DNA was removed using DNase I digestion for 15 minutes at 37ºC and the resulting RNA was further cleaned and concentrated using the

RNA clean up and concentration kit (Norgen Biotek, Canada) following the manufacturer's protocol.

2.2.3.2 Tumor cell transfection

For *in vitro* transfection 1.2 x 10^4 tumor cells were seeded per well in 96-well flat bottom plates or 2.0 x 10^5 cells/well in 6-well plates. RNA transfection was accomplished through Lipofectamine™ RNAiMAX mediated delivery and the RNA-Lipofectamine complex was prepared in the Opti-MEM medium. Cultures in 96-well plates received 10 µl/well and 6-well plates received 200 µl/well complexed RNA.

T110299-EpCAM and T110299-EpCAM-OVA cells were transfected with 160 nM of RNA, complexed with 0.9 µl Lipofectamine for 96-well plates and cultured in the adherent tumor cell medium supplemented with 2% FCS. Panc02-EpCAM-OVA and SUIT-02-MSLN cells were transfected with 80 nM RNA complexed with 0.45 µl and 0.2 µl Lipofectamine respectively onto 96-well plates and cultured in adherent tumor cell media with 10% FCS.

2.2.3.3 Quantitative real time polymerase chain reaction

2.2.3.3.1 Total RNA isolation

To assess chemokine expression in response to 3p-RNA transfection, tumor cells were lysed, and their RNA isolated using the RNeasy mini kit from Qiagen according to the manufacturers protocol. In short, upon cell lysis, RNA is selectively bound to a spin column. Contaminants are removed after a series of washing steps and purified RNA is eluted and its concentration measured determined via a photometrical method using NanoDrop®.

2.2.3.3.2 cDNA transcription

cDNA synthesis from RNA was accomplished with the RevertAID™ first strand cDNA synthesis kit following the manufacturer's protocol. In brief, the reaction was carried out for 1 hour at 42°C, followed by a 10 min incubation step at 70° C to inactivate the transcriptase.

Mastermix for cDNA synthesis

	Stock concentration	1x reaction
RNA		1000 ng
Oligo(dT)	10 µM	1 µl
Ribolock™	20 U/µl	1 µl
dNTP	10 mM	2 µl
RevertAid™	200 U/µl	1 µl
5x Reaction buffer		4 µl
H_2O		up to 12 µl

2.2.3.3.2 qPCR

The expression levels of messenger RNA (mRNA) were measured by quantitative PCR (qPCR). Probes were assigned to each primer set using the Roche Universal probe library and the PCR program was performed in a Roche LightCycler 480 II device following the manufacturer's protocol.

qPCR Mastermix

	Stock concentration	1x reaction
cDNA		3 µl
Fwd Primer	10 µM	0.2 µl
Rev Primer	10 µM	0.2 µl
Probe		0.1 µl
Kapa probe fast universal qPCR mastern (2x)		5 µl
H_2O		up to 10 µl

Roche LightCycler 480 II mRNA expression program

	Temperature (ºC)	Time	Quantification	
Pre-incubation	95	10 min	--	
Denaturation	95	15 sec	--	40 cycles
Elongation	60	60 sec	Yes	
Cooling	40	∞	--	

2.2.4 Animal experiments

All animal testing was approved by the Regierung von Oberbayern in Munich, Germany; according to the animal protocol number ROB-55.2-2532.Vet_02-17-12. All experiments were done in the central laboratory animal facility in Munich city center (ZVH) under specific pathogen-free (SPF) conditions. Parameters such as body weight, behavior and clinical conditions were assessed to monitor the health status of the animals. A score was assigned, in line with the guidelines described in the animal protocol score sheet and in accordance with the EU-severity guidelines. A severity score of four or higher translated into immediate mice euthanasia.

2.2.4.1 Subcutaneous tumor induction and tumor growth monitoring

2.2.4.2 Syngeneic tumor models

C57BL/6 female mice were purchased from Charles River and were used to establish syngeneic subcutaneous tumor models using T110299-EpCAM (with or without OVA expression) tumor cells. Tumor cells were split at a 1:2 ratio one day prior to tumor induction. On the day of tumor induction, the tumor cells were detached and washed three times with PBS to remove residing FBS and cell numbers were adjusted to 1 x 10^6 tumor cells in 100 μl PBS. Mice were injected with 100 μl of tumor cells suspension in the right flank. When the tumors reached 9 mm^2 in size, they were treated intra-tumorally (i.t.) with 10 μg of *in vivo*-jetPEI complexed 3p-RNA or PBS as the control. The volume of i.t. injections was of 50 μl. Six hours later, the mice received 1 x 10^7 retrovirally-transduced syngeneic murine T cells expressing a second generation anti-EpCAM CAR through the tail vein (i.v.). Maximum 100 μl volume was injected in the tail vein. Intra-tumoral treatment with 10 μg *in vivo*-jetPEI complexed 3p-RNA was repeated once or twice after the first dose depending on the experiment. Tumor growth was measured every second day by a blinded observer.

2.2.4.2 Xenograft tumor model

NSG female mice (NOD.Cg-PrkdcscidIl2rgtm1WjI/SzJ) were purchased from Charles River and used to establish a xenograft pancreatic subcutaneous model using Suit-2-MSLN$^+$ tumor cell line. Tumor cell splitting one day prior to tumor inoculation and the preparation of the tumor cells on the day of injection was performed as described above in section 2.2.4.2.

Mice were inoculated in the right flank with 1 x 10^6 Suit-2-MSLN tumor cells. When the tumors reached 4 mm^2 in size, they were treated with 10 μg of *in vivo*-jetPEI complexed 3p-RNA or PBS i.t., six hours later 1-10^7 human anti-mesothelin CAR T cells were injected through i.v. Intra-tumoral treatment with 10 μg *in vivo*-jetPEI complexed 3p-RNA was repeated three days after the first dose and tumor growth was measured every second day by a blinded observer.

2.2.4.3 Orthotopic pancreas tumor induction

T110299-EpCAM tumor cell splitting one day prior to tumor inoculation and the preparation of the tumor cells on the day of injection was performed as described above in section 2.2.4.2. However, in this case cell numbers were adjusted to 2 x 10^5 cells in 25 μl PBS. General anesthesia and analgesia were administered intraperitoneally (i.p.). Eye cream was used to protect the eyes from exsiccation and body temperature was maintained using warming pads. After disinfecting the fur, both skin and peritoneal cavity were cut open (approximately 1 cm), pancreatic tissue was carefully dislocated and 25 μl PBS was injected into the tail of the pancreas. Organs were carefully relocated, and cuts were sewn (Philipp Metzger, 2019). General anesthesia was antagonized using the antidote described in section 2.1.13 of Material and Methods. Analgesia was administered at the beginning of the procedure with an injection of Buprenorphine (dose: 0.05 mg/kg, s.c.). This dose was repeated as necessary every 6-12 hours for 2 days and animals with clear signs of surgery associated distress were immediately sacrificed.

2.2.4.4 Treatment of mice with orthotopic pancreatic tumors

3p-RNA was complexed with *in vivo*-jetPEI in a 5 % glucose solution following the manufacturer's protocol with an N/P ratio of 6. Mice were treated 5 days after surgery with 50 μg 3p-RNA systemically (i.v.). Six hours later, the mice received 1 x 10^7 retrovirally-transduced syngeneic murine T cells expressing anti-EpCAM CAR through the tail vein (i.v.). 3p-RNA systemic treatment was repeated on day 8 after surgery. Animal conditions and survival was evaluated by a blinded observer.

2.2.5 Organ and single cell preparation

2.2.5.1 Splenocyte isolation

Spleens were passed through 70 μm strainers to obtain single cell suspensions. Obtained cells were centrifuged at 400xg for 5 min at room temperature (RT) and erythrocyte lysis was performed using 3 ml of ammonium chloride-Tris (ACT) buffer for 3 min at RT. Erythrocyte lysis was stopped using 1x PBS and the obtained cells were washed, counted, and further used for downstream applications.

2.2.5.2 Blood cell isolation

Mice were briefly anesthetized using Isoflurane and blood withdrawal was performed retro-orbitally using heparinized capillary tubes. Two rounds of erythrocyte lysis were performed using 10 times the volume of 1x BD Pharm Lyse™ lysing solution for 5 min at RT in the dark. Cell lysis was stopped using 1x PBS and cells were centrifuged at 400 x g for 7 min at RT.

2.2.5.3 Tumor composition analysis

Tumors were sliced into 1 to 2 mm² pieces and dissociated in the presence of digestion enzymes according to the Tumor Dissociation Kit® protocol, using the gentleMACS Dissociator (Miltenyi Biotec, Germany).

2.2.6 Generation of iCD103⁺ bone marrow-derived dendritic cells

Bone marrow was isolated from murine femur. The bone epiphyses were cut off and bone marrow was flushed out with the help of a syringe and PBS. The obtained bone marrow content was pelleted at 400xg for 5 min at RT and erythrocyte lysis was performed as described above. The obtained cells were differentiated in non-tissue culture dishes, seeding 2 x 10^6 cells in 10 ml DC medium for 9 days. The culture medium was enriched with 200 ng/ml recombinant murine FLT3L and 5 ng/ml recombinant murine GM-CSF. On day 3 the culture volume was duplicated using new fresh DC medium with cytokines and on day 5, 66% of media volume was replaced with new fresh media with cytokines.

2.2.7 Murine T cell isolation and retroviral T cell transduction

Spleens from donor mice were processed as described in section 2.2.5.1 of Materials and Methods. The number of obtained splenocytes was adjusted to 2 x 10^6 cells per ml in murine T cell media supplemented with 4 μg/ml IL-2, and the cells were stimulated for 24 hours with 1 μg/ml murine anti-CD3 and 0.1 μg/ml murine anti-CD28 antibodies. The stimulated T cells were retrovirally transduced using supernatant from the viral producer cell lines described in section 2.1.7.2 following previously described protocols (Karches et al., 2019). In short, non-tissue culture 24-well plates were coated overnight with 400 μl/well of 6.25 μg/ml RetroNectin at 4°C. On the day of transduction, 2 % BSA diluted in PBS was used to block the RetroNectin-coated wells for 30 min, followed by one wash with 25 mM HEPES in 1 ml PBS. Upon removal of the washing buffer 2 ml of viral

supernatant was added per well and the virus particles were attached to the RetroNectin by centrifugation at 3000 x g for 2 hours at 4 °C. Once the centrifugation step was completed, the viral supernatant was discarded and 1 x 10^6 activated murine T cells were added per well in 1 ml murine T cell media enriched with 10 U/ml IL-2, 50 μM 2-mercaptoethanol and 4 x 10^5 mouse CD3/CD28 T cell activator Dynabeads. The cells were cultured in virus-coated plates for 48 hours and then expanded with T cell medium enriched with 50 ng/ml recombinant IL-15 and 50 μM ß-mercaptoethanol every second day. Transduction efficiency was assessed by flow cytometry.

2.2.8 Human T cell isolation and CAR T cell transduction

Pheripheral blood was donated by healthy human donors and processed using density gradient centrifugation with the Biocoll separating solution to isolate peripheral blood mononuclear cells (PBMC). The human Pan T Cell Isolation Kit (Miltenyi Biotec) was used in order to obtain untouched human T cells from PBMC. Isolation quality was assessed by flow cytometry assessment of $CD4^+$ and $CD8^+$ cells. Isolated human T cells were cultured and stimulated for 48 h in human T cell media using 8.25 µl of human anti-CD3-anti-CD28 dynabeads per 1 x 10^6 cells. Viral transduction and CAR T cell expansion were then performed following previously described protocols (Karches et al., 2019).

2.2.9 Migration assay

T110299_$EpCAM^+$ Tumor cells were plated and transfected on the next day with Lipofectamine™ RNAiMAX complexed 3p-RNA (160 nM) or OH-RNA (160 nM). Transfected tumor cells were further cultured in migration media (no phenol red RPMI supplemented with 1% BSA) and 24 h later the supernatant with secreted chemokines was collected and purified from cellular debris by centrifugation.

Primary murine T cells were retrovirally transduced to express individual chemokine receptor constructs and tagged with GFP to evaluate their migration

towards chemokines secreted by 3p-RNA transfected T110299_EpCAM tumor cells. Migration of T cells was assessed using trans-well plates with a 3 μm pore membrane as previously described (Rapp et al., 2016a). Briefly, 5 x 10^5 transduced T cells were platted in the upper chamber of the plate while the lower chamber contained supernatant from 3p-RNA or OH-RNA transfected T110299_EpCAM tumor cells. After 4 hours of incubation at 37°C the cells that migrated to the lower chamber were counted and analyzed using flow cytometry.

2.2.10 T cell proliferation assays

T cell proliferation was assessed either by staining with 2.5 μM CFSE or by culturing the T cells for 24 h in the presence of 10 μM Click-iT® EdU and subsequently stained and fixed following the manufacturer´s protocol.

2.2.11 T cell cytotoxicity assays

2.2.11.1 xCELLigence assay

The xCELLigence system was used to monitor tumor cell adhesion as an indicator of viability. Tumor cells were transfected with Lipofectamine™ RNAiMAX complexed 3p-RNA or controls and 2.5 x 10^4 cells per well were plated in a 96-well plate. The cell index was monitored every 20 min and upon reaching a value of 1, transduced T cells were added to the cultures at different effector to target ratios (10:1, 5:1 and 2.5:1). Impedance values were further quantified for 48 h.

2.2.11.2 Cell Titer Blue viability assay

The viability of tumor cells seeded and treated in transparent 96 well plates was assessed using the Cell Titer Blue (CTB) reagent from Promega. Each well received 20% of the culture volume CTB reagent. After 2-3 hours of incubation at 37ºC the fluorescence signal was measured using a luminometer adjusted for

excitation at 560 nm and emission 590 nm. Calculations of cell viability were performed by subtracting the background signal given by the media and normalizing the obtained data to the signal of untreated tumor cells using GraphPad Prism software.

2.2.12 Flow cytometry

Staining of single cell suspensions was performed in FACS buffer. Dead cells were excluded by staining them with fixable viability violet dye (1:5000) for 15 min at RT. Cell surface proteins were generally stained for 30 min at 4 ºC with the exception of chemokine receptors which were stained at 37 ºC for 15 min.
Intracellular stains were performed using the BD Cytofix/Cytoperm™ Fixation/Permeabilization Solution Kit following the manufacturer's protocol. Absolute cell numbers were determined using Count Bright counting beads according to the manufacturer's protocol. Compensation was performed either with stained cells or UltraComp eBeads®. Fluorescence signal was acquired on BD FACSCanto II or BD LSRFortessa flow cytometers, and resulting data were analyzed with the FlowJo software version 10.3.

2.2.13 Statistical analysis

Data are generally shown as the mean with either standard deviation (SD) or standard error of the mean (SEM) as specified in the figure legends. Data for individual mice are mostly summarized using the mean with SEM. Differences between two groups were generally assessed for statistical significance using the nonparametric Mann Whitney U test. For comparisons across multiple groups, two-way ANOVA with the Bonferroni correction (multiple time-points) or one-way ANOVA with the Tukey posthoc (single time-points) were conducted. All statistical testing was carried out with GraphPad Prism 8 software and P values < 0.05 were considered to be significant. Significance levels are indicated as *, **, *** for <0.05, <0.01 and <0.001 respectively.

3 Results

3.1 Generation of a preclinical PDAC model for assessment of 3p-RNA and CAR T cell combination therapy

Pre-clinical models are of great importance for studying therapeutic efficacy and safety before trials in humans. Ideally, results observed in pre-clinical models such as rodents, or non-human primates, would then be extrapolated to predict efficacy and safety in humans. Nevertheless, translation between studies with pre-clinical models and human clinical studies has a success rate of less than 8% (Mak et al., 2014). The many reasons behind this low success rate include discrepancies in biological processes between species (Brubaker & Lauffenburger, 2020) and failure to reproduce the many factors that contribute to the complexity of the diseases. Therefore, it is of great importance to use pre-clinical models that reproduce key characteristics observed in human disease.

In the case of PDAC, several murine models have been established harboring the main genetic alterations regularly identified in human PDAC patients. One example is the KPC murine model ($Ptf1a^{Cre+/-}$, $LSL\text{-}Kras^{G12D}$, $p53^{fl/R172H}$). These mice have been engineered using the Cre-Lox system to specifically introduce mutations in the *Kras* and *p53* genes in pancreatic cells. Consequently, the mice develop spontaneous, stroma-rich neoplasms, specifically in the pancreas, which exhibit many of the typical clinical, histopathological and TME features of human PDAC patients (Lee et al., 2016). The T110299 cell line used in the current study is derived from this murine model. It has been shown in previous work from our group that this cell line closely reflects histological features from the original murine primary tumor and also of human PDAC tumors (Adunka, 2014). As a second murine model for PDAC, we used Panc02 tumor cells. This cell line was generated by inducing mutations with the carcinogen 3-methylcholanthrene (3-MCA) in the pancreas of C57BL/6 wild-type mice. Finally, as a human model of PDAC we utilized the SUIT-2 cell line which is derived from a liver metastasis from a PDAC patient.

3.1.1 Engineering of EpCAM expressing T110299 tumor cells as a CAR T cell target

In recent years, CAR T cell therapy has displayed remarkable outcomes against several hematological malignancies. Nevertheless, their efficacy against solid tumors, such as PDAC, is still limited. Appropriate tumor models that exemplify the challenges opposing CAR T cell efficacy are of vital importance to understand and overcome therapeutic limitations.

For the purpose of studying the therapeutic effects of combining 3p-RNA treatment with CAR T cell therapy in PDAC, the murine KPC-derived T110299 tumor cell line was chosen, as this cell line embodies many key features observed in human PDAC, including immune TME composition, strong inflammatory reaction, and exclusion of effector T cells (Lee et al., 2016a).
The epithelial cell adhesion molecule (EpCAM) is highly overexpressed in many human epithelial cancers in different organs (Sankpal et al., 2021), with a high fraction of PDAC tumors being strongly positive (Went et al., 2004). It has been clinically tested as a target antigen for various targeted therapies and therefore was chosen in this study as target for CAR T cell therapy in our murine PDAC models.

Flow cytometric assessment of T110299 tumor cells shows that they do not endogenously express EpCAM in the cell membrane (Figure 6A). Therefore, they are not responsive to treatment with anti-EpCAM CAR T cells, evidenced in the unaltered cell viability of T110299 tumor cells cultured with EpCAM targeting CAR T cells (Figure 6B). Engineering of this cell line using retroviral vectors permitted the generation of T110299-EpCAM tumor cells, where the antigen is expressed in the membrane of the tumor cells at both a high and low level (Figure 6A). Induced EpCAM expression sensitized the tumor cells to CAR T cell mediated cytotoxicity in a dose-dependent manner (Figure 6C). Moreover, unaltered cell viability of T110299-EpCAM tumor cells, when co-cultured with mock transduced T cells, confirmed that the observed cytotoxicity was entirely antigen dependent

(Figure 6D). These results corroborate that the engineered T110299-EpCAM tumor cell line is a suitable model to study antigen-specific CAR T cell cytotoxicity.

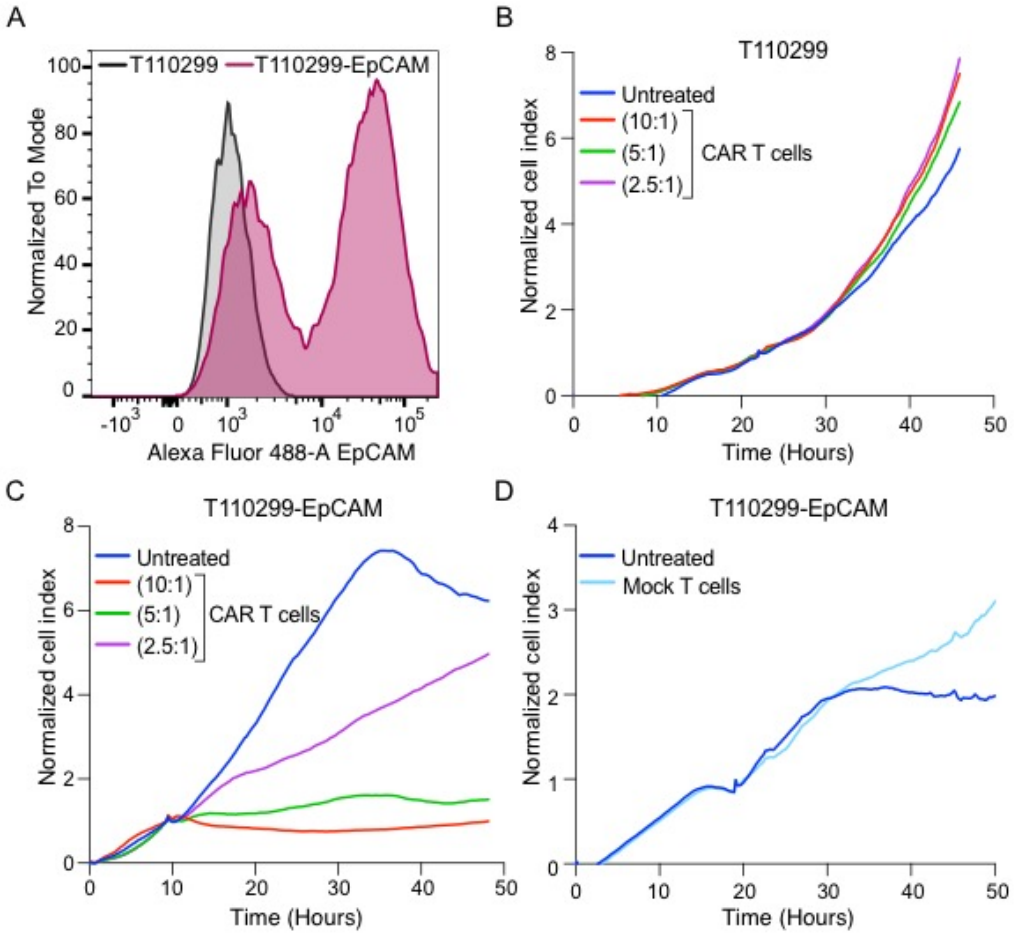

Figure 6. Generation of T110299-EpCAM tumor cells and validation of antigen-specific CAR T cell cytotoxicity.

A) Histogram representation of EpCAM expression on T110299 tumor cells (black curve) compared to engineered T110299-EpCAM tumor cells (purple curve). Impedance-based cytotoxicity assays (xCELLigence) showing real-time quantification of **B)** T110299 and **C)** T110299-EpCAM tumor cell lysis upon co-culture with anti-EpCAM CAR T cells in three different effector to target (E:T) ratios (10:1, 5:1 and 2.5:1). **D)** T110299-EpCAM tumor cell lysis upon co-culture with mock transduced T cells in a 5:1 E:T ratio. Graphs show one representative experiment out of three independent repeats.

3.1.2 Validation of 3p-RNA effects on T110299-EpCAM tumor model

Further characterization of the T110299-EpCAM model demonstrated that 3p-RNA transfection of the tumor cells induced strong secretion of type I IFN, evaluated in the form of IFN-β presence in the culture supernatant, when compared to cells transfected with RIG-I non-activating OH-RNA control (Figure 7A). Moreover, an increase in the membrane expression of MHC-I was detected in cells transfected with 3p-RNA (Figure 7B) Together, these results indicate an intact IFNAR signaling pathway as both molecules are induced by IFN signaling. Furthermore, real-time quantification of tumor cell adhesion indicated that 3p-RNA transfection affects tumor cell growth *in vitro* (Figure 7C) but does not influence membrane expression of EpCAM (Figure 7D). These results confirm that the engineered T110299-EpCAM tumor cells respond to cytosolic RNA sensing without influencing the expression of the CAR T cell targeted antigen, making this cell line a suitable model for evaluating the effects of combining 3p-RNA therapy with CAR T cells.

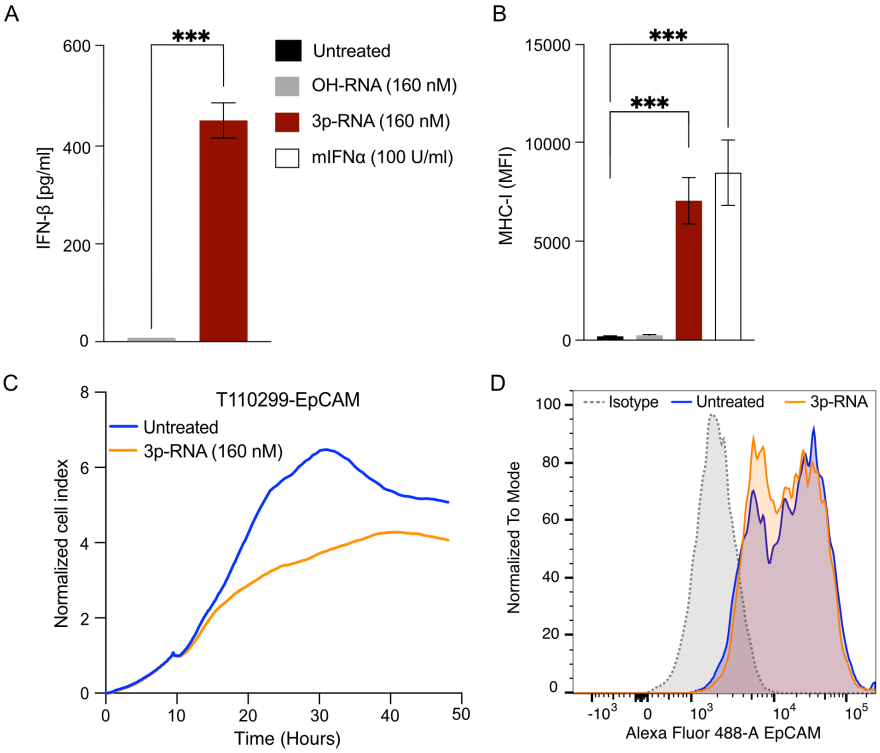

Figure 7. Effects of 3p-RNA transfection on T110299-EpCAM tumor cells.

A) Detection of murine IFN-β in the supernatant of untreated or treated T110299-EpCAM tumor cells by ELISA 24 hours after transfection with either 3p-RNA or OH-RNA transfection control. Assessment of surface expression of **B)** MHC-I on live T110299-EpCAM tumor cells 24 hours after transfection with either 3p-RNA, OH-RNA, or exposure to 100 U/ml of murine IFN-α. **C)** Impedance-based quantification of T110299-EpCAM tumor cell lysis upon transfection with 3p-RNA. **D)** Histogram representation of EpCAM expression on T110299-EpCAM tumor cells untransfected (blue) compared to those transfected with 3p-RNA (yellow) and isotype control (dotted gray line). Graphs are representative of two to three independent repeats, error bars indicate mean values ± SD of technical replicates for the shown experiment. Statistical analysis was calculated using unpaired t-test for A) and ordinary one-way ANOVA with Dunnett's multiple comparison test for B).

3.2 Combination of 3p-RNA with CAR T cells shows improved anti-tumoral effect in murine pancreatic cancer models

To evaluate the potential therapeutic advantage of combining 3p-RNA treatment with CAR T cell therapy, the T110200-EpCAM tumor model was used in two different settings. First, assessment of local 3p-RNA delivery was performed on subcutaneous T110299-EpCAM tumors induced in the right flank of female C57Bl/6 mice. One week after tumor induction, the mice received one intra-tumoral injection of 3p-RNA or PBS control followed by a systemic injection of 1 x 10^7 retrovirally-transduced, syngeneic murine T cells expressing anti-EpCAM CAR. Intra-tumoral treatment with 3p-RNA or PBS control was repeated 3 days later, and changes in tumor size were assessed every second day until termination criteria were met (Figure 8A). Intra-tumoral injections of PBS control alone or in combination with anti-EpCAM CAR T cell monotherapy had no significant effect on tumor growth. However, intra-tumoral injections of 3p-RNA showed a significant decrease in tumor size when compared to CAR T cell monotherapy (Figure 8B), and the combination of intra-tumoral 3p-RNA with CAR T cells further induced complete tumor regression in 60% (3/5) of the mice (Figure 8C).

Second, evaluation of the therapeutic effects of systemic delivery of both 3p-RNA and CAR T cells was performed in female C57BL/6 mice bearing orthotopically induced T110299-EpCAM tumors in the pancreas. Mice were injected with 3p-RNA or PBS control followed by i.v. injection of 1 x 10^7 syngeneic anti-EpCAM CAR T cells six hours later. Systemic 3p-RNA treatment was repeated three days later (Figure 8D). High levels of murine IFN-β were detected in the serum of mice that received 3p-RNA treatment (Figure 8E). Both 3p-RNA and CAR T cell monotherapy had no effect on survival compared to PBS-treated controls, whereas the combination of 3p-RNA with CAR T cell therapy showed a therapeutic benefit by prolonging survival (Figure 8F). These results indicate the superiority of the combination treatment over monotherapy in terms of enhanced tumor control and extended survival in PDAC tumor models with both local and systemic administration of 3p-RNA.

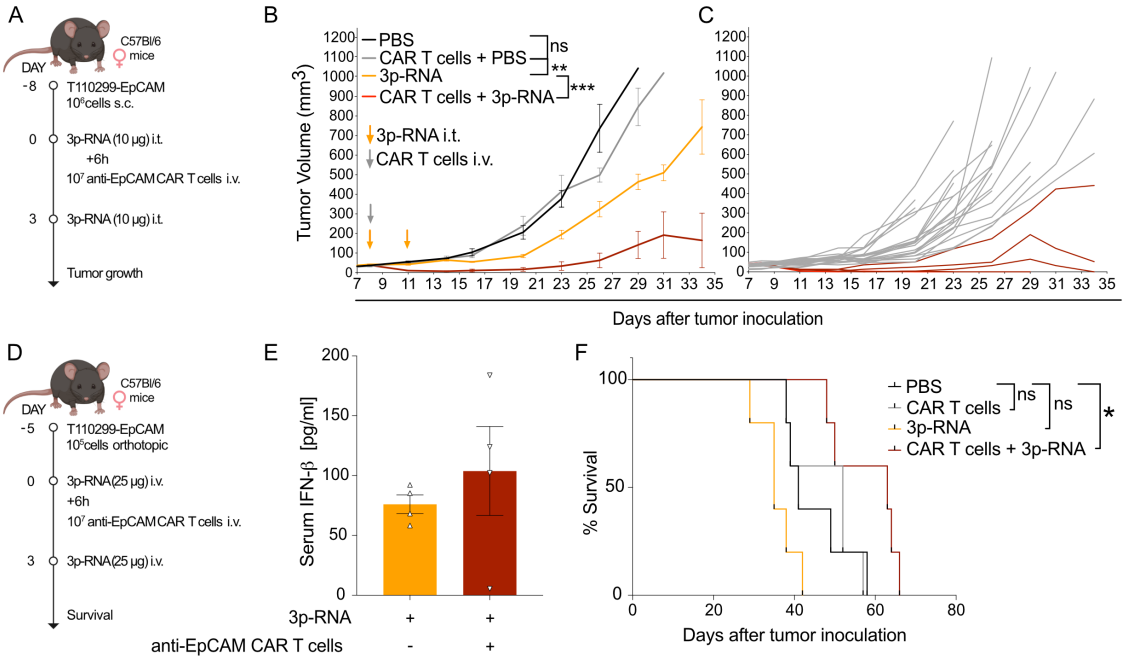

Figure 8. Combination of 3p-RNA with CAR T cells promotes tumor control and survival in s.c. and orthotopic murine T110299-EpCAM tumor models.

A) Experimental timeline of s.c. T110299-EpCAM tumor challenge experiments. **B)** Growth curves of T110299-EpCAM tumors in mice treated with 10 *µ*g of *in vivo*-JetPEI-complexed 3p-RNA and/or 1 x 10^7 anti-EpCAM CAR T cells as indicated (n = min. 5 mice/ group). **C)** Spaghetti plot depicting all individual mice, with those receiving either monotherapy in gray and those receiving the combination treatment in red. **D)** Experimental layout of orthotopic T110299-EpCAM tumor induction experiments. **E)** Serum IFN-β levels 24 hours after systemic treatment with *in vivo*-JetPEI complexed 3p-RNA (25 *µ*g) **F)** Survival curves of orthotopic T110299-EpCAM tumor challenge experiments. Mice were treated systemically with 25 *µ*g of *in vivo*-JetPEI complexed 3p-RNA and/or 10^7 anti-EpCAM CAR T cells as indicated (n = min. 4-5 mice/ group). Error bars indicate mean values ± SEM. Differences between groups in B) were assessed using two-way ANOVA with correction for multiple testing by the Bonferroni method. Comparison of survival curves in F) was done with the Logrank (Mantel-Cox) test.

3.3 3p-RNA treatment reshapes the myeloid compartment of PDAC tumors

The immunosuppressive TME poses an important challenge for CAR T cell therapy in solid tumors (Marofi et al., 2021). In a previous study, it was shown that activation of RLR can reshape the myeloid compartment in the TME, thereby reducing immunosuppression in a type I IFN-dependent manner (Metzger et al., 2019). To evaluate if the combination of 3p-RNA and CAR T cells induced changes in the cellular composition of the TME, we analyzed the myeloid cell infiltrate after three days of treatment (Figure 9A).

CAR T cell monotherapy had no effect on the frequency of live PMN-MDSC, TAM, monocytes or DC found in the tumor when compared to untreated tumor bearing mice (data not shown). Meanwhile, the addition of 3p-RNA treatment together with CAR T cell therapy prompted a significant reduction in the relative frequency of PMN-MDSC and TAM. Additionally, an increase in the presence of monocytes was observed in the tumor of the mice that received the combination therapy (Fig 9B). Despite an unaltered composition in the DC populations, 3p-RNA in combination with CAR T cell therapy stimulated an increase in the expression of MHC-I in DC suggesting an increase in activation and antigen-presentation capabilities (Fig 9C). 3p-RNA treatment also upregulated PD-L1 expression on PMN-MDSC and DC populations in response to the combination therapy (Fig 9D), likely via type I IFN signalling. Altogether, the data show that 3p-RNA treatment reshapes the myeloid compartment of PDAC tumors into a more immune-permissive TME.

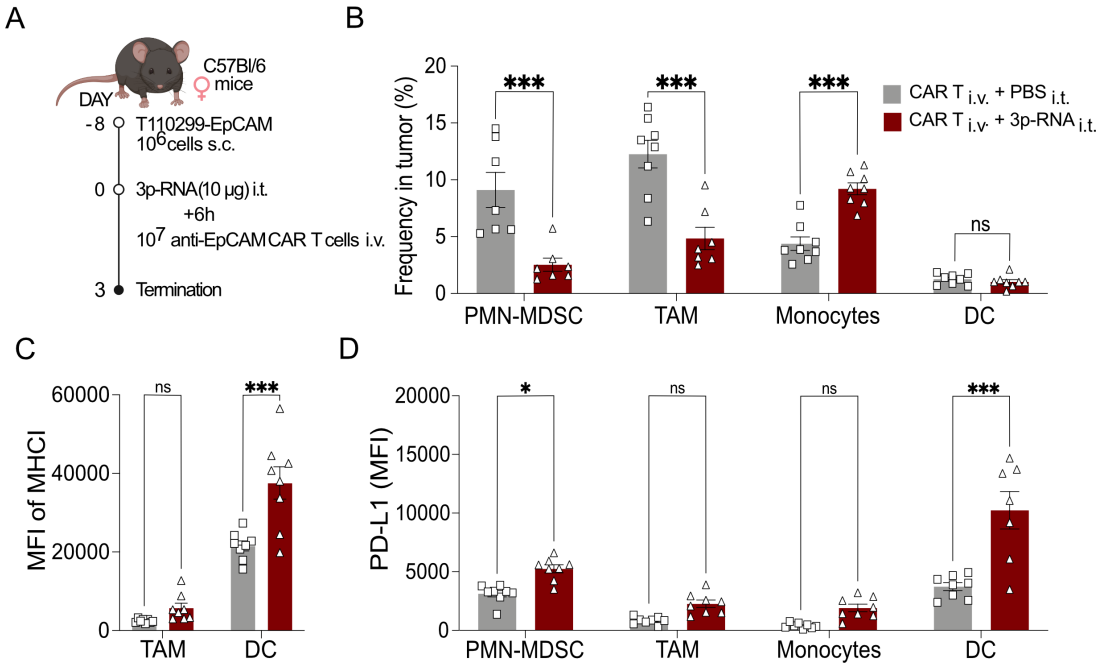

Figure 9. 3p-RNA reshapes the myeloid compartment in T110299-EpCAM PDAC tumors.

A) Experimental layout for evaluation of TME composition of T110299-EpCAM tumors after treatment. C57BL/6 tumor-bearing mice were treated with 10 µg of *in vivo*-JetPEI complexed 3p-RNA and/or 10^7 anti-EpCAM CAR T cells as indicated. Three days after treatment, the experiment was terminated, and tumors were resected and digested for flow cytometry analysis. Flow cytometry assessment of **B)** frequency of live $CD11b^+Ly6C^{int}Ly6G^+$ PMN-MDSC, $CD11b^+Ly6C^-F4/80^+$ Macrophages, $CD11b^+Ly6C^{high}Ly6G^-$ Monocytes and $CD11b^+CD11c^+MHC\text{-}II^+$ DC in the tumor. Gating strategy is depicted in Figure S1. **C)** MHC-I expression in live Macrophages and DC. **D)** PD-L1 expression in the different live myeloid cell types. Data is depicted as mean values ± SEM (n=8 mice per group). Statistical significance was calculated using ordinary two-way ANOVA with Turkey's multiple comparison test, ns: non-significant.

3.4 3p-RNA treatment augments T cell trafficking into the TME

3.4.1 3p-RNA treatment increases both CAR T cell and endogenous T cell infiltration into PDAC tumors

Hampered trafficking and infiltration into solid tumors is another widely described limitation for CAR T cell therapy (Lim & June, 2017). Therefore, increased CAR T cell infiltration in response to 3p-RNA treatment could contribute to the observed therapeutic effect *in vivo*. To evaluate this hypothesis the number of viable CAR T cells was assessed in the tumors three days after ACT using an mCherry reporter which was co-expressed in the CAR T cells. 3p-RNA pre-treatment induced an increased infiltration of $CD8^+$, but not $CD4^+$, CAR T cells (Figure 10A). Similar effects were revealed for mCherry-negative endogenous T cell populations, were 3p-RNA treatment had no effects on the numbers of $CD4^+$ T cells present in the tumor, while the number of $CD8^+$ T cells was increased ($p= 0.028$) (Figure 10B). Taken together, this data suggest that 3p-RNA treatment triggers increased infiltration of both $CD8^+$ CAR T and endogenous $CD8^+$ T cells into PDAC tumors.

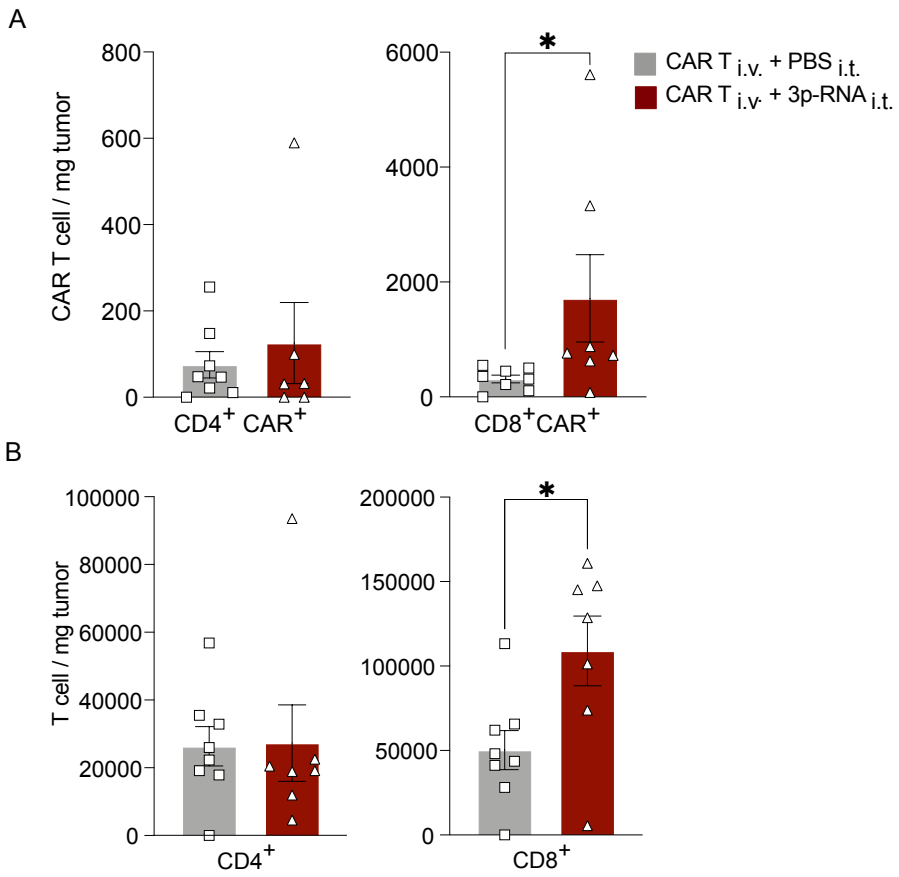

Figure 10. 3p-RNA therapy increases both CAR T cell as well as endogenous T cell infiltration into PDAC tumors

A) Flow cytometry tracking of live CD45⁺ CD4⁺ or CD8⁺ CAR T cells co-expressing mCherry-reporter protein and **B)** CD4⁺ or CD8⁺ mCherry-negative endogenous T cells. Cell counts are calculated using counting beads and further normalized to the weight of the tumor. Error bars depict mean values ± SEM of (n = 8 mice) and statistical analysis was calculated with Mann-Whitney test. Flow cytometric gating strategies are shown in Figure S2.

3.4.2 Chemokine release in response to 3p-RNA treatment drives CAR T cell migration

Chemokines play a crucial role in the migration of hematopoietic cells (Foeng et al., 2022). qPCR expression profiling in T110299-EpCAM tumor cells transfected with 3p-RNA or OH-RNA control indicated high expression levels of a variety of chemokines. We hypothesized that the observed chemokine profile potentially explains the increased infiltration of T cells into the tumor observed in PDAC-bearing mice, treated with combination therapy. Increased expression levels of Ccl2, Ccl4, Ccl5, Ccl7, Cxcl2, Cxcl9, Cxcl10 and Cxcl11 were observed in transfected tumor cells (Figure 11A).

In order to evaluate which chemokine receptors could be associated with the increased CAR T cell trafficking and infiltration *in vivo,* primary murine T cells were retrovirally transduced to express each individual chemokine receptor while co-expressing a GFP reporter. Flow cytometric identification of the GFP signal enabled the assessment of genetic engineering efficiency as well as the behavior of the transduced T cells in a Boyden chamber migration assay. The supernatant of 3p-RNA or control transfected tumor cells, containing the secreted chemokines, was used to attract chemokine receptor-transduced T cells to determine their migration preference (Figure 11B). Significant enrichment of GFP positive T cells was observed for those transduced to express CCR5 ($p=0.004$) or CXCR3 ($p=0.001$) (Figure 11C). Interestingly, CCL2 and CCL5 as well as CXCL9-11 (which were upregulated by 3p-RNA transfected tumor cells) are described ligands for CCR5 and CXCR3, respectively (Hughes & Nibbs, 2018). Moreover, membrane expression of CCR5 (Figure 11D) or CXCR3 (Figure 11E) was confirmed on the CAR T cells used for ACT at the timepoint of treatment. Together, this data suggests that 3p-RNA transfection of T110299-EpCAM tumor cells induces the expression of a variety of chemokines that attract CAR T cells via their cognate receptors CXCR3 and CCR5.

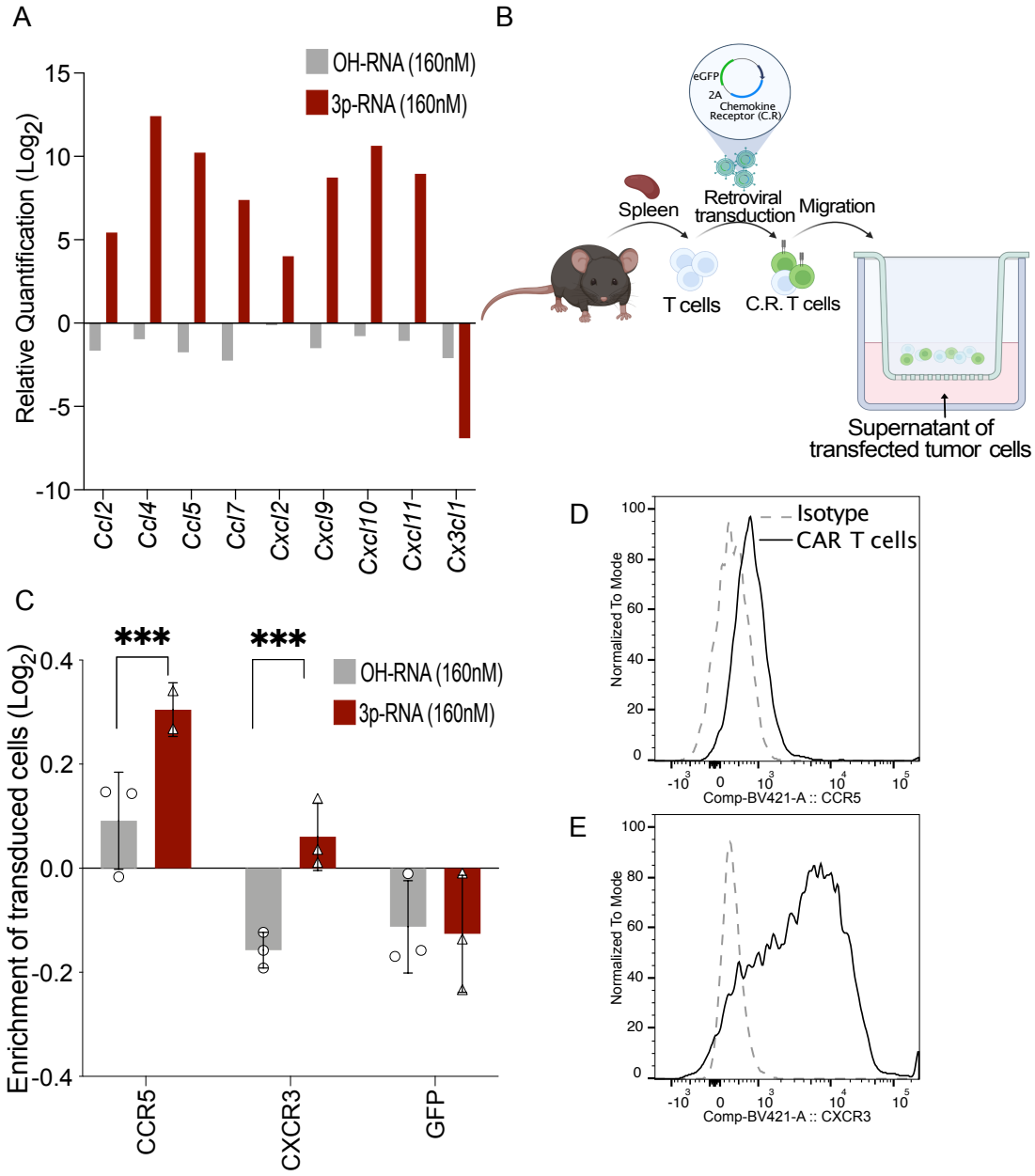

Figure 11. T110299-EpCAM tumor cells transfected with 3p-RNA express a wide range of chemokines that attract T cells.

A) qPCR of chemokines induced by 3p-RNA in T110299-EpCAM tumor cells. RNA was isolated 24 hours after transfection with either 3p-RNA or OH-RNA transfection control. Expression levels relative to β-actin are shown. **B)** Schematic representation for the generation of primary T cells retrovirally transduced to co-express individual chemokine receptors and eGFP. The migration of chemokine receptor transduced T cells towards supernatant from T110299-EpCAM tumor cells transfected with 3p-RNA or OH-RNA was assessed through a Boyden chamber migration assay. **C)** Log_2 enrichment between the percentage of GFP positive T cells in the lower well compartment containing the tumor supernatant versus the percentage of originally plated transduced T cells. **D)** CCR5 and **E)** CXCR3 expression on EpCAM CAR-transduced T cells (black) at the timepoint of ACT. Error bars indicate mean values ± SD of three independent experiments Mann-Whitney test was performed for statistical analysis.

3.5 3p-RNA treatment increases CAR T cell proliferation, persistence, and functionality

3.5.1 3p-RNA treatment of tumor cells has a positive bystander effect on the proliferation and persistence of CAR T cells

Poor T cell expansion and lack of persistence are known limiting factors for CAR T cell therapy in solid tumors. Even in hematological malignancies, where the TME does not play a critical role, initially responsive patients risk relapse, due partly to these two aspects (Pietrobon et al., 2021b). To investigate the influence of 3p-RNA therapy and the consequent secretion of type I IFN and chemokines on CAR T cell proliferation, 3p-RNA treated tumor cells were cultured together with CAR T cells overnight in the presence of 5-Ethynyl-2′-deoxyuridine (EdU) thymidine analogue to measure proliferation. Analysis of the CAR T cells by flow cytometry indicated an increase in the level of EdU incorporated into the cells which were co-cultured with 3p-RNA transfected tumor cells ($p= 0.006$) when compared with untreated or control transfected tumor cells ($p= 0.02$). This increase of EdU incorporation was not recapitulated by the sole presence of murine IFN-α in the culture (Figure 12A). Of note, an increased incorporation of EdU was also observed in untransduced T cells (CAR^-), in the co-cultures with 3p-RNA transfected tumor cells ($p= 0.06$) (Figure 12B). Similar results were observed when culturing CAR T cells with a second PDAC tumor model i.e., Panc02-OVA-EpCAM (Figure S3). These results suggest that factors induced and/or secreted by the transfection of tumor cells with 3p-RNA can, potentiate CAR T cell proliferation, as indicated by an increase in DNA synthesis.

In line with these results, flow cytometric analysis of $CD8^+$ $mCherry^+$ CAR T cells in the blood of T110299-EpCAM tumor bearing mice indicated that only one out of six mice treated with CAR T cell monotherapy had detectable numbers of circulating CAR T cells at day 9 after treatment. In contrast, six out of eight mice that received 3p-RNA in combination with ACT had measurable CAR T cells in circulation at the same timepoint, and the overall number of detected CAR T cells detected per mL of blood was higher in the mice that received the combination

therapy (p= 0.04) (Figure 12C). Similar trends were observed at a later timepoint (Figure 12D) where none of the mice from the CAR T cell monotherapy group had detectable numbers of CAR T cells in the blood, while almost 50% of the mice in the combination therapy group still had CAR T cells circulating in blood. Taken together, these findings suggest that 3p-RNA treatment has a positive bystander effect on the persistence and proliferation of CAR T cells.

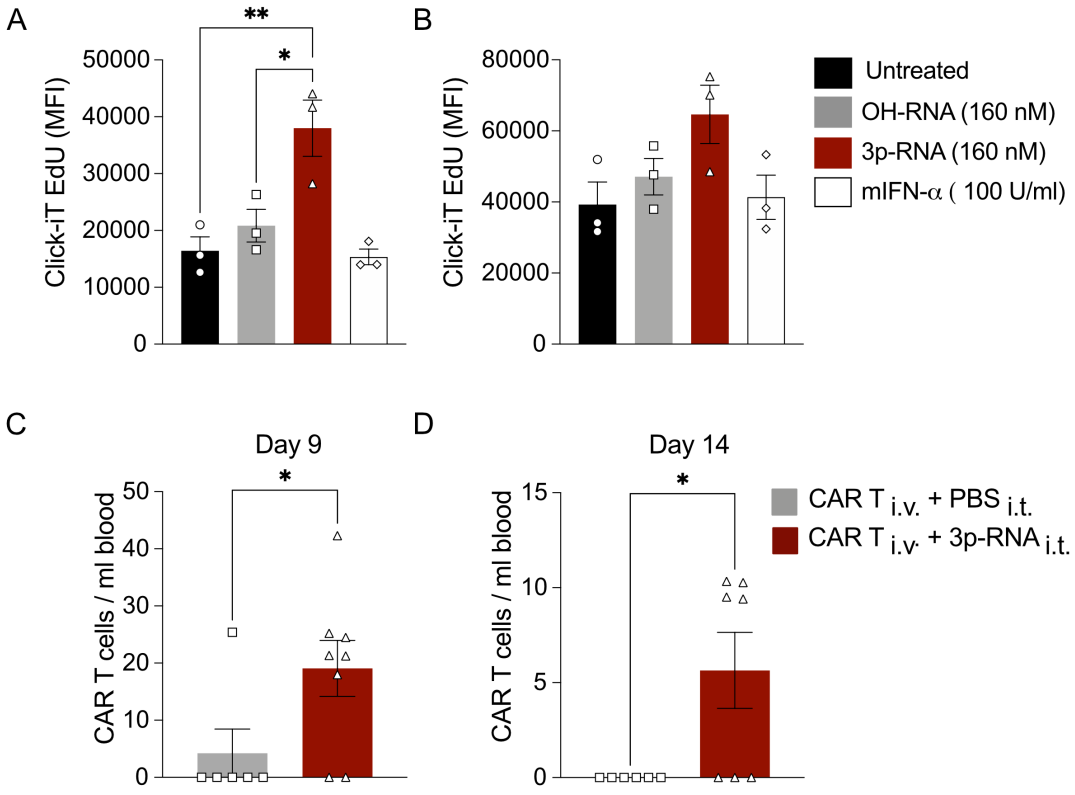

Figure 12. 3p-RNA therapy increases CAR T cell proliferation and prolongs their persistence in blood.

A) Proliferation assessment through incorporation of EdU thymidine analogue by $CD8^+$ CAR T cells co-expressing mCherry and **B)** CD8+ mCherry- untransduced T cells upon 18 hours co-culture with T110299-EpCAM tumor cells transfected with 3p-RNA or controls as indicated. Graphs show mean values ± SEM of three biological replicates and are representative of three independent experiments. Statistical analysis is based on ordinary one-way ANOVA with correction for multiple comparisons using Tukey test. **C)** Flow cytometry tracking of live $CD45^+$ $CD8^+$ CAR T cells co-expressing mCherry in the blood of mice after nine days and **D)** 14 days of treatment with 10 *µg in vivo*-JetPEI complexed 3p-RNA and/or 10^7 anti-EpCAM CAR T cells. Cell counts are calculated using counting beads and normalized to ml of blood. Error bars indicate mean values ± SEM of (n = 8 mice) and statistical analysis was performed using unpaired t-test.

3.5.2 3p-RNA therapy increases CAR T cell activation and cytotoxicity

Increase of $CD8^+$ T cell activation and cytotoxicity have been reported in response to type I IFN stimulation (Medrano et al., 2017). Consequently, we used flow cytometry to look at the expression of activation markers of CAR T cells cultured together with 3p-RNA treated tumor cells. CAR T cells cultured with tumor cells in the presence of IFN-α or transfected with 3p-RNA had a significantly higher percentage of CD69 expression (p= 0.001) (Figure 13A). This increase in the percentage of CD69-expressing cells was also observed in untransduced T cells in the presence of IFN-α (Figure S4). Interestingly, no changes in the expression patterns of PD1 (Figure 13B), TIM3 (Figure 13C) and LAG3 (Figure 13D) were detected at the time-point measured.

In line with increased CD69 expression, CAR T cells co-cultured with 3p-RNA treated tumor cells secreted significantly higher levels of IFNγ (p= 0.03) compared to those cultured with untreated tumor cells (Figure 13E). Likewise, supernatant levels of granzyme B assessed by ELISA indicated higher concentrations present in the co-cultures of CAR T cells with 3p-RNA treated tumor cells (p= 0.0001) when compared to cultures with untreated tumor cells. Here, the presence of IFN-α was sufficient to recapitulate this increase (p= 0.0003) (Figure 13F). Interestingly an opposite tendency was observed for IL-2; CAR T cells co-cultured with 3p-RNA treated tumor cells secreted lower levels of IL-2 when compared to cultures with untreated tumor cells (p= 0.002) and this observation was not IFN-α dependent (Figure 13G).

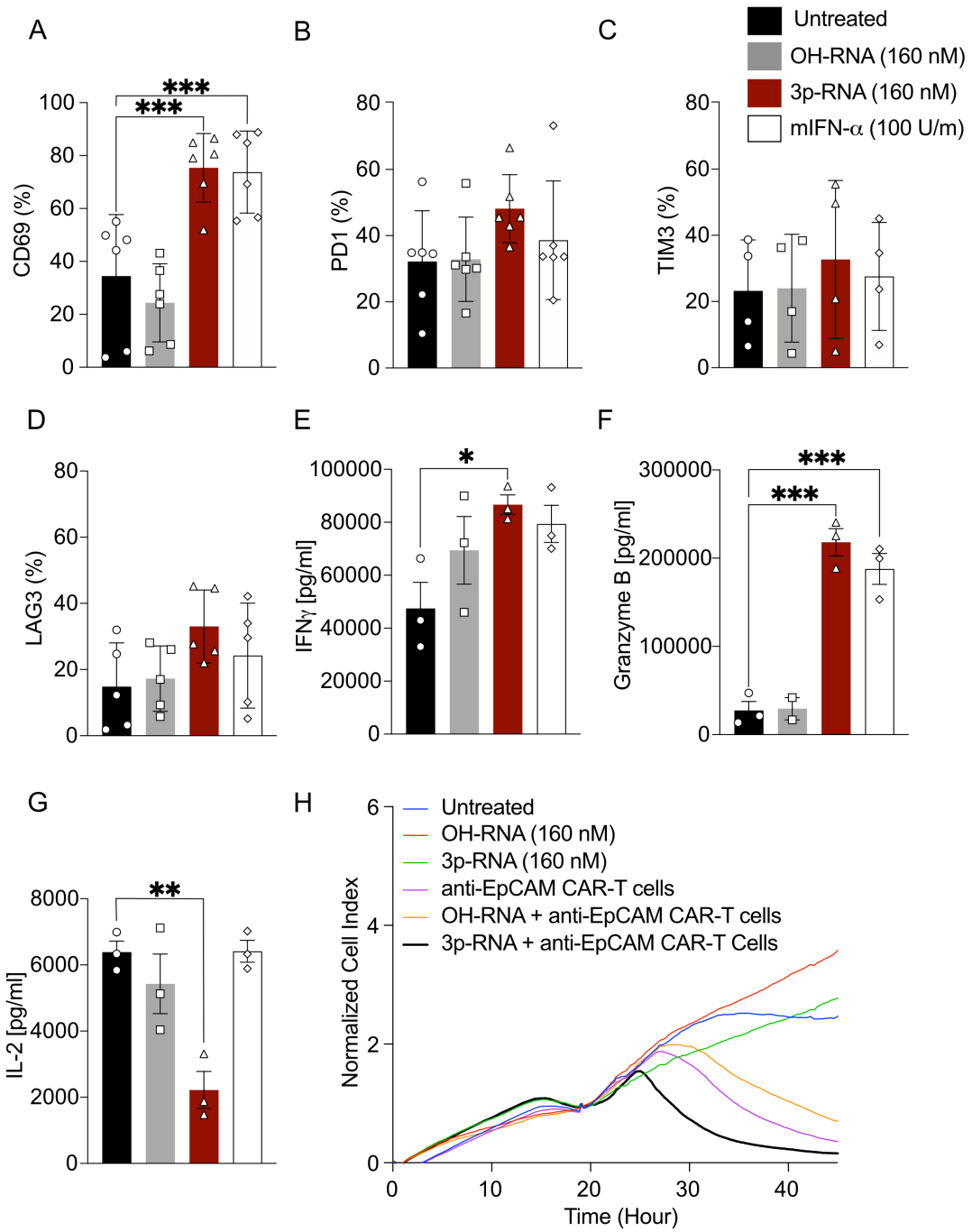

Figure 13. 3p-RNA therapy increases CAR T cell activation and cytotoxicity.

Percentage of **A)** CD69 **B)** PD1 **C)** TIM3 and **D)** LAG3 expressing anti-EpCAM CAR T cells cultured for 24 hours together with T110299-EpCAM tumor cells transfected with 3p-RNA or controls. Graphs show mean values ± SD of five independent experiments. Statistical analysis was performed using ordinary one-way ANOVA with correction for multiple comparisons using Tukey test. **E)** ELISA detection of IFNγ **F)** granzyme B and **G)** IL-2, in the supernatant of the co-cultures. Error bars indicate mean values ± SEM of three biological replicates **H)** xCELLigence real-time quantification of T110299-EpCAM tumor cell lysis upon co-culture with anti-EpCAM CAR T cells in a 10:1 E:T ratio, depending on tumor cell transfection with OH-RNA or 3p-RNA. Graph is representative of three independent experiments.

Further analysis of the cytotoxic capacity of the CAR T cells when combined with 3p-RNA treatment was performed by assessing real-time quantification of tumor cell lysis in an xCELLigence assay (Figure 13H). As observed previously, the moderate decrease in the cell index curve of tumor cells transfected with 3p-RNA (green curve) confirmed its influence on delaying tumor cell growth when compared to OH-RNA transfected cells (red curve) or untreated controls (blue curve). Anti-EpCAM-mediated killing by the CAR T cells alone induced almost complete cell lysis within 48 h of co-culture (purple curve). However, the combination of 3p-RNA transfection of tumor cells with CAR T cell killing showed a drastic acceleration in the killing kinetics (black curve). Similar activation and cytotoxicity results were observed when culturing CAR T cells with Panc02-OVA-EpCAM cells (Figure S5). Overall, these results indicate that 3p-RNA transfection of tumor cells induces an increase in early activation levels of the CAR T cells and promotes higher secretion of IFNγ and granzyme B ultimately leading to faster tumor cell killing.

3.6 Combining 3p-RNA with CAR T cell therapy induces an immunogenic form of cell death

3.6.1 3p-RNA therapy enhances calreticulin exposure and HMGB1 release in CAR T cell mediated killing

An additional factor contributing to the risk of relapse in initially responsive CAR T cell treated patients is the decrease in or loss of target antigen expression (Majzner & Mackall, 2018). Immunogenic cell death of cancer cells and the consequent antigen spreading assists the immune system in mounting an efficient immune response against other cancer-associated antigens, thereby preventing relapse. Cell death induction mediated by 3p-RNA has been previously described to induce an immunogenic form of cell death (Duewell et al., 2014).

Cell death induction by 3p-RNA, CAR T cell monotherapy or the combination therapy was validated through a cell titer blue assay. Within 24 h, a roughly 20% reduction in viability of T110299-EpCAM tumor cells in response to 3p-RNA and CAR T cell monotherapy was observed, while the combination induced 40% cell death (Figure 14A). Assays with Panc02-OVA-EpCAM showed 80% and 40% reductions in viability for 3p-RNA and CAR T cell monotherapy respectively, while the combination induced approximately 80% of cell death (Figure 14D).

Cell surface exposure of calreticulin on the tumor cells and HMGB1 release are two hallmarks of immunogenic cell death. Therefore, these were measured in order to assess the immunogenicity of the cell death induced by the combination of CAR T cells with 3p-RNA treatment in the T110299-EpCAM and Panc02-OVA-EpCAM PDAC models.

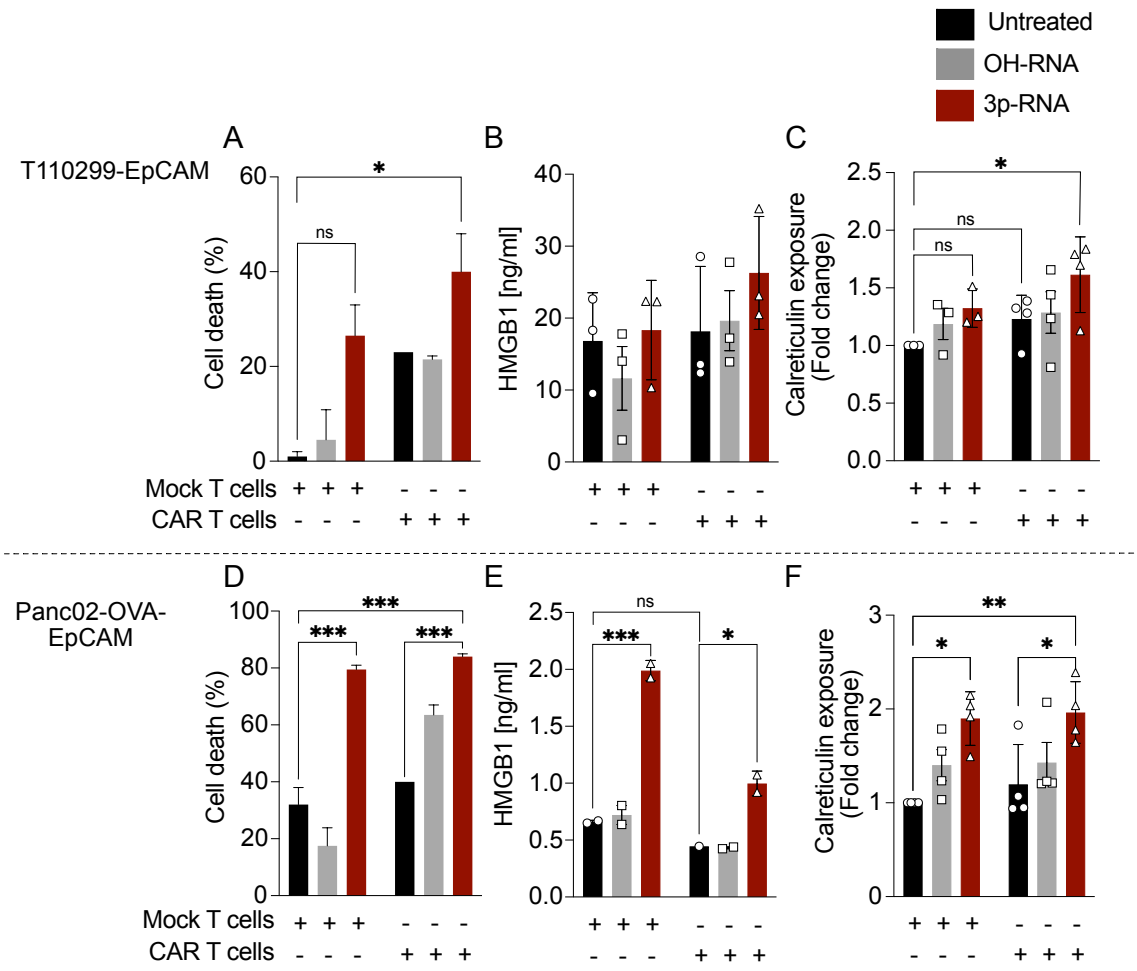

Figure 14. 3p-RNA therapy enhances CAR T cell cytotoxicity while augmenting calreticulin exposure and release of DAMP.

Viability of **A)** T110299-EpCAM and **D)** Panc02-OVA-EpCAM tumor cells either untreated (black) or transfected with OH-RNA (gray) or 3p-RNA (red) and co-cultured for 24 hours with mock transduced T cells or anti-EpCAM CAR T cells. Error bars represent mean values ± SD of two technical replicates and are representative of three independent experiments. ELISA detection of HMGB1 in the supernatant of **B)** T110299-EpCAM and **E)** Panc02-OVA-EpCAM tumor cells either untreated or transfected and co-cultured for 24 hours with mock transduced T cells or anti-EpCAM CAR T cells. Flow cytometry assessment of calreticulin exposure on live (FVD^-) **C)** T110299-EpCAM and **F)** Panc02-OVA-EpCAM tumor cells after transfection and/or co-culture with mock transduced or anti-EpCAM transduced CAR T cells for 24 hours. Bar charts represent mean values ± SEM of three to four independent experiments normalized to the values obtained for the co-culture of untreated tumor cells with mock transduced T cells. Differences between groups were calculated using ordinary two-way ANOVA with Dunnett's multiple comparison test.

HMGB1 release by T110299-EpCAM tumor cells in response to 3p-RNA and CAR T cell monotherapy did not differ when compared to untreated tumor cells co-cultured with mock-transduced T cells. Nevertheless, higher levels of HMGB1 were detected when tumor cells were treated with 3p-RNA without T cells in the culture (data not shown). Moreover, the combination of 3p-RNA and CAR T cells slightly increased the concentration of HMGB1 detectable in the culture media, but this was not statistically significant (p= 0.6) (Figure 14B). On the other hand, the same setup with Panc02-OVA-EpCAM tumor cells showed a drastic increase of HMGB1 release when the tumor cells were treated with 3p-RNA in the presence of mock-transduced T cells (p= 0.001) when compared to untreated cells. Interestingly, CAR T cell monotherapy did not induce an increase of HMGB1 release compared to untreated tumor cells but combining 3p-RNA with CAR T cells potentiated HMGB1 release (p= 0.018) (Figure 14E).

Assessment of calreticulin exposure on the tumor cell membrane indicated that 3p-RNA or CAR T cell monotherapy did not induce a difference compared to untreated T110299-EpCAM tumor cells. However, the combination of 3p-RNA and CAR T cells increased the amount of calreticulin exposed in the surface of the tumor cells (p= 0.02) (Figure 14C). Moreover, in line with the HMGB1 release data, 3p-RNA treatment of Panc02-OVA-EpCAM tumor cells induced higher calreticulin exposure compared to untreated tumor cells (p= 0.01), while CAR T cell monotherapy did not result in a strong difference at the timepoint analyzed. Interestingly, combining 3p-RNA with CAR T cells strongly increased calreticulin exposure compared to both CAR T cell monotherapy (p= 0.04) and untreated cells (p=0.007) (Figure 14F).

In summary, these data indicate that combining 3p-RNA with CAR T cells increases tumor cell death while simultaneously leading to the exposure and release of immunogenic cell death markers with the potential of inducing further anti-tumoral T cell activation via antigen spreading.

3.6.2 3p-RNA therapy enhances antigen uptake and activation of DC

The induction of an immunogenic form of cell death is important for the engagement of APC and the formation of *de novo* immune responses (Lin et al., 2021). To validate the potential of combining 3p-RNA with CAR T cells in increasing antigen uptake, presentation, and activation of APC, iCD103$^+$ BMDC were differentiated from BM of C57BL/6 mice. eFluro450 stained Panc02-OVA-EpCAM tumor cells were transfected with 3p-RNA or controls and then co-cultured with anti-EpCAM CAR T cells for 48 h. iCD103$^+$BMDC were then added to the culture and uptake of stained tumor antigen, presentation of OVA-derived peptide SIINFEKL on MHC-I as well as DC activation were assessed by flow cytometry.

3p-RNA-mediated tumor cell death significantly increased antigen uptake by iCD103$^+$ BMDC ($p= 0.0001$) while cell death induced by CAR T cell monotherapy had no effect. Interestingly, combining 3p-RNA with CAR T cells restored antigen uptake by iCD103$^+$ BMDC ($p=0.0001$) (Figure 15A). In line with these results, iCD103$^+$ BMDC activation measured by the expression levels of CD86 was increased by 3p-RNA treatment of the tumor cells as well as by CAR T cell monotherapy or combination therapy (Figure 15B). Detection of SIINFEKL peptide presented in MHC-I on iCD103$^+$ BMDC indicated a slight but not significant increase in the BMDC cultured with 3p-RNA-treated Panc02-OVA-EpCAM tumor cells compared to untreated tumor cells while no difference was evident in the CAR T cell monotherapy or combination therapy conditions (Figure 15C).

These data suggest that 3p-RNA-mediated cell death enhances both antigen uptake and activation of BMDC. Moreover, although CAR T cell mediated cytotoxicity induces BMDC activation, the amount of antigen uptake elicited is limited. Thus, combining 3p-RNA with CAR T cells not only enhances DC activation but also rescues antigen uptake by BMDC.

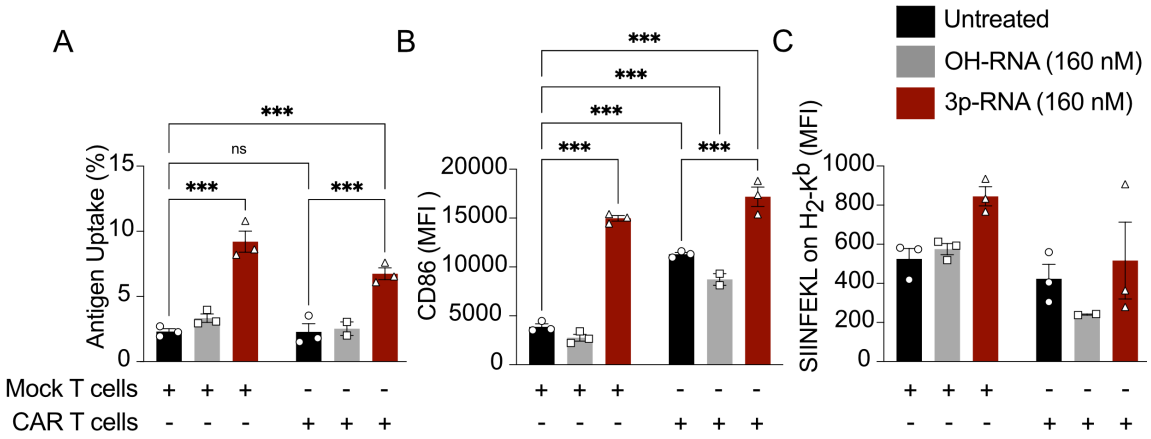

Figure 15. 3p-RNA treatment enhances antigen uptake and activation by BMDC.

A) Panc02-OVA-EpCAM were labelled with 5 μM efluor450 proliferation dye and either left untreated or were transfected with 3p-RNA or OH-RNA control. Mock transduced T cells or anti-EpCAM CAR T cells were added to the cultures for 24 hours. Immediately after, iCD103$^+$ BMDC were added to the cultures for six hours and antigen uptake by CD11b$^+$CD11c$^+$MHCII$^+$CD103$^+$XCR1$^+$ BMDC was analyzed with flow cytometry (efluor450 positivity). **B)** BMDC activation measured by CD86 expression and **C)** flow cytometric quantification of H-2Kb (MHC-I)-bound SIINFEKL peptide (OVA257–264) on iCD103$^+$BMDC after coculture with RNA-treated and/or CAR T cell co-cultured Panc02-OVA-EpCAM tumor cells. Statistical analysis of differences between groups was calculated with ordinary two-way ANOVA with Dunnett's multiple comparison test.

3.6.3 Combination of 3p-RNA with CAR T cells induces *in vivo* antigen spreading

The observed increase in antigen uptake and activation of DC in response to the combination therapy may translate into tumor antigen spreading and the formation of a *de novo* immune response against non-CAR tumor antigens *in vivo*. To address this hypothesis, immune competent mice were subcutaneously injected with T110299-EpCAM-OVA tumor cells, in which EpCAM represents the CAR target and OVA a non-CAR tumor antigen. Tumors were treated with 3p-RNA, anti-EpCAM CAR T cell monotherapy, or combination therapy. The mice were euthanized nine days after the initial therapy and cells isolated from the blood were stimulated using SIINFEKL peptide. IFNγ secretion in response to SIINFEKL stimulation was assessed through an ELISpot assay, to determine the presence of OVA-specific T cells (Figure 16A). Quantification of IFNγ spot forming units indicated a substantial increase in the number of SIINFEKL responsive cells

coming from the mice that received the combination therapy compared to CAR T cell monotherapy (p= 0.006) (Figure 16B). Together these results suggest that combining 3p-RNA with CAR T cells enhances *in vivo* antigen spreading leading to the induction of a *de novo* tumor antigen (OVA)-specific immune response.

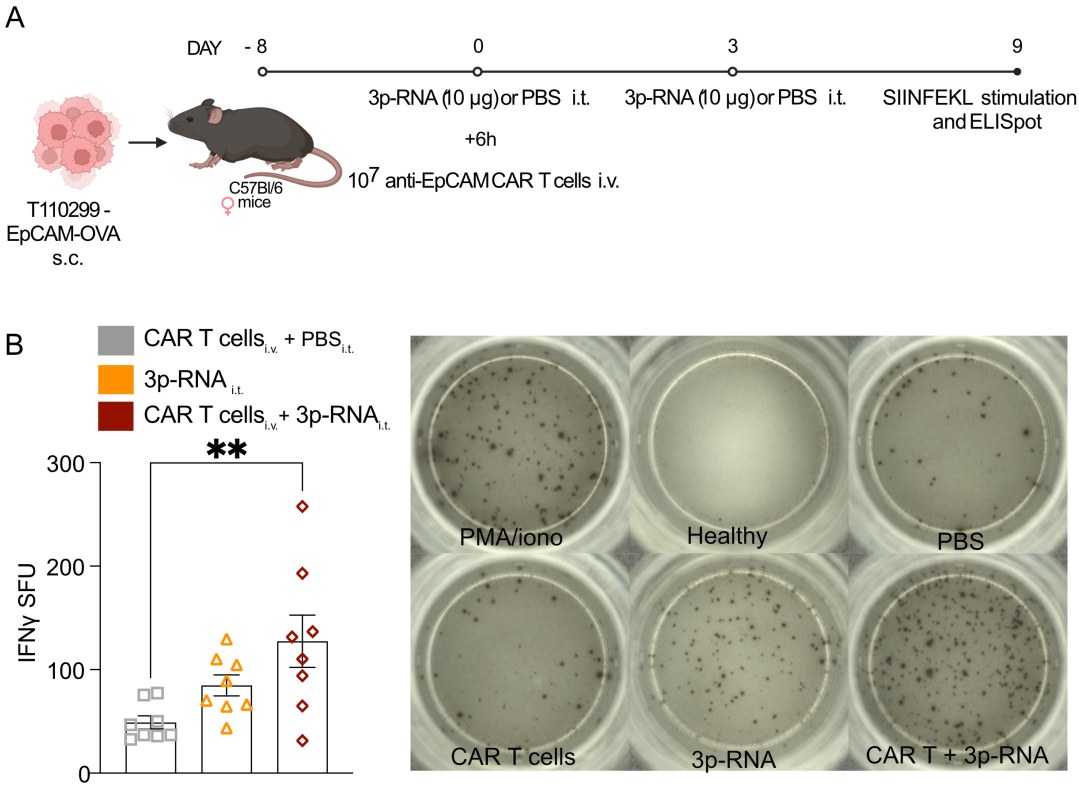

Figure 16. 3p-RNA treatment enhances antigen spreading permitting the generation of a de novo immune response in vivo.

A) Experimental layout for evaluation of tumor antigen spreading using OVA as non-CAR model antigen. Mice with s.c. T110299- EpCAM-OVA tumors were treated with 10 µg of *in vivo*-JetPEI complexed 3p-RNA and/or 1 x 10^7 anti-EpCAM CAR T cells as indicated. The experiment was terminated at nine days after treatment and cells isolated from blood were stimulated for 24 hours with 1 µg/ml SIINFEKL peptide to evaluate IFNγ response by ELISpot. **B)** Quantification of IFNγ spot forming units (n=8 mice per group). The quantification includes three technical replicates per mouse. Representative wells are shown, including a well of isolated cells stimulated with PMA and Ionomycin as positive control. Differences between groups was evaluated using ordinary one-way ANOVA with correction for multiple testing by Tukey method.

3.7 Therapeutic response of combining 3p-RNA and CAR T cell therapy in a human PDAC model

Due to its strong upregulation in the majority of PDAC tumors, mesothelin (MSLN) has been widely explored as a relevant antigen for targeted immunotherapies. To evaluate if the therapeutic advantage achieved by combining 3p-RNA and CAR T cells in PDAC murine models holds true in a human setting, SUIT-2 tumor cells engineered to express MSLN were used as a model. As expected, upon transfection with 3p-RNA, SUIT-2-MSLN tumor cells secreted high levels of CXCL10 (Figure 17A) and upregulated the membrane expression of both CD95 ($p = 0.009$) (Figure 17B) and HLA ($p = 0.009$) (Figure 17C). The same effect on CD95 and HLA expression was observed in the presence of exogenous type I IFN.

In contrast to what was observed in the murine models, tumor cell transfection with 3p-RNA had no significant effect on the proliferation of $CD4^+$ or $CD8^+$ CAR T cells when compared to unstimulated CAR T cells or to co-cultures between CAR T cells and untreated tumor cells (Figure 17D). Nevertheless, tumor cell treatment with 3p-RNA did induce IFNγ secretion by CAR T cells ($p=0.06$) (Figure 17E). This was paralleled by a decrease in IL-2 release ($p= 0.0001$) (Figure 17F) and a slight but not significant increase in the secretion of granzyme B (Figure 17G). The activation of $CD4^+$ CAR T cells was not significantly altered by 3p-RNA transfection of SUIT-2-MSLN tumor cells (Figure 17H). Nonetheless, $CD8^+$ CAR T cells showed CD69 upregulation in response to both 3p-RNA transfection ($p = 0.02$) an exogenous IFN-α2a addition ($p = 0.03$) (Figure 17I).

Overall, increased activation and cytokine secretion induced by 3p-RNA transfection of tumor cells was paralleled by a higher cytotoxic capacity of the CAR T cells assessed by real time quantification of tumor cell viability in response to the combination therapy (black curve), anti-MSLN CAR T cell monotherapy (purple curve), 3p-RNA monotherapy (green curve), and untreated tumor cells (blue curve) (Figure 17J). Moreover, flow cytometric evaluation of the number of detected anti-MSLN CAR T cells in NSG mice bearing SUIT-2-MSLN tumors

revealed that the combination therapy greatly enhanced CD8⁺ CAR T cells infiltration into the tumors (p=0.003) (Figure 17K).

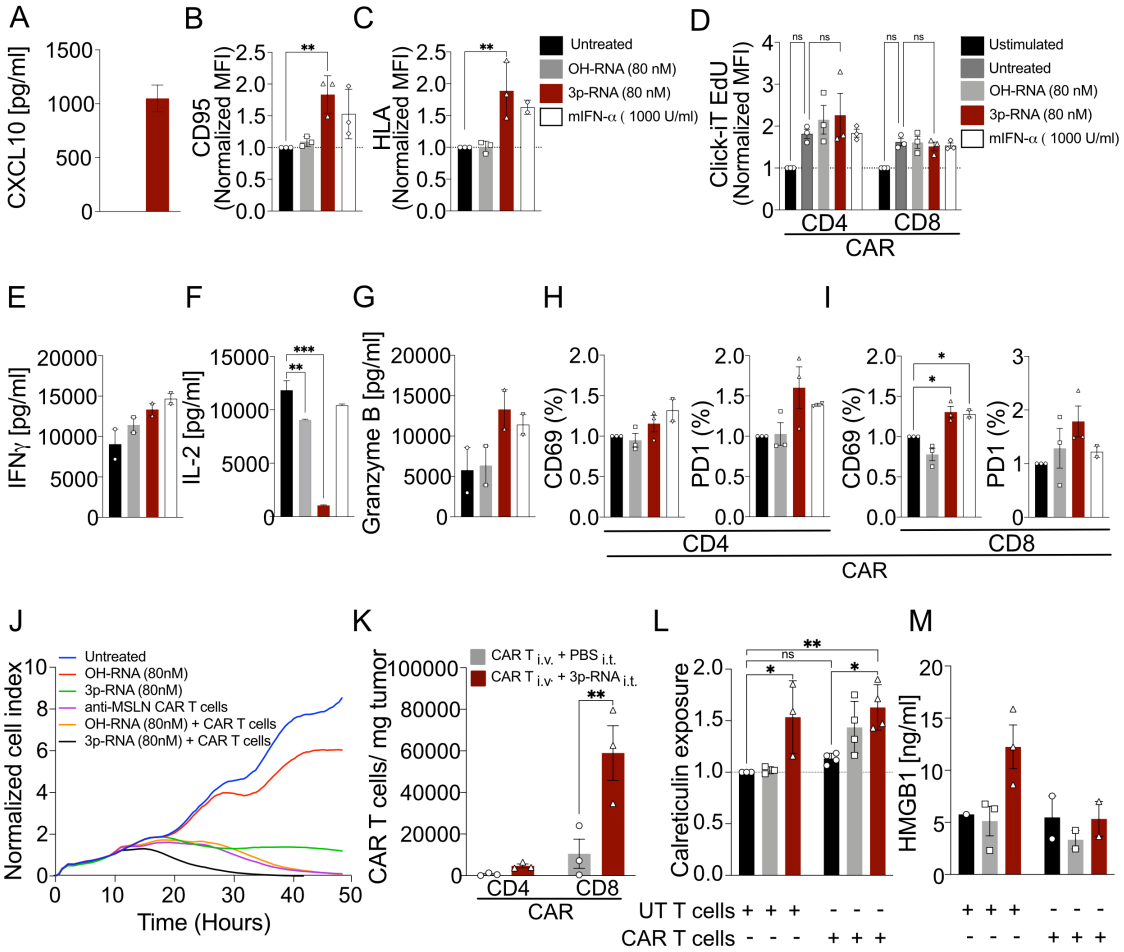

Figure 17. Therapeutic response of combining 3p-RNA and CAR T cells in human SUIT-2-MSLN PDAC model.

A) ELISA detection of human CXCL10 in the supernatant of SUIT-2-MSLN tumor cells 24 hours after transfection with either 3p-RNA or OH-RNA. Assessment of surface expression of **B)** CD95 (Fas) and **C)** HLA (MHC-I) on live SUIT-2-MSLN tumor cells 24 hours after transfection with 3p-RNA or controls as indicated. Data shown in B and C are normalized to the signal detected in untreated tumor cells. Error bars indicate mean ±SD of two to three pooled independent experiments. **D)** Proliferation assessment through incorporation of EdU thymidine analogue by CD4⁺ and CD8⁺ anti-MSLN CAR T cells upon 18 hours co-culture with SUIT-2-MSLN tumor cells transfected with 3p-RNA or controls. Data shown are normalized to signal from unstimulated CAR T cells. Error bars indicate mean values ± SEM of three biological replicates and are representative of three independent experiments. **E)** ELISA detection of IFNγ **F)** IL-2 and **G)** granzyme B in the supernatant of anti-MSLN CAR T cells co-cultured for 24 hours with SUIT-2-MSLN tumor cells transfected with 3p-RNA or controls. Percentage of CD69 and PD1 expression on **H)** CD4⁺ and **I)** CD8⁺ CAR T cells co-cultured for five hours with SUIT-2-MSLN tumor cells transfected with 3p-RNA or controls. Data shown are normalized to the signal detected in co-cultures of CAR T cells with untreated tumor cells. Error bars in E-I indicate mean values ± SEM of two to three biological replicates. **J)** xCELLigence real-

time quantification of SUIT-2-MSLN tumor cell lysis upon co-culture with anti-MSLN CAR T cells in a 10:1 E:T ratio. Graph is representative of three independent experiments. **K)** Flow cytometry assessment of live $CD45^+$ $CD4^+$ or $CD8^+$ CAR T cells co-expressing a *myc* tag. Cells were isolated three days after therapy from SUIT-2-MSLN tumors implanted in NSG mice. Cell counts were calculated using counting beads and normalized to tumor weight. Error bars indicate mean values ± SEM three mice and statistical analysis was performed using ordinary two-way ANOVA with Dunnett's multiple comparison test. **L)** Flow cytometry assessment of calreticulin exposure on Live (FVD^-) SUIT-2-MSLN tumor cells after transfection and/or co-culture with untransduced T cells or anti-MSLN CAR T cells for 24 hours. Error bars depict mean values ± SEM of three to four independent experiments normalized to the values for the co-culture of untreated tumor cells with untransduced T cells. **M)** ELISA detection of HMGB1 in the supernatant of SUIT-2-MSLN tumor cells either untreated or transfected and co-cultured for 24 hours with untransduced T cells or anti-MSLN CAR T cells. Error bars show mean values ± SEM of two to three biological replicates. Statistical analysis for A-I and K was calculated using ordinary one-way ANOVA with correction for multiple comparisons using Tukey test. Statistical analysis for L and M was calculated using ordinary two-way ANOVA with Dunnett's multiple comparison test.

Finally, 3p-RNA transfection of SUIT-2-MSLN tumor cells was sufficient to induce the exposure of calreticulin in the membrane of live cells ($p=0.03$). On the contrary, CAR T cell monotherapy did not significantly induce calreticulin exposure in the tumor cells but adding 3p-RNA treatment together with CAR T cells recapitulated the calreticulin exposure of 3p-RNA monotherapy (Figure 17L). Simultaneously, HMGB1 release was slightly enhanced by tumor cell treatment with 3pRNA monotherapy but not the addition of CAR T cells. The combination of both therapies had no effect on HMGB1 secretion in the SUIT-2-MSLN tumor model (Figure 17M).

These results suggest that combining 3p-RNA with CAR T cells recapitulates some of the findings observed in murine PDAC tumor models. Tumor cells upregulate type I IFN, CD95 and HLA in response to 3p-RNA treatment and CAR T cells show an increase in activation and cytokine release, thereby leading to superior cytotoxicity. Moreover, 3p-RNA therapy enhanced the *in vivo* infiltration of CAR T cells into the tumor and promoted the exposure of calreticulin as well as release of DAMP, such as HMGB1. These signs of immunogenic tumor cell death are not detectable upon CAR T cell monotherapy.

4 Discussion

This study proposes a strategy to improve the therapeutic efficacy of CAR T cell therapy in solid tumors by combination with 3p-RNA treatment. The delivery of *in vitro*-transcribed 3p-RNA as a RIG-I agonist mimics a viral infection in tumor cells triggering the expression of type I IFN, pro-inflammatory cytokines and chemokines. RIG-I agonists and other PRR agonists have been shown to promote an antitumoral immune response by enhancing infiltration of effector cells in various preclinical tumor models (Y. Jiang et al., 2023) (Lurescia et al., 2020). In this thesis I investigated how the immune cell recruiting and activating function via RIG-I signaling affects CAR T cell therapy and wether a combinatorial approach would overcome the limitations of CAR T cell-based therapies observed for solid tumors, such as PDAC.

In the case of PDAC, the highly complex TME, often entails a dense stroma and a high abundance of immunosuppressive factors and cells, which limits overall T cell infiltration and dampens potential cytotoxic immune responses (Orth et al., 2019).

To investigate strategies for overcoming these limitations, such as the one proposed in this study, experiments should be carried out in pertinent models that recapitulate not only key characteristics of the biology of the disease, but also portray fundamental features such as a membrane expression of relevant antigens that can be targeted by CAR T cells, and a functional type I IFN signaling pathway.

4.1 Engineering and validation of PDAC relevant tumor models

In this study, the murine T110299 and Panc02 cell lines, and the human SUIT-2 cell lines were chosen as relevant models that represent many of the described characteristics of PDAC disease. In particular, the KPC-derived tumor cell line T110299 resembles numerous histological features of the human disease.

EpCAM and mesothelin were used as model antigens for CAR therapy, as both are known to be expressed in a high proportion of PDAC patients and are thus currently being tested as target antigens in clinical trials (Schaft, 2020). As expression levels were low to undetectable in the tumor cell lines used in this study, expression was synthetically induced.

One key factor when evaluating the use of RIG-I targeted therapies for cancer is the functionality of the type I IFN pathway in the tumor cells. Epigenetic silencing or overall deletion of genes involved in IFN pathways can induce several survival and growth advantages and has therefore been commonly observed in cancer cells (Matveeva & Chumakov, 2018). Functionality of both the RIG-I and the interferon-α/β receptor pathways in the studied tumor models was confirmed by the observed secretion of IFN-β following 3p-RNA treatments, as well as the upregulation of ISG (such as MHCI) in response to both treatment and stimulation with exogenous IFN-α.

The use of cell lines derived both from murine and human origin helps to ensure that the observed outcomes are not merely characteristic of a single tumor cell line, and aid delineating what could be species-specific findings. Moreover, *in vivo* implantation of T110299 cells either s.c. or orthotopically into the pancreas of immune competent, syngeneic mice is a good tool to investigate the immune mechanisms behind the anti-tumor effects of combining CAR T cells with 3p-RNA. While using a variety of models is helpful in extrapolating information, it is important to remember that model are only approximations of the reality of human disease, and thus have limitations. Cultured cell lines, despite their origin, tend to have limited tumor cell clonal heterogeneity, which alter tumor characteristics and disease progression. Additionally, due to technical limitations many of the experiments need to be carried out in subcutaneously induced tumors, which do not strictly recapitulate the organ-specific microenvironment, and its effect on tumor progression and therapy response (Talmadge et al., 2007). Therefore, clinical studies will eventually be needed to confirm the therapeutic advantages of combining CAR T cell therapy with 3p-RNA for the treatment of human PDAC.

4.2 RIG-I targeted therapy improves CAR T cell efficacy and enhances anti-tumoral effects in PDAC murine models

We showed that the combination of 3p-RNA treatment and CAR T cell therapy is superior to both monotherapies in controlling subcutaneously and orthotopically induced PDAC tumors. In line with observations from human clinical trials that attempted to treat solid tumors solely with CAR T cells, no significant effect on tumor control or survival were observed in the mice treated with CAR T cells alone, thereby reinforcing the urgent need of exploring new strategies to improve CAR T cell efficiency for solid tumors (Zhang et al., 2022).

When it comes to 3p-RNA, intra-tumoral administration of this RIG-I agonist contributed to a delay in tumor growth. However, the observed effects were not strong enough to debulk the tumors and clear them entirely. Similar results in response to RLR lignads, including 3p-RNA and poly(I:C), have been previously reported in syngeneic murine PDAC models (Duewell et al., 2014). When using orthotopic tumor models, repeated delivery of 3p-RNA in the pancreas presented a technical limitation that forced us to evaluate the effects of systemic (i.v.) administration. Systemic delivery of any medication has the advantage of easier administration in a clinical setting. However, in the evaluated tumor model 3p-RNA did not confer any survival benefit as a monotherapy when delivered systemically. One speculation for this lack of therapeutic effect is that the amount of RNA that reaches the tumor after systemic delivery is greatly reduced due to degradation and distribution in other organs. Moreover, unintended transfection of non-target cells could have occurred, which can be detrimental due to the generation of a strong systemic cytokine release. This can result in the recruitment and activation of immunosuppresive immune cells at the tumor site, such as macrophages and neutrophils, which can contribute to tumor progression (Stickdorn et al., 2022).

Overall, the superior therapeutic effect of combined 3p-RNA and CAR T cell therapy suggests a synergistic effect capable of delaying tumor growth and even inducing tumor clearance in subcutaneous models. In addition, combination

therapy significantly prolonged survival of mice with orthotopic tumors**,** however tumor clearance was not achieved in this setting**.** The reduced antitumoral effect of 3p-RNA in this setting could be explained by the administration route, which was systemic in the orthotropic models as compared to intra-tumoral in the s.c tumor model. Another explanation could be the development of a more potent immunosuppressive network in the TME of orthotopic tumors. More work is required to evaluate whether the lack of curative effect observed in mice with orthotopically induced tumors can be explained by enhanced immunosuppression, e.g., via CAR T cell exhaustion, and could thus potentially be reverted with the addition of checkpoint blockade therapy. Moreover, i.t. delivery of 3p-RNA, e.g., via ultrasound-guided injection techniques, should be explored to evaluate whether this approach can improve efficacy.

4.3 RIG-I targeted therapy remodels the immunosuppressive TME in PDAC tumors

Widely described aspects that reduce the efficacy of CAR T cell therapy in solid tumors are the occurrence of immunosuppressive cells and molecules and the lack of T cell-attracting chemokines in the TME, which reduce T cell infiltration and dampen potential immune responses (J. Li et al., 2018). In particular, a dense infiltration of MDSC with a strong immunosuppressive capability has been described in human PDAC tissue (Stromnes et al., 2017).

Our results show that localized treatment with 3p-RNA reshapes the myeloid compartment in the tumors, reducing the relative frequency of PMN-MDSC and TAM, while increasing the frequency of Ly6C^{high} monocytes. The changes in the frequencies of these MDSC populations are in accordance with what has been shown in studies carried out in the context of TLR9-based therapies (Zoglmeier et al., 2011), and acute viral infection models (Dangi et al., 2018). Moreover, recent work from our group revealed that both M-MDSC (CD11b^{+} Ly6G^{-}Ly6C^{high}) and PMN-MDSC (CD11b^{+} Ly6G^{+} Ly6C^{int}) are enriched in the tumor and spleen of T110299 bearing mice and wield strong T cell suppression capability. However, in response to RLR ligand therapy using poly(I:C), MDSC populations are

reprogrammed into a less suppressive phenotype (Metzger et al., 2019). Currently, there is no strategy to differentiate inflammatory Ly6C^{high} monocytes and M-MDSC based on their surface markers. As these cells have been shown to be less suppressive, it may be preferable to refer to them as “pro-inflammatory monocytes” rather than M-MDSC in the acute therapeutic setting. Both the reduction of the suppressive activity of these cells, as well as the phenotypic shift of MDSC and TAM from M2/G2 towards a M1/G1 inflammatory phenotype have been shown to depend on type I IFN signaling (Metzger et al., 2019). Although we did not assess changes in the suppressive capability of the MDSC populations in response to 3p-RNA treatment, one can infer from previous studies that 3p-RNA-mediated type I IFN secretion likely promoted a decrease in MDSC suppressive activity alongside with the observed reduction of their frequency.

In many of the analyzed cell types in the TME, an expected increase in the expression of ISG such as PD-L1 and MHC-I, was observed following 3p-RNA treatment. Considering that PD-1/PD-L1 signaling is a widely known mechanism for cytotoxic T cell suppression (Oh et al., 2020), the observed upregulation of PDL1 suggests that adding an anti-PD1/PDL-1 blocking agent could be a successful strategy to further enhance the anti-tumoral immune response.

Increased expression of MHC-I in DC suggests stronger activation and antigen presentation capacities. This has been observed in studies carried out using CAR T cell-delivered stimulatory RNA (Johnson et al., 2021), and in the context of viral infections (Shirley et al., 2020) or virus-like particle therapy (Zepeda-Cervantes et al., 2020). In these studies, activation of PRR in the membrane or endosome of DC leads to type I IFN production, driving increased activation and cross-priming capacities mainly of cDC1, but also recently described in an interferon activation state of CD11b^{+} conventional cDC2 (Duong et al., 2022).

Overall, the reprogramming and reduction of suppressive populations in combination with the induction of pro-inflammatory cytokines imply that 3p-RNA therapy induces a more immune-permissive TME that promotes CAR T cell efficacy in PDAC tumors. This is in accordance with results observed in strategies

that combine other PRR activation modalities with CAR T cells. For example, poly(I:C) used as a TLR3 (and MDA5) ligand, improves CAR T cell anti-tumoral effects in models of colon and breast cancer due to TME remodeling but also enhancement of CAR T cell infiltration and cytotoxic functions (Di et al., 2019). Furthermore, Xu and colleagues reported in 2021 that treatment of pre-clinical models of breast cancer with STING agonists induced the remodeling of the TME facilitating CAR T cell trafficking and persistence and improving tumor control when combined with checkpoint blockade (N. Xu et al., 2021)

Considering that 3p-RNA induces a more immune-permissive TME and that RIG-I sensing leads to the expression of several chemokines due to the activation of NF-κB (Richmond, 2002), we hypothesized that the superior therapeutic effect observed in mice treated with the combination therapy could be explained by an increase of trafficking and infiltration of CAR T cells into the tumor.

4.4. Cytokine secretion in response to RIG-I targeted therapy increases T cell trafficking and infiltration

Our results show that treatment with 3p-RNA significantly increased the number of endogenous $CD8^+$ T cells and adoptively transferred $CD8^+$ CAR T cells in the tumors. Interestingly, no effect on the $CD4^+$ populations was detected. These observations are in line with what has been reported by others evaluating RLH-targeted therapies. Systemic treatment of T110299 orthotopic PDAC tumors with poly(I:C) induced an increase of the percentage of $CD8^{+\ but}$ not $CD4^+$ T cells in the tumors (Metzger et al., 2019). Furthermore, selective delivery of RN7SL1 RNA to immune cells in the TME increased infiltration of both adoptively transferred CAR T cells and endogenous immune cells in response to the activation of inflammatory DC, monocytes, and macrophages (Johnson et al., 2021).

Assessment of the chemokines expressed by T110299-EpCAM tumor cells in response to 3p-RNA treatment showed upregulation of CCL2, CCL4, CCL5, CCL7, CXCL2, CXCL9, CXLC10 and CXCL11. Most of these chemokines have

been associated with increase of survival and invasion of tumor cells due to their attraction of immune inhibitory cells such as TAM, MDSC and Treg (M. Xu et al., 2021). However, in the context of acute inflammation, CCL2 enhances the anti-tumor activity of inflammatory monocytes and neutrophils (Jin et al., 2021), whilst CCL7 facilitates the recruitment of inflammatory monocytes and activated DC, triggering Th1 responses (Liu et al., 2018). CXCL2 has been described to promote cellular growth arrest and delay early phases of tumorigenesis through CXCR2 in the context of oncogene-induced tumor senescence (Mukaida, 2014).

Of particular interest is the observed upregulation of both CCL4 and CCL5, as well as CXCL9, CXCL10 and CXCL11. The first two chemokines can promote anti-tumor effects through CCR5-mediated recruitment of cytolytic lymphocytes and phagocytic macrophages (Mukaida et al., 2020). Meanwhile, CXCL9, CXCL10 and CXCL11 are IFN-inducible chemokines that influence immune cell migration, differentiation, and activation via CXCR3. Interestingly, *in vitro* migration assays with chemokine receptor--transduced primary T cells showed a preferential migration of CCR5- and CXCR3-expressing T cells towards the supernatant of 3p-RNA transfected tumor cells. These observations, together with the fact that both CCR5 and CXCR3 are upregulated in the membrane of the CAR T cells used for ACT, suggest that the CCL4-5/CCR5 and CXCL9-10-11/CXCR3 axes are likely involved in the enhancement of CAR T cell infiltration upon 3p-RNA treatment in our PDAC models. However, further experiments are required to prove this causal relationship in our setting, which could be done by exploiting chemokine receptor-knockout CAR T cells. Encouragingly, such experiments have been performed by other groups in the context of lung cancer, showing that immunogenic chemotherapy can enhance CAR T cell recruitment in a time-restricted manner. Srivastava *et al.,* showed that initial T cell infiltration relies partially on CXCR6 and CCR5. Once within the tumor, IFNγ secretion by the CAR T cells activates M1-like iNOS^{+} macrophages that express CXCL9-10, mediating further CXCR3-mediated recruitment of CAR T cells and endogenous immune cells (Srivastava et al., 2021) .

Chemokine directed trafficking of CAR T cell into solid tumors is a long-studied strategy to improve therapy. In the context of PDAC tumor models, high expression of both CCL1 and CXCL16 has been reported in murine cancer models and human tumor biopsies. Studies that generated CCR8 (B. L. Cadilha et al., 2021), and CXCR6 expressing CAR T cells (Lesch et al., 2021), demonstrated enhanced trafficking and infiltration in murine and human PDAC models, which ultimately contributed to better tumor control. Consequently, 3p-RNA mediated upregulation of CCR5 and CXCR3 ligands is an attractive feature that offers great potential for exploiting both the CCL5/CCR5 and CXCL9-10-11/CXCR3 axis to enhance CAR T cell recruitment to the tumor.

4.5 RIG-I targeted therapy increases CAR T cell proliferation, persistence, activation, and cytotoxic capacity.

In parallel to enhanced tumor infiltration and persistence in the blood of 3p-RNA-treated mice, we observed an enhancement of *in vitro* CAR T cell proliferation activation and lytic capacity. Similar findings were also reported upon combination of CAR T cells with poly(I:C) (Di et al., 2019), STING agonists (N. Xu et al., 2021), and targeted delivery of immunostimulatory RNA (Johnson et al., 2021).

Type I IFNs have extensively described pro-tumorigenic and anti-tumor immunomodulatory functions. Acute exposure to type I IFN in the TME contributes to inhibition of tumor cell growth and induces apoptosis in some types of cancer (Murata et al., 2006). These cytokines have also been shown to decrease angiogenesis in some tumors (Sidky & Borden, 1987), and to increase MHC-I expression in immunogenic tumor clones, facilitating tumor antigen recognition by reactive T cells. Moreover, type I IFN-mediated maturation of DC induces upregulation of co-stimulatory and MHC molecules as well as chemokine receptors, enhancing their ability to process antigens and migrate to the LN to cross-present antigens to T cells. Additionally, enhanced secretion of IL-12 and IL-23 by type I IFN activated DC supports Th1 and Th17 responses, and contributes to $CD8^+$ memory T cell survival, degranulation, and lytic ability

(Medrano et al., 2017). Therefore, it is reasonable to think that many of the observed enhanced CAR T cell characteristics are linked to type I IFN induction by 3p-RNA treatment.

Upregulation of CD69 and increased secretion of IFNγ and granzyme B were observed when adding IFNα to co-cultures of CAR T cells with target cells. CD69 has been described before to be directly induced by IFNα/β (Shiow et al., 2006). Increased IFNγ secretion in response to IFNα was described for $CD4^+$ T cells, promoting the induction and maintenance of Th1 responses (Brinkmann et al., 1993). Specifically in the case of mouse $CD8^+$ T cells, it has been described that IFNα and IFNβ in combination with antigen detection and co-stimulation enhances both IFNγ and granzyme B secretion (Huber & David Farrar, 2011). This suggests that the observed increase on CAR T cell activation and cytokine secretion, paired with the enhanced lytic capacity and faster killing kinetic are a direct result of the exposure to type I IFN secreted by 3p-RNA activated cells in the tumor. Blockade of IFNAR signaling in the T cells should be conducted to further validate this point.

Interestingly, in contrast to findings from Di and colleagues, who reported increased IL-2 secretion by CAR T cells when combined with poly(I:C) treatment (Di et al., 2019), we observed reduced IL-2 secretion when co-culturing CAR T cells with 3p-RNA-treated tumor cells. This observation was not recapitulated by addition of IFNα to the co-cultures. Both IFNα and IFNβ share the same receptor and induce similar immunomodulatory responses. However, they can exhibit differences in the association of receptor subunits with certain proteins (Runkel et al., 1998). This translates into differences in the strength of some responses or even IFNα- or IFNβ-specific biological responses (Platanias et al., 1996). Dennis et al. described IFNβ-specific epigenetic silencing of IL-2 in T cells through the upregulation of the transcriptional suppressor CREM, which recruits histone deacetylases (HDAC) to the IL-2 promoter thereby silencing it (Dennis C. Otero et al., 2015). Thus, strong secretion of IFNβ by 3p-RNA transfected tumor cells could lead to epigenetic modifications of the IL-2 promoter. This may explain why we observed reduction in IL-2 secretion in the co-cultures setting, but not in

response to exogenous IFNα stimulation. This is an intriguing possibility which should be further evaluated.

The increased proliferation and persistence of CAR T cells when combined with 3p-RNA treatment are most likely indirectly linked to type I IFN responses. The proliferation status of CAR T cells was checked with *in vitro* assays that assess DNA synthesis. These assays are however limited, as they overlook the influence that type I IFN-activated immune cells in the TME may have on CAR T cell proliferation. The fact that the mere presence of IFNα in the cultures did not recapitulate an enhancement of CAR T cell proliferation suggests that either IFNβ is also required to induce higher proliferation or other secreted factors are needed to enhance CAR T cell proliferation. CCL5 has been described as a T cell co-stimulatory molecule in the context of CD3 stimulation, inducing proliferation and cytokine production at low concentrations (Taub et al., 1996). Moreover, antigen-independen CCL5-mediated T cell proliferation has been observed at concentrations of approximately 1 μM (Murooka et al., 2006), potentially explaining the higher proliferative tendency we observed on untransduced T cells when cultured with 3p-RNA transfected tumor cells. Further experiments blocking the CCL5/CCR5 axis and IFNAR receptor are required to validate these hypotheses.

In accordance with what is observed in the clinics for many types of cancer, lack of CAR T cell expansion and persistence correlate with tumor progression and/or relapse (Pietrobon et al., 2021). In this study, attempts to treat PDAC tumors with CAR T cell monotherapy had no significant effect on tumor control, presumably because in many mice CAR T cells were no longer detectable as early as 9 days after therapy. In contrast, 3p-RNA treatment significantly enhanced CAR T cell persistence with detectable numbers even 14 days after therapy administration. Despite the low numbers detected, the superior therapeutic efficacy of combining 3p-RNA with CAR T cells is likely associated with the simultaneous enhancement of CAR T cell persistence. It would be interesting to evaluate whether persistence could be further enhanced by combining 3p-RNA therapy with CAR T cells bearing a different co-stimulatory domain (Guedan et al., 2020).

4.6 RIG-I targeted therapy enhances immunogenic tumor cell death promoting the generation of a *de-novo* immune response

Our results indicate that combining 3p-RNA treatment with CAR T cells does not only enhance tumor cell death, but also simultaneously increases the release and exposure of DAMP. This may lead to the engagement of APC, contributing to *in vivo* antigen spreading. Such engagement of the innate immune system in collaboration with an adaptive immune response has the potential to fight disease relapse due to antigen downregulation or loss.

Interestingly, we observed substantial differences between cell lines in regard to the exposure or secretion of immunogenic cell death markers which could be attributed to the sensitivity of each cell line towards 3p-RNA transfection (T. K. Kim & Eberwine, 2010). Despite T110299 cells showing fewer striking differences in DAMP exposure *in vitro*, we observed differences *in vivo* when it came to the generation of OVA-specific T cells in response to the different treatments. One limitation of studying antigen spreading with this method comes from the intrinsic immunogenic nature of the xenoantigen ovalbumin, which easily induces immune responses on its own. Therefore, more experiments on antigen cross-presentation and assessment of immune protection against other antigens would be crucial to fully describe the extent of antigen spreading and memory formation as a result of our combination treatment.

Despite outstanding results in the therapeutic handling of hematological malignancies, around 50% of the patients treated with anti-CD19 CAR T cells show progressive disease, associated in the majority of those patients with either CD19 antigen loss or diminished surface expression (Majzner & Mackall, 2018). Many strategies are currently being pursued to tackle the issue of disease relapse due to antigen loss. One could summarize those efforts into two branches. On one hand there are strategies that focus on antigen targeting, aimed at improving CAR T cell sensitivity to detect low-expressing antigen or adding secondary

targets simultaneously. On the other hand, a second CAR T cell target could be used.

In the case of complete antigen loss, one would require the engagement of the innate immune system and consequent mounting of a *de novo* immune response against new tumor-associated antigens to prevent disease relapse. During the course of our study, Johnson and colleagues reported the engineering of CAR T cells that selectively deliver RIG-I/MDA5 stimulatory RNA and peptide antigens to immune cells to overcome CAR T cell limitations in solid tumors. They argue that triggering PRR signaling in tumor cells is detrimental and therefore an immune cell targeted delivery approach is required (Johnson et al., 2021). This affirmation deviates from our observations in that despite a non-targeted delivery of 3p-RNA, our experiments show similar TME remodeling accompanied by enhancement of CAR T cell infiltration, efficacy, tumor control and some signs of antigen spreading. Future steps would be to validate this antigen spreading in other tumor models and using alternative methods to assess immunological memory formation towards intrinsic physiological tumor antigens.

4.7 Advantages of enhancing CAR T cell therapy with 3p-RNA compared to other combination strategies

The idea of optimizing solid tumor responses to CAR T cell therapy by combining it with a second agent is not novel. Combinations of CAR T cells with radio- or chemotherapy, checkpoint inhibitors, oncolytic viruses, and small molecules, are some of the currently explored strategies to improve solid tumor therapeutic responses (A. Nguyen et al., 2022). Of particular interest are the strategies that propose combining CAR T cells with PRR agonists, such as STING agonists, or immunostimulatory RNA. Like 3p-RNA, these molecules trigger an anti-viral immune response, attracting and activating CAR T cells together with other immune cells against the tumor as a consequence of type I IFN and other pro-inflammatory cytokines and chemokines. However, the pleiotropic effect of pro-inflammatory cytokines and chemokines, including type I IFN, in the cancer setting has led to differential arguments supporting or refuting the exploitation of

PRR signaling directly in tumor cells as compared to immune cells, bringing up additional questions regarding potential toxicities and side effects due to local versus systemic delivery.

In line with our results, recent publications that combine STING agonists or poly(I:C) with CAR T cells have also shown improved anti-tumoral effects on solid tumors such as breast and colon cancer. However, in the case of poly(I:C) both systemic and intraperitoneal delivery, induced strong toxicities ranging from weight loss to hepatic and pulmonary complications in mice (Di et al., 2019).

In the case of STING agonists like DMXAA or cGAMP, Xu and colleagues reported that despite local delivery, strong toxicities were observed in the mice affecting their weight and inducing mortality (N. Xu et al., 2021). Additionally, both the strength of STING activation (Sivick et al., 2018), as well as the stimulation of IFN-independent pathways by STING activation in T cells are described to induce T cell apoptosis (Kuhl et al., 2023) and may lead to pro-tumorigenic effects (Wu et al., 2020).

In our study, no limiting toxicities were observed with either systemic or local 3pRNA treatment of the mice. Moreover, due to the challenging nature of primary T cells transfection, 3p-RNA does not exercise any toxic effects directly on the T cells, suggesting an overall superior safety profile of the 3p-RNA treatment compared to STING agonists. In addition, the observed therapeutic advantage of combining 3pRNA with CAR T cell therapy in murine PDAC models was recapitulated also in human pre-clinical models. This validates that our observations are not species-specific and suggests that this combination should be further explored as a therapeutic strategy in the clinic.

One important aspect in favor of developing clinical studies that explore CAR T cell and 3p-RNA combination therapy is the fact that tolerability of RLH ligand treatment has already been confirmed in two distinct phase I/Ib clinical trials targeting injectable tumors (NCT03739138, NCT02828098). Both trials showed good toxicity profiles but were stopped for undisclosed or business reasons.

In conclusion, RIG-I targeted therapy is an interesting and encouraging combination scheme to overcome known limitations of CAR T cell therapy in solid tumors and improve their therapeutic potential.

References

Adunka, T. (2014). Characterization of murine pancreatic carcinoma models regarding immunosuppressive mechanisms and therapy with bifunctional siRNA targeting galectin-1. Dissertation, LMU München: Medizinische Fakultät.

Alberts, B., Johnson, A., Lewis, J., Raff, M., Roberts, K., & Walter, P. (2002). Molecular Biology of the Cell (4th ed.). Garland Science.

Aldous, A. R., & Dong, J. Z. (2018). Personalized neoantigen vaccines: A new approach to cancer immunotherapy. Bioorganic and Medicinal Chemistry, 26(10), 2842–2849. https://doi.org/10.1016/j.bmc.2017.10.021

Beatty, G. L., O'Hara, M. H., Lacey, S. F., Torigian, D. A., Nazimuddin, F., Fang, C., Kulikovskaya, I. M., Soulen, M. C., McGarvey, M., Nelson, A. Marie., Gladney, W. L., Levine, B. L., Melenhorst, J. J., Plesa, G., & June, C. H. (2018). Activity of mesothelin-specific chimeric antigen receptor T cells against pancreatic carcinoma metastases in a phase 1 trial. Gastroenterology, 155, 29–32. https://doi.org/10.1053/j.gastro.2018.03.029.Activity

Bellone, M., & Calcinotto, A. (2013). Ways to Enhance Lymphocyte Trafficking into Tumors and Fitness of Tumor Infiltrating Lymphocytes. Frontiers in Oncology, 11;3:231. https://doi.org/10.3389/fonc.2013.00231

Besch, R., Poeck, H., Hohenauer, T., Senft, D., Häcker, G., Berking, C., Hornung, V., Endres, S., Ruzicka, T., Rothenfusser, S., & Hartmann, G. (2009). Proapoptotic signaling induced by RIG-I and MDA-5 results in type I interferon–independent apoptosis in human melanoma cells. Journal of Clinical Investigation. 2009 Aug;119(8):2399-411. https://doi.org/10.1172/JCI37155

Beyer, K., Normann, L., Sendler, M., Käding, A., Heidecke, C.-D., Partecke, L. I., & von Bernstorff, W. (2016). TRAIL Promotes Tumor Growth in a Syngeneic Murine Orthotopic Pancreatic Cancer Model and Affects the Host Immune Response. Pancreas, 45(3), 401–408. https://doi.org/10.1097/MPA.0000000000000469

Bezu, L., Gomes-de-Silva, L. C., Dewitte, H., Breckpot, K., Fucikova, J., Spisek, R., Galluzzi, L., Kepp, O., & Kroemer, G. (2015). Combinatorial Strategies for the Induction of Immunogenic Cell Death. Frontiers in Immunology, 6:187. https://doi.org/10.3389/fimmu.2015.00187

Boehmer, D. F. R., Formisano, S., de Oliveira Mann, C. C., Mueller, S. A., Kluge, M., Metzger, P., Rohlfs, M., Hörth, C., Kocheise, L., Lichtenthaler, S. F., Hopfner, K. P., Endres, S., Rothenfusser, S., Friedel, C. C., Duewell, P., Schnurr, M., & Koenig, L. M. (2021). OAS1/RNase L executes RIG-I ligand–dependent tumor cell apoptosis. Science Immunology, 6(61), 1–16. https://doi.org/10.1126/sciimmunol.abe2550

Bonaventura, P., Shekarian, T., Alcazer, V., Valladeau-Guilemond, J., Valsesia-Wittmann, S., Amigorena, S., Caux, C., & Depil, S. (2019). Cold tumors: A therapeutic challenge for immunotherapy. Frontiers in Immunology, 10(FEB), 1–10. https://doi.org/10.3389/fimmu.2019.00168

Brinkmann, V., Geiger, T., Alkan, S., & Heusser, C. H. (1993). Interferon alpha increases the frequency of interferon gamma-producing human CD4+ T cells. Journal of Experimental Medicine, 178(5), 1655–1663. https://doi.org/10.1084/jem.178.5.1655

Bronte, V., Brandau, S., Chen, S. H., Colombo, M. P., Frey, A. B., Greten, T. F., Mandruzzato, S., Murray, P. J., Ochoa, A., Ostrand-Rosenberg, S., Rodriguez, P. C., Sica, A., Umansky, V., Vonderheide, R. H., & Gabrilovich, D. I. (2016). Recommendations for myeloid-derived suppressor cell nomenclature and characterization standards. In Nature Communications (2016) Jul 6;7:12150. https://doi.org/10.1038/ncomms12150

Brouwer, T. P., Vahrmeijer, A. L., & de Miranda, N. F. C. C. (2021). Immunotherapy for pancreatic cancer: chasing the light at the end of the tunnel. Cellular Oncology, 44(2), 261–278. https://doi.org/10.1007/s13402-021-00587-z

Brubaker, D. K., & Lauffenburger, D. A. (2020). Translating preclinical models to humans. Science, 367(6479), 742–743. https://doi.org/10.1126/science.aay8086

Busnardo, A. C., Didio, L. J. A., Tidrick, R. T., & Thomford, N. R. (1983). History of the pancreas. American Journal of Surgery, 146(5), 539–550. https://doi.org/10.1016/0002-9610(83)90286-6

Cadilha, B., Dorman, K., Rataj, F., Endres, S., & Kobold, S. (2017). Enabling T Cell Recruitment to Tumours as a Strategy for Improving Adoptive T Cell Therapy. European Oncology & Haematology, 13(01), 66-73. https://doi.org/10.17925/EOH.2017.13.01.66

Cadilha, B. L., Benmebarek, M.-R., Dorman, K., Oner, A., Lorenzini, T., Obeck, H., Vänttinen, M., di Pilato, M., Pruessmann, J. N., Stoiber, S., Huynh, D., Märkl, F., Seifert, M., Manske, K., Suarez-Gosalvez, J., Zeng, Y., Lesch, S., Karches, C. H., Heise, C., … Kobold, S. (2021). Combined tumor-directed recruitment and protection from immune suppression enable CAR T cell efficacy in solid tumors. In Sci. Adv. 7(24). doi: 10.1126/sciadv.abi5781. PMID: 34108220

Cance, J. C., Crozat, K., Dalod, M., & Mattiuz, R. (2019). Are conventional type 1 dendritic cells critical for protective antitumor immunity and how? In Frontiers in Immunology. 10(9). Frontiers Media S.A. https://doi.org/10.3389/fimmu.2019.00009

Castiello, L., Zevini, A., Vulpis, E., Muscolini, M., Ferrari, M., Palermo, E., Peruzzi, G., Krapp, C., Jakobsen, M., Olagnier, D., Zingoni, A., Santoni, A., & Hiscott, J. (2019). An optimized retinoic acid-inducible gene I agonist M8 induces immunogenic cell death markers in human cancer cells and dendritic cell activation. Cancer Immunology, Immunotherapy, 68(9), 1479–1492. https://doi.org/10.1007/s00262-019-02380-2

Chang, Z. N. L., & Chen, Y. Y. (2017). CARs: Synthetic Immunoreceptors for Cancer Therapy and Beyond. Trends in Molecular Medicine, 23(5), 430–450. https://doi.org/10.1016/j.molmed.2017.03.002

Chen, D. S., & Mellman, I. (2013). Oncology meets immunology: The cancer-immunity cycle. Immunity, 39(1), 1–10. https://doi.org/10.1016/j.immuni.2013.07.012

Chen, Y. G., & Hur, S. (2022). Cellular origins of dsRNA, their recognition and consequences. In Nature Reviews Molecular Cell Biology. 23(4), 286–301. Nature Research. https://doi.org/10.1038/s41580-021-00430-1

Collin, M., & Bigley, V. (2018). Human dendritic cell subsets: an update. In Immunology. 154(1), 3–20. Blackwell Publishing Ltd. https://doi.org/10.1111/imm.12888

Condamine, T., Mastio, J., & Gabrilovich, D. I. (2015). Transcriptional regulation of myeloid-derived suppressor cells. Journal of Leukocyte Biology, 98(6), 913–922. https://doi.org/10.1189/jlb.4RI0515-204R

Connor, A. A., Denroche, R. E., Jang, G. H., Timms, L., Kalimuthu, S. N., Selander, I., McPherson, T., Wilson, G. W., Chan-Seng-Yue, M. A., Borozan, I., Ferretti, V., Grant, R. C., Lungu, I. M., Costello, E., Greenhalf, W., Palmer, D., Ghaneh, P., Neoptolemos, J. P., Buchler, M., … Gallinger, S. (2017). Association of distinct mutational signatures with correlates of increased immune activity in pancreatic ductal adenocarcinoma. In JAMA Oncology. 3(6), 774–783. https://doi.org/10.1001/jamaoncol.2016.3916

Conroy, T., Desseigne, F., Ychou, M., Bouché, O., Guimbaud, R., Bécouarn, Y., Adenis, A., Raoul, J.-L., Gourgou-Bourgade, S., de la Fouchardière, C., Bennouna, J., Bachet, J.-B., Khemissa-Akouz, F., Péré-Vergé, D., Delbaldo, C., Assenat, E., Chauffert, B., Michel, P., Montoto-Grillot, C., & Ducreux, M. (2011). FOLFIRINOX versus Gemcitabine for Metastatic Pancreatic Cancer. New England Journal of Medicine, 364(19), 1817–1825. https://doi.org/10.1056/nejmoa1011923

Contento, R. L., Molon, B., Boularan, C., Pozzan, T., Manes, S., Marullo, S., & Viola, A. (2008). CXCR4–CCR5: A couple modulating T cell functions. Proceedings of the National Academy of Sciences, 105(29), 10101–10106. https://doi.org/10.1073/pnas.0804286105

Cruz, F. M., Colbert, J. D., Merino, E., Kriegsman, B. A., & Rock, K. L. (2017). The biology and underlying mechanisms of cross-presentation of exogenous antigens on MHC-I molecules. Annual Review of Immunology, 35(December 2016), 149–176. https://doi.org/10.1146/annurev-immunol-041015-055254

Dangi, A., Zhang, L., Zhang, X., & Luo, X. (2018). Murine CMV induces type 1 IFN that impairs differentiation of MDSCs critical for transplantation tolerance. Blood Advances, 2(6), 669–680. https://doi.org/10.1182/bloodadvances.2017012187

Daßler-Plenker, J., Paschen, A., Putschli, B., Rattay, S., Schmitz, S., Goldeck, M., Bartok, E., Hartmann, G., & Coch, C. (2019). Direct RIG-I activation in human NK cells induces TRAIL-dependent cytotoxicity toward autologous melanoma cells. International Journal of Cancer, 144(7), 1645–1656. https://doi.org/10.1002/ijc.31874

Dennis C. Otero, Nancy J. Fares-Frederickson, Menghong Xiao, Darren P. Baker, & Michael David. (2015). Interferon β selectively Inhibits Interleukin-2 (IL-2)

production through cAMP responsive element modulator (CREM)-mediated chromatin remodeling. J Immunol, (2015) Jun 1;194(11):5120-8.https://doi.org/10.1159/000444169.Carotid

Di, S., Zhou, M., Pan, Z., Sun, R., Chen, M., Jiang, H., Shi, B., Luo, H., & Li, Z. (2019). Combined adjuvant of poly I:C improves antitumor effects of CAR-T cells. Frontiers in Oncology, 9(APR), 1–11. https://doi.org/10.3389/fonc.2019.00241

Dias Junior, A. G., Sampaio, N. G., & Rehwinkel, J. (2019). A Balancing Act: MDA5 in Antiviral Immunity and Autoinflammation. In Trends in Microbiology. 27(1), 75–85. Elsevier Ltd. https://doi.org/10.1016/j.tim.2018.08.007

Dinarello, C. A. (2006). The paradox of pro-inflammatory cytokines in cancer. In Cancer and Metastasis Reviews. 25(3), 307–313. https://doi.org/10.1007/s10555-006-9000-8

Duewell, P., Beller, E., Kirchleitner, S. V, Adunka, T., Bourhis, H., Siveke, J., Mayr, D., Kobold, S., Endres, S., & Schnurr, M. (2015). Targeted activation of melanoma differentiation-associated protein 5 (MDA5) for immunotherapy of pancreatic carcinoma. OncoImmunology, 4(10), e1029698. https://doi.org/10.1080/2162402X.2015.1029698

Duewell, P., Steger, A., Lohr, H., Bourhis, H., Hoelz, H., Kirchleitner, S. V., Stieg, M. R., Grassmann, S., Kobold, S., Siveke, J. T., Endres, S., & Schnurr, M. (2014). RIG-I-like helicases induce immunogenic cell death of pancreatic cancer cells and sensitize tumors toward killing by CD8(+) T cells. Cell Death and Differentiation, 21(12), 1825–1837. https://doi.org/10.1038/cdd.2014.96

Duong, E., Fessenden, T. B., Lutz, E., Dinter, T., Yim, L., Blatt, S., Bhutkar, A., Wittrup, K. D., & Spranger, S. (2022). Type I interferon activates MHC class I-dressed CD11b+ conventional dendritic cells to promote protective anti-tumor CD8+ T cell immunity. Immunity, 55(2), 308-323.e9. https://doi.org/10.1016/j.immuni.2021.10.020

Ehrlich, P. (1909). Ueber den jetzigen Stand der Karzinomforschung. In Ned. Tijdschr. Geneeskd. 5(3), 273–290.

Eisenbarth, S. C. (2019). Dendritic cell subsets in T cell programming: location dictates function. Nature Reviews Immunology, 19(2), 89–103. https://doi.org/10.1038/s41577-018-0088-1

Elion, D. L., Jacobson, M. E., Hicks, D. J., Rahman, B., Sanchez, V., Gonzales-Ericsson, P. I., Fedorova, O., Pyle, A. M., Wilson, J. T., & Cook, R. S. (2018). Therapeutically Active RIG-I Agonist Induces Immunogenic Tumor Cell Killing in Breast Cancers. Cancer Research, 78(21), 6183–6195. https://doi.org/10.1158/0008-5472.CAN-18-0730

Ellermeier, J., Wei, J., Duewell, P., Hoves, S., Stieg, M. R., Adunka, T., Noerenberg, D., Anders, H.-J., Mayr, D., Poeck, H., Hartmann, G., Endres, S., & Schnurr, M. (2013). Therapeutic Efficacy of Bifunctional siRNA Combining TGF-β1 Silencing with RIG-I Activation in Pancreatic Cancer. Cancer Research, 73(6), 1709–1720. https://doi.org/10.1158/0008-5472.CAN-11-3850

Erkan, M., Michalski, C. W., Rieder, S., Reiser-Erkan, C., Abiatari, I., Kolb, A., Giese, N. A., Esposito, I., Friess, H., & Kleeff, J. (2008). The Activated Stroma Index Is a Novel and Independent Prognostic Marker in Pancreatic Ductal Adenocarcinoma. Clinical Gastroenterology and Hepatology, 6(10), 1155–1161. https://doi.org/10.1016/j.cgh.2008.05.006

Eshhar, Z., Waks, T., Gross, G., & Schindler, D. G. (1993). Specific activation and targeting of cytotoxic lymphocytes through chimeric single chains consisting of antibody-binding domains and the γ or ζ subunits of the immunoglobulin and T-cell receptors. Proceedings of the National Academy of Sciences of the United States of America, 90(2), 720–724. https://doi.org/10.1073/pnas.90.2.720

Fallarino, F., Grohmann, U., Hwang, K. W., Orabona, C., Vacca, C., Bianchi, R., Belladonna, M. L., Fioretti, M. C., Alegre, M.-L., & Puccetti, P. (2003). Modulation of tryptophan catabolism by regulatory T cells. Nature Immunology, 4(12), 1206–1212. https://doi.org/10.1038/ni1003

Foeng, J., Comerford, I., & McColl, S. R. (2022). Harnessing the chemokine system to home CAR-T cells into solid tumors. Cell Reports Medicine, 3(3), 100543. https://doi.org/10.1016/j.xcrm.2022.100543

Froelich, W. (2021). CAR NK Cell Therapy Directed Against Pancreatic Cancer. Oncology Times, 43(11), 46–46. https://doi.org/10.1097/01.COT.0000754736.41993.ee

Fuchs, Y., & Steller, H. (2011). Programmed Cell Death in Animal Development and Disease. Cell, 147(4), 742–758. https://doi.org/10.1016/j.cell.2011.10.033

Fuchs, Y., & Steller, H. (2015). Live to die another way: modes of programmed cell death and the signals emanating from dying cells. Nature Reviews Molecular Cell Biology, 16(6), 329–344. https://doi.org/10.1038/nrm3999

Fucikova, J., Kepp, O., Kasikova, L., Petroni, G., Yamazaki, T., Liu, P., Zhao, L., Spisek, R., Kroemer, G., & Galluzzi, L. (2020). Detection of immunogenic cell death and its relevance for cancer therapy. Cell Death and Disease, 11(11). https://doi.org/10.1038/s41419-020-03221-2

Gabrilovich, D. I. (2017). Myeloid-Derived Suppressor Cells. Cancer Immunology Research, 5(1), 3–8. https://doi.org/10.1158/2326-6066.CIR-16-0297

Galluzzi, L., Buqué, A., Kepp, O., Zitvogel, L., & Kroemer, G. (2017). Immunogenic cell death in cancer and infectious disease. In Nature Reviews Immunology. 17(2), 97–111. Nature Publishing Group. https://doi.org/10.1038/nri.2016.107

Ganss, R., Ryschich, E., Klar, E., Arnold, B., & Hämmerling, G. J. (2002). Combination of T-cell therapy and trigger of inflammation induces remodeling of the vasculature and tumor eradication. Cancer Research, 62(5), 1462–1470.

Gesteland RF, Cech TR, & Atkins JF. (1999). The RNA World . Cold Spring Harbor Laboratory Press.

Gillen, S., Schuster, T., Büschenfelde, C. M. Zum, Friess, H., & Kleeff, J. (2010). Preoperative/neoadjuvant therapy in pancreatic cancer: A systematic review and

meta-analysis of response and resection percentages. PLoS Medicine, 7(4), 1–15. https://doi.org/10.1371/journal.pmed.1000267

Golan, T., Hammel, P., Reni, M., Custem, E., Macarulla, T., Hall, M., Park, J.-O., Hochhauser, D., Arnold, D., Oh, D.-Y., Reinacher-Schick, A., Tortora, G., Algül, H., O'Reilly, E., McGuinness, D., Cui, K., Schlienger, Ka., Locker, G., & Kindler, H. (2019). Maintenance Olaparib for Metastatic Pancreatic Cancer. In New England Journal of Medicine. 38(15), 1491–1493. https://doi.org/10.1056/nejmc1911185

Gorchs, L., Oosthoek, M., Yucel-Lindberg, T., Moro, C. F., & Kaipe, H. (2022). Chemokine Receptor Expression on T Cells Is Modulated by CAFs and Chemokines Affect the Spatial Distribution of T Cells in Pancreatic Tumors. Cancers, 14(15), 3826. https://doi.org/10.3390/cancers14153826

Groom, J. R., & Luster, A. D. (2011). CXCR3 in T cell function. Experimental Cell Research, 317(5), 620–631. https://doi.org/10.1016/j.yexcr.2010.12.017

Gross, G., Waks, T., & Eshhar, Z. (1989). Expression of immunoglobulin-T-cell receptor chimeric molecules as functional receptors with antibody-type specificity. Proceedings of the National Academy of Sciences of the United States of America, 86(24), 10024–10028. https://doi.org/10.1073/pnas.86.24.10024

Guedan, S., Madar, A., Casado-Medrano, V., Shaw, C., Wing, A., Liu, F., Young, R. M., June, C. H., & Posey, A. D. (2020). Single residue in CD28-costimulated CAR-T cells limits long-term persistence and antitumor durability. Journal of Clinical Investigation, 130(6), 3087–3097. https://doi.org/10.1172/JCI133215

Gumber, D., & Wang, L. D. (2022). Improving CAR-T immunotherapy: Overcoming the challenges of T cell exhaustion. EBioMedicine, 77, 103941. https://doi.org/10.1016/j.ebiom.2022.103941

Harlin, H., Meng, Y., Peterson, A. C., Zha, Y., Tretiakova, M., Slingluff, C., McKee, M., & Gajewski, T. F. (2009). Chemokine Expression in Melanoma Metastases Associated with CD8+ T-Cell Recruitment. Cancer Research, 69(7), 3077–3085. https://doi.org/10.1158/0008-5472.CAN-08-2281

Heidegger, S., Kreppel, D., Bscheider, M., Stritzke, F., Nedelko, T., Wintges, A., Bek, S., Fischer, J. C., Graalmann, T., Kalinke, U., Bassermann, F., Haas, T., & Poeck, H. (2019). RIG-I activating immunostimulatory RNA boosts the efficacy of anticancer vaccines and synergizes with immune checkpoint blockade. EBioMedicine, 41, 146–155. https://doi.org/10.1016/j.ebiom.2019.02.056

Ho, W. J., Jaffee, E. M., & Zheng, L. (2020). The tumour microenvironment in pancreatic cancer — clinical challenges and opportunities. In Nature Reviews Clinical Oncology. 17(9), 527–540. Nature Research. https://doi.org/10.1038/s41571-020-0363-5

Hong, M., Puaux, A.-L., Huang, C., Loumagne, L., Tow, C., Mackay, C., Kato, M., Prévost-Blondel, A., Avril, M.-F., Nardin, A., & Abastado, J.-P. (2011). Chemotherapy Induces Intratumoral Expression of Chemokines in Cutaneous Melanoma, Favoring T-cell Infiltration and Tumor Control. Cancer Research, 71(22), 6997–7009. https://doi.org/10.1158/0008-5472.CAN-11-1466

Hornung, V., Ellegast, J., Kim, S., Brzózka, K., Jung, A., Kato, H., Poeck, H., Akira, S., Conzelmann, K.-K., Schlee, M., Endres, S., & Hartmann, G. (2006). 5'-Triphosphate RNA Is the Ligand for RIG-I. Science, 314(5801), 994–997. https://doi.org/10.1126/science.1132505

Hruban, R. H., Adsay, N. V., Albores-Saavedra, J., Compton, C., Garrett, E. S., Goodman, S. N., Kern, S. E., Klimstra, D. S., Klöppel, G., Longnecker, D. S., Lüttges, J., & Offerhaus, G. J. A. (2001). Pancreatic intraepithelial neoplasia: A new nomenclature and classification system for pancreatic duct lesions. American Journal of Surgical Pathology, 25(5), 579–586. https://doi.org/10.1097/00000478-200105000-00003

Hu, H., Hang, J.-J., Han, T., Zhuo, M., Jiao, F., & Wang, L.-W. (2016). The M2 phenotype of tumor-associated macrophages in the stroma confers a poor prognosis in pancreatic cancer. Tumor Biology, 37(7), 8657–8664. https://doi.org/10.1007/s13277-015-4741-z

Huber, J. P., & David Farrar, J. (2011). Regulation of effector and memory T-cell functions by type I interferon. Immunology, 132(4), 466–474. https://doi.org/10.1111/j.1365-2567.2011.03412.x

Huffman, A. P., Lin, J. H., Kim, S. I., Byrne, K. T., & Vonderheide, R. H. (2020). CCL5 mediates CD40-driven CD4+ T cell tumor infiltration and immunity. JCI Insight. 2020 May 21;5(10):e137263. https://doi.org/10.1172/jci.insight.137263

Hughes, C. E., & Nibbs, R. J. B. (2018). A guide to chemokines and their receptors. In FEBS Journal. 285(16), 2944–2971. https://doi.org/10.1111/febs.14466

Ichim, C. V. (2005). Revisiting immunosurveillance and immunostimulation: Implications for cancer immunotherapy. Journal of Translational Medicine, 3, 1–13. https://doi.org/10.1186/1479-5876-3-8

Iurescia, S., Fioretti, D., & Rinaldi, M. (2020). The Innate Immune Signalling Pathways: Turning RIG-I Sensor Activation against Cancer. Cancers (Basel). 27;12(11):3158. https://doi.org/10.3390/cancers12113158

Janeway, C. A., Travers, P., Walport, M., & Shlomchik, M. J. (2001). Immunobiology (5th ed.). Garland Science.

Jiang, X., Muthusamy, V., Fedorova, O., Kong, Y., Kim, D. J., Bosenberg, M., Pyle, A. M., & Iwasaki, A. (2019). Intratumoral delivery of RIG-I agonist SLR14 induces robust antitumor responses. Journal of Experimental Medicine. 2;216(12):2854-2868. https://doi.org/10.1084/jem.20190801

Jiang, Y., Zhang, H., Wang, J., Chen, J., Guo, Z., Liu, Y., & Hua, H. (2023). Exploiting RIG-I-like receptor pathway for cancer immunotherapy. Journal of Hematology & Oncology, 16(1), 8. https://doi.org/10.1186/s13045-023-01405-9

Jin, J., Lin, J., Xu, A., Lou, J., Qian, C., Li, X., Wang, Y., Yu, W., & Tao, H. (2021). CCL2: An Important Mediator Between Tumor Cells and Host Cells in Tumor Microenvironment. Front Oncol. 2021 Jul 27;11:722916.https://doi.org/10.3389/fonc.2021.722916

Johansson, A., Hamzah, J., Payne, C. J., & Ganss, R. (2012). Tumor-targeted TNFα stabilizes tumor vessels and enhances active immunotherapy. Proceedings of the National Academy of Sciences, 109(20), 7841–7846. https://doi.org/10.1073/pnas.1118296109

Johnson, L. R., Lee, D. Y., Eacret, J. S., Ye, D., June, C. H., & Minn, A. J. (2021). The immunostimulatory RNA RN7SL1 enables CAR-T cells to enhance autonomous and endogenous immune function. Cell, 1–15. https://doi.org/10.1016/j.cell.2021.08.004

Kagoya, Y., Tanaka, S., Guo, T., Anczurowski, M., Wang, C. H., Saso, K., Butler, M. O., Minden, M. D., & Hirano, N. (2018). A novel chimeric antigen receptor containing a JAK-STAT signaling domain mediates superior antitumor effects. Nature Medicine, 24(3), 352–359. https://doi.org/10.1038/nm.4478

Kamisawa, T., Wood, L. D., Itoi, T., & Takaori, K. (2016). Pancreatic cancer. The Lancet, 388(10039), 73–85. https://doi.org/10.1016/S0140-6736(16)00141-0

Kantari, C., Pederzoli-Ribeil, M., & Witko-Sarsat, V. (2008). The Role of Neutrophils and Monocytes in Innate Immunity. Contrib Microbiol, 15, 118–146. https://doi.org/doi: 10.1159/000136335.

Karches, C. H., Benmebarek, M. R., Schmidbauer, M. L., Kurzay, M., Klaus, R., Geiger, M., Rataj, F., Cadilha, B. L., Lesch, S., Heise, C., Murr, R., Vom Berg, J., Jastroch, M., Lamp, D., Ding, J., Duewell, P., Niederfellner, G., Sustmann, C., Endres, S., … Kobold, S. (2019). Bispecific antibodies enable synthetic agonisti receptor-transduced T cells for tumor immunotherapy. Clinical Cancer Research, 25(19), 5890–5900. https://doi.org/10.1158/1078-0432.CCR-18-3927

Karin, N. (2020). CXCR3 Ligands in Cancer and Autoimmunity, Chemoattraction of Effector T Cells, and Beyond. Frontiers in Immunology. 29;11:976. https://doi.org/10.3389/fimmu.2020.00976

Kim, S., Park, M., & Cho, M. (2018). Interleukin-10 produced by myeloid-derived suppressor cells is critical for the induction of tregs and attenuation of rheumatoid inflammation in mice. Cytotherapy, 20(5), e8. https://doi.org/10.1016/j.jcyt.2018.03.026

Kim, T. K., & Eberwine, J. H. (2010). Mammalian cell transfection: The present and the future. Analytical and Bioanalytical Chemistry, 397(8), 3173–3178. https://doi.org/10.1007/s00216-010-3821-6

Kroemer, G., Galassi, C., Zitvogel, L., & Galluzzi, L. (2022). Immunogenic cell stress and death. In Nature Immunology . 23(4), 487–500. Nature Research. https://doi.org/10.1038/s41590-022-01132-2

Krysko, D. v., Garg, A. D., Kaczmarek, A., Krysko, O., Agostinis, P., & Vandenabeele, P. (2012). Immunogenic cell death and DAMPs in cancer therapy. Nature Reviews Cancer, 12(12), 860–875. https://doi.org/10.1038/nrc3380

Kuhl, N., Linder, A., Philipp, N., Nixdorf, D., Fischer, H., Veth, S., Kuut, G., Xu, T. T., Theurich, S., Carell, T., Subklewe, M., & Hornung, V. (2023). STING agonism

turns human T cells into interferon-producing cells but impedes their functionality. EMBO Reports, 6;24(3):e55536.https://doi.org/10.15252/embr.202255536

Le, D., Durham, J., Smith, K., Wnag, H., Bartlett, B., Aulakh, L., Lu, S., Kemberling, H., Wilt, C., Luber, B. S., Wong, F., Azad, N. S., Rucki, A. A., Laheru, D., Donehower, R., Zaheer, A., Fisher, G. A., Crocenzi, T. S., Lee, J. J., … Diaz, L. A. (2017). Mismatch-repair deficiency predicts response of solid tumors to PD-1 blockade. Physiology & Behavior, 176(12), 139–148. https://doi.org/10.1126/science.aan6733.Mismatch-repair

Lee, J. W., Komar, C. A., Bengsch, F., Graham, K., & Beatty, G. L. (2016a). Genetically engineered mouse models of pancreatic cancer: The KPC model (LSL-KrasG12D/+;LSL-Trp53R172H/+;Pdx-1-Cre), its variants, and their application in immuno-oncology drug discovery. Current Protocols in Pharmacology, 2016, 14.39.1-14.39.20. https://doi.org/10.1002/cpph.2

Lee, J. W., Komar, C. A., Bengsch, Fee., Graham, Kathleen., & Beatty, G. L. (2016b). Genetically Engineered Mouse Models of Pancreatic Cancer : The. Current Protocols in Pharmacology, 465, 1–28. https://doi.org/10.1002/cpph.2.Genetically

Lemoine, J., Ruella, M., & Houot, R. (2021). Born to survive : how cancer cells resist CAR T cell therapy. Journal of Hematology & Oncology 14,199 1–12. https://doi.org/10.1186/s13045-021-01209-9

Lesch, S., Blumenberg, V., Stoiber, S., Gottschlich, A., Ogonek, J., Cadilha, B. L., Dantes, Z., Rataj, F., Dorman, K., Lutz, J., Karches, C. H., Heise, C., Kurzay, M., Larimer, B. M., Grassmann, S., Rapp, M., Nottebrock, A., Kruger, S., Tokarew, N., … Kobold, S. (2021). T cells armed with C-X-C chemokine receptor type 6 enhance adoptive cell therapy for pancreatic tumours. Nature Biomedical Engineering, 5(11), 1246–1260. https://doi.org/10.1038/s41551-021-00737-6

Li, C., Yang, N., Li, H., & Wang, Z. (2020). Robo1-specific chimeric antigen receptor natural killer cell therapy for pancreatic ductal adenocarcinoma with liver metastasis. Journal of Cancer Research and Therapeutics, 16(2):393-396. https://doi.org/10.4103/jcrt.JCRT_190_20

Li, J., Byrne, K. T., Yan, F., Yamazoe, T., Chen, Z., Baslan, T., Richman, L. P., Lin, J. H., Sun, Y. H., Rech, A. J., Balli, D., Hay, C. A., Sela, Y., Merrell, A. J., Liudahl, S. M., Gordon, N., Norgard, R. J., Yuan, S., Yu, S., … Stanger, B. Z. (2018). Tumor Cell-Intrinsic Factors Underlie Heterogeneity of Immune Cell Infiltration and Response to Immunotherapy. Immunity, 17;49(1):178-193.e7. https://doi.org/10.1016/j.immuni.2018.06.006

Li, Q., Wang, Y., Lin, M., Xia, L., Bao, Y., Sun, X., & Yang, L. (2019). Abstract A014: Phase I clinical trial with PD-1/MUC1 CAR-pNK92 immunotherapy. Cancer Immunology Research, 7(2_Supplement), A014–A014. https://doi.org/10.1158/2326-6074.CRICIMTEATIAACR18-A014

Lim, W. A., & June, C. H. (2017). The Principles of Engineering Immune Cells to Treat Cancer. Cell, 168(4), 724–740. https://doi.org/10.1016/j.cell.2017.01.016

Lin, R. A., Lin, J. K., & Lin, S. Y. (2021). Mechanisms of immunogenic cell death and immune checkpoint blockade therapy. Kaohsiung Journal of Medical Sciences, 37(6), 448–458. https://doi.org/10.1002/kjm2.12375

Liu, Y., Cai, Y., Liu, L., Wu, Y., & Xiong, X. (2018). Crucial biological functions of CCL7 in cancer. PeerJ, 2018(6). https://doi.org/10.7717/peerj.4928

Liu, Y., Guo, Y., Wu, Z., Feng, K., Tong, C., Wang, Y., Dai, H., Shi, F., Yang, Q., & Han, W. (2020). Anti-EGFR chimeric antigen receptor-modified T cells in metastatic pancreatic carcinoma: A phase I clinical trial. Cytotherapy, 22(10):573-580. https://doi.org/10.1016/j.jcyt.2020.04.088

Loetscher, M., Loetscher, P., Brass, N., Meese, E., & Moser, B. (1998). Lymphocyte-specific chemokine receptor CXCR3: regulation, chemokine binding and gene localization. European Journal of Immunology, 28(11), 3696–3705. https://doi.org/10.1002/(SICI)1521-4141(199811)28:11<3696::AID-IMMU3696>3.0.CO;2-W

Loo, Y. M., & Gale, M. (2011). Immune Signaling by RIG-I-like Receptors. Immunity, 34(5), 680–692. https://doi.org/10.1016/j.immuni.2011.05.003

Luo, Q., Napoleon, J. v., Liu, X., Zhang, B., Zheng, S., & Low, P. S. (2022). Targeted Rejuvenation of Exhausted Chimeric Antigen Receptor T Cells Regresses Refractory Solid Tumors. Molecular Cancer Research, 20(5), 823–833. https://doi.org/10.1158/1541-7786.MCR-21-0711

Majzner, R. G., & Mackall, C. L. (2018). Tumor antigen escape from car t-cell therapy. Cancer Discovery, 8(10), 1219–1226. https://doi.org/10.1158/2159-8290.CD-18-0442

Mak, I. W. Y., Evaniew, N., & Ghert, M. (2014). Lost in translation: Animal models and clinical trials in cancer treatment. American Journal of Translational Research, 6(2), 114–118.

Maleki Vareki, S. (2018). High and low mutational burden tumors versus immunologically hot and cold tumors and response to immune checkpoint inhibitors. Journal for ImmunoTherapy of Cancer, 6(1), 4–8. https://doi.org/10.1186/s40425-018-0479-7

Marofi, F., Motavalli, R., Safonov, V. A., Thangavelu, L., Yumashev, A. V., Alexander, M., Shomali, N., Chartrand, M. S., Pathak, Y., Jarahian, M., Izadi, S., Hassanzadeh, A., Shirafkan, N., Tahmasebi, S., & Khiavi, F. M. (2021). CAR T cells in solid tumors: challenges and opportunities. Stem Cell Research and Therapy, 12(1), 1–16. https://doi.org/10.1186/s13287-020-02128-1

Matveeva, O. V., & Chumakov, P. M. (2018). Defects in interferon pathways as potential biomarkers of sensitivity to oncolytic viruses. Reviews in Medical Virology, 28(6), 1–13. https://doi.org/10.1002/rmv.2008

Medrano, R. F. V., Hunger, A., Mendonça, S. A., Barbuto, J. A. M., & Strauss, B. E. (2017). Immunomodulatory and antitumor effects of type I interferons and their application in cancer therapy. In Oncotarget. 8(41), 71249-71284 https://doi.org/10.18632/oncotarget.19531

Mehta, R. S., Randolph, B., Daher, M., & Rezvani, K. (2018). NK cell therapy for hematologic malignancies. In International Journal of Hematology. 107(3), 262–270. Springer Tokyo. https://doi.org/10.1007/s12185-018-2407-5

Metzger, P., Kirchleitner, S. v., Kluge, M., Koenig, L. M., Hörth, C., Rambuscheck, C. A., Böhmer, D., Ahlfeld, J., Kobold, S., Friedel, C. C., Endres, S., Schnurr, M., & Duewell, P. (2019). Immunostimulatory RNA leads to functional reprogramming of myeloid-derived suppressor cells in pancreatic cancer. Journal for ImmunoTherapy of Cancer, 7(1), 1–16. https://doi.org/10.1186/s40425-019-0778-7

Moore, M. J., Goldstein, D., Hamm, J., Figer, A., Hecht, J. R., Gallinger, S., Au, H. J., Murawa, P., Walde, D., Wolff, R. A., Campos, D., Lim, R., Ding, K., Clark, G., Voskoglou-Nomikos, T., Ptasynski, M., & Parulekar, W. (2007). Erlotinib plus gemcitabine compared with gemcitabine alone in patients with advanced pancreatic cancer: A phase III trial of the National Cancer Institute of Canada Clinical Trials Group. Journal of Clinical Oncology, 25(15), 1960–1966. https://doi.org/10.1200/JCO.2006.07.9525

Morgan, R. A., Yang, J. C., Kitano, M., Dudley, M. E., Laurencot, C. M., & Rosenberg, S. A. (2010). Case Report of a Serious Adverse Event Following the Administration of T Cells Transduced With a Chimeric Antigen Receptor Recognizing ErbB2. Molecular Therapy, 18(4), 843–851. https://doi.org/10.1038/mt.2010.24

Morrison, A. H., Byrne, K. T., & Vonderheide, R. H. (2018). Immunotherapy and Prevention of Pancreatic Cancer. Trends in Cancer, 4(6), 418–428. https://doi.org/10.1016/j.trecan.2018.04.001

Motz, G. T., & Coukos, G. (2013). Deciphering and Reversing Tumor Immune Suppression. Immunity, 39(1), 61–73. https://doi.org/10.1016/j.immuni.2013.07.005

Mukaida, N. (2014). Chemokines. Reference Module in Biomedical Sciences. https://doi.org/10.1016/B978-0-12-801238-3.04041-1

Mukaida, N., Sasaki, S., & Baba, T. (2020). CCL4 Signaling in the Tumor Microenvironment. 1231:23-32. https://doi.org/10.1007/978-3-030-36667-4_3

Murakami, T., Hiroshima, Y., Matsuyama, R., Homma, Y., Hoffman, R. M., & Endo, I. (2019). Role of the tumor microenvironment in pancreatic cancer. In Annals of Gastroenterological Surgery. 3(2), 130–137. Wiley-Blackwell Publishing Ltd. https://doi.org/10.1002/ags3.12225

Murata, M., Nabeshima, S., Kikuchi, K., Yamaji, K., Furuyso, N., & Hayashi, J. (2006). A comparison of the antitumor effects of interferon-α and β on human hepatocellular carcinoma cell lines. Cytokine, 33(3), 121–128. https://doi.org/10.1016/j.cyto.2005.08.011

Murooka, T. T., Wong, M. M., Rahbar, R., Majchrzak-Kita, B., Proudfoot, A. E. I., & Fish, E. N. (2006). CCL5-CCR5-mediated apoptosis in T cells: Requirement for glycosaminoglycan binding and CCL5 aggregation. Journal of Biological Chemistry, 281(35), 25184–25194. https://doi.org/10.1074/jbc.M603912200

Neesse, A., Bauer, C. A., Öhlund, D., Lauth, M., Buchholz, M., Michl, P., Tuveson, D. A., & Gress, T. M. (2019). Stromal biology and therapy in pancreatic cancer: ready for clinical translation? Gut, 68(1), 159–171. https://doi.org/10.1136/gutjnl-2018-316451

Neoptolemos, J. P., Kleeff, J., Michl, P., Costello, E., Greenhalf, W., & Palmer, D. H. (2018). Therapeutic developments in pancreatic cancer: Current and future perspectives. Nature Reviews Gastroenterology and Hepatology, 15(6), 333–348. https://doi.org/10.1038/s41575-018-0005-x

Nguyen, A., Johanning, G., & Shi, Y. (2022). Emerging Novel Combined CAR-T Cell Therapies. In Cancers. 14(6), 1403. MDPI. https://doi.org/10.3390/cancers14061403

Nguyen, L. T., Saibil, S. D., Sotov, V., Le, M. X., Khoja, L., Ghazarian, D., Bonilla, L., Majeed, H., Hogg, D., Joshua, A. M., Crump, M., Franke, N., Spreafico, A., Hansen, A., Al-Habeeb, A., Leong, W., Easson, A., Reedijk, M., Goldstein, D. P., … Butler, M. O. (2019). Phase II clinical trial of adoptive cell therapy for patients with metastatic melanoma with autologous tumor-infiltrating lymphocytes and low-dose interleukin-2. Cancer Immunology, Immunotherapy, 68(5), 773–785. https://doi.org/10.1007/s00262-019-02307-x

Oh, S. A., Wu, D. C., Cheung, J., Navarro, A., Xiong, H., Cubas, R., Totpal, K., Chiu, H., Wu, Y., Comps-Agrar, L., Leader, A. M., Merad, M., Roose-Germa, M., Warming, S., Yan, M., Kim, J. M., Rutz, S., & Mellman, I. (2020). PD-L1 expression by dendritic cells is a key regulator of T-cell immunity in cancer. Nature Cancer, 1(7), 681–691. https://doi.org/10.1038/s43018-020-0075-x

Öhlund, D., Handly-Santana, A., Biffi, G., Elyada, E., Almeida, A. S., Ponz-Sarvise, M., Corbo, V., Oni, T. E., Hearn, S. A., Lee, E. J., Chio, I. I. C., Hwang, C.-I., Tiriac, H., Baker, L. A., Engle, D. D., Feig, C., Kultti, A., Egeblad, M., Fearon, D. T., … Tuveson, D. A. (2017). Distinct populations of inflammatory fibroblasts and myofibroblasts in pancreatic cancer. Journal of Experimental Medicine, 214(3), 579–596. https://doi.org/10.1084/jem.20162024

Onomoto, K., Onoguchi, K., & Yoneyama, M. (2021). Regulation of RIG-I-like receptor-mediated signaling: interaction between host and viral factors. In Cellular and Molecular Immunology. 18(3), 539–555. Springer Nature. https://doi.org/10.1038/s41423-020-00602-7

Orth, M., Metzger, P., Gerum, S., Mayerle, J., Schneider, G., Belka, C., Schnurr, M., & Lauber, K. (2019). Pancreatic ductal adenocarcinoma: Biological hallmarks, current status, and future perspectives of combined modality treatment approaches. Radiation Oncology, 14(1), 1–20. https://doi.org/10.1186/s13014-019-1345-6

Padrón, L. J., Maurer, D. M., O'Hara, M. H., O'Reilly, E. M., Wolff, R. A., Wainberg, Z. A., Ko, A. H., Fisher, G., Rahma, O., Lyman, J. P., Cabanski, C. R., Yu, J. X., Pfeiffer, S. M., Spasic, M., Xu, J., Gherardini, P. F., Karakunnel, J., Mick, R., Alanio, C., … Vonderheide, R. H. (2022). Sotigalimab and/or nivolumab with chemotherapy in first-line metastatic pancreatic cancer: clinical and immunologic analyses from the randomized phase 2 PRINCE trial. Nature Medicine, 28(6), 1167–1177. https://doi.org/10.1038/s41591-022-01829-9

Pandiyan, P., Zheng, L., Ishihara, S., Reed, J., & Lenardo, M. J. (2007). CD4+CD25+Foxp3+ regulatory T cells induce cytokine deprivation–mediated apoptosis of effector CD4+ T cells. Nature Immunology, 8(12), 1353–1362. https://doi.org/10.1038/ni1536

Pant, A., & Jackson, C. M. (2022). Supercharged chimeric antigen receptor T cells in solid tumors. Journal of Clinical Investigation, 132(16). https://doi.org/10.1172/JCI162322

Park, J. H., Isabelle Rivière, Gonen, M., Wang, X., Sénéchal, B., Curran, K. J., Sauter, C., Wang, Y., Santomasso, B., Ph.D., E. M., Roshal, M., Maslak, P., Davila, M., Ph.D., R., Brentjens, J., & Sadelain, M. (2018). Long-Term Follow-up of CD19 CAR Therapy in Acute Lymphoblastic Leukemia. Physiology & Behavior, 378(5), 449–459. https://doi.org/10.1056/NEJMoa1709919.Long-Term

Parkin, J., & Bryony, C. (2001). An overview of the immune system. Lancet, 357, 1777–1789. https://doi.org/10.7748/ns2008.12.23.15.47.c6738

Patel, U., Abernathy, J., Savani, B. N., Oluwole, O., Sengsayadeth, S., & Dholaria, B. (2021). CAR T cell therapy in solid tumors: A review of current clinical trials. EJHaem, 3(S1), 24–31. https://doi.org/10.1002/jha2.356

Philipp Metzger. (2019). Myeloid-derived suppressor cells (MDSC) in murine pancreatic cancer: Role of IRF4 in development and function of MDSC in RIG-I-like helicase-based immunotherapy. LMU.

Pietrobon, V., Todd, L. A., Goswami, A., Stefanson, O., Yang, Z., & Marincola, F. (2021a). Improving CAR T-Cell Persistence. International Journal of Molecular Sciences, 22(19), 10828. https://doi.org/10.3390/ijms221910828

Pietrobon, V., Todd, L. A., Goswami, A., Stefanson, O., Yang, Z., & Marincola, F. (2021b). Improving car t-cell persistence. International Journal of Molecular Sciences, 22(19), 1–27. https://doi.org/10.3390/ijms221910828

Platanias, L. C., Uddin, S., Domanski, P., & Colamonici, O. R. (1996). Differences in Interferon α and β Signaling. Journal of Biological Chemistry, 271(39), 23630–23633. https://doi.org/10.1074/jbc.271.39.23630

Poh, A. R., & Ernst, M. (2021). Tumor-Associated Macrophages in Pancreatic Ductal Adenocarcinoma: Therapeutic Opportunities and Clinical Challenges. Cancers, 13(12), 2860. https://doi.org/10.3390/cancers13122860

Previdi, A. (1968). Contribution to the knowledge of osteopetrosis. In Minerva Ortopedica e Traumatologica. 19(6), 274–281.

Provenzano, P. P., Cuevas, C., Chang, A. E., Goel, V. K., Von Hoff, D. D., & Hingorani, S. R. (2012). Enzymatic Targeting of the Stroma Ablates Physical Barriers to Treatment of Pancreatic Ductal Adenocarcinoma. Cancer Cell, 21(3), 418–429. https://doi.org/10.1016/j.ccr.2012.01.007

Rapp, M., Grassmann, S., Chaloupka, M., Layritz, P., Kruger, S., Ormanns, S., Rataj, F., Janssen, K. P., Endres, S., Anz, D., & Kobold, S. (2016a). C-C chemokine receptor type-4 transduction of T cells enhances interaction with dendritic cells,

tumor infiltration and therapeutic efficacy of adoptive T cell transfer. OncoImmunology, 5(3), 1–12. https://doi.org/10.1080/2162402X.2015.1105428

Rapp, M., Grassmann, S., Chaloupka, M., Layritz, P., Kruger, S., Ormanns, S., Rataj, F., Janssen, K.-P., Endres, S., Anz, D., & Kobold, S. (2016b). C-C chemokine receptor type-4 transduction of T cells enhances interaction with dendritic cells, tumor infiltration and therapeutic efficacy of adoptive T cell transfer. OncoImmunology, 5(3), e1105428. https://doi.org/10.1080/2162402X.2015.1105428

Rehwinkel, J., & Gack, M. U. (2020). RIG-I-like receptors: their regulation and roles in RNA sensing. In Nature Reviews Immunology. 20(9), 537–551. Nature Research. https://doi.org/10.1038/s41577-020-0288-3

Richmond, A. (2002). NF-κB, chemokine gene transcription and tumour growth. In Nature Reviews Immunology. 2(9), 664–674. https://doi.org/10.1038/nri887

Rojas, L. A., Sethna, Z., Soares, K. C., Olcese, C., Pang, N., Patterson, E., Lihm, J., Ceglia, N., Guasp, P., Chu, A., Yu, R., Chandra, A. K., Waters, T., Ruan, J., Amisaki, M., Zebboudj, A., Odgerel, Z., Payne, G., Derhovanessian, E., … Balachandran, V. P. (2023). Personalized RNA neoantigen vaccines stimulate T cells in pancreatic cancer. Nature, 1–7. https://doi.org/10.1038/s41586-023-06063-y

Rosenberg, S. A., & Restifo, N. P. (2015). Adoptive cell transfer as personalized immunotherapy for human cancer. Science, 348(6230), 62–68. https://doi.org/10.1126/science.aaa4967

Royal, R. E., Levy, C., Turner, K., Mathur, A., Hughes, M., Kammula, U. S., Sherry, R. M., Topalian, S. L., Yang, J. C., Lowy, I., & Rosenberg, S. A. (2010). Phase 2 trial of single agent ipilimumab (Anti-CTLA-4) for locally advanced or metastatic pancreatic adenocarcinoma. In Journal of Immunotherapy. 33(8), 828–833). https://doi.org/10.1097/CJI.0b013e3181eec14c

Runkel, L., Pfeffer, L., Lewerenz, M., Monneron, D., Yang, C. H., Murti, A., Pellegrini, S., Goelz, S., Uzé, G., & Mogensen, K. (1998). Differences in Activity between α and β Type I Interferons Explored by Mutational Analysis. Journal of Biological Chemistry, 273(14), 8003–8008. https://doi.org/10.1074/jbc.273.14.8003

Ruzicka, M., Koenig, L. M., Formisano, S., Boehmer, D. F. R., Vick, B., Heuer, E.-M., Meinl, H., Kocheise, L., Zeitlhöfler, M., Ahlfeld, J., Kobold, S., Endres, S., Subklewe, M., Duewell, P., Schnurr, M., Jeremias, I., Lichtenegger, F. S., & Rothenfusser, S. (2020). RIG-I-based immunotherapy enhances survival in preclinical AML models and sensitizes AML cells to checkpoint blockade. Leukemia, 34(4), 1017–1026. https://doi.org/10.1038/s41375-019-0639-x

Sankpal, N. V., Brown, T. C., Fleming, T. P., Herndon, J. M., Amaravati, A. A., Loynd, A. N., & Gillanders, W. E. (2021). Cancer-associated mutations reveal a novel role for EpCAM as an inhibitor of cathepsin-L and tumor cell invasion. BMC Cancer, 21(1), 1–13. https://doi.org/10.1186/s12885-021-08239-z

Sarén, T. (2022). CAR T cells for Immunotherapy of Cancer. Dissertation, Uppsala University: Department of Immunology, Genetics and Pathology.

Schaft, N. (2020). The landscape of car-t cell clinical trials against solid tumors—a comprehensive overview. Cancers, 12(9), 1–36. https://doi.org/10.3390/cancers12092567

Schlee, M., Roth, A., Hornung, V., Hagmann, C. A., Wimmenauer, V., Barchet, W., Coch, C., Janke, M., Mihailovic, A., Wardle, G., Juranek, S., Kato, H., Kawai, T., Poeck, H., Fitzgerald, K. A., Takeuchi, O., Akira, S., Tuschl, T., Latz, E., … Hartmann, G. (2009). Recognition of 5′ Triphosphate by RIG-I Helicase Requires Short Blunt Double-Stranded RNA as Contained in Panhandle of Negative-Strand Virus. Immunity, 31(1), 25–34. https://doi.org/10.1016/j.immuni.2009.05.008

Schneider, W. M., Chevillotte, M. D., & Rice, C. M. (2014). Interferon-stimulated genes: A complex web of host defenses. In Annual Review of Immunology. 32, 513–545. Annual Reviews Inc. https://doi.org/10.1146/annurev-immunol-032713-120231

Schnittert, J., Bansal, R., & Prakash, J. (2019). Targeting Pancreatic Stellate Cells in Cancer. In Trends in Cancer. 5(2), 128–142. Cell Press. https://doi.org/10.1016/j.trecan.2019.01.001

Schoggins, J. W., & Rice, C. M. (2011). Interferon-stimulated genes and their antiviral effector functions. Current Opinion in Virology, 1(6), 519–525. https://doi.org/10.1016/j.coviro.2011.10.008

Shiow, L. R., Rosen, D. B., Brdičková, N., Xu, Y., An, J., Lanier, L. L., Cyster, J. G., & Matloubian, M. (2006). CD69 acts downstream of interferon-α/β to inhibit S1P1 and lymphocyte egress from lymphoid organs. Nature, 440(7083), 540–544. https://doi.org/10.1038/nature04606

Shirley, J. L., Keeler, G. D., Sherman, A., Zolotukhin, I., Markusic, D. M., Hoffman, B. E., Morel, L. M., Wallet, M. A., Terhorst, C., & Herzog, R. W. (2020). Type I IFN Sensing by cDCs and CD4+ T Cell Help Are Both Requisite for Cross-Priming of AAV Capsid-Specific CD8+ T Cells. Molecular Therapy, 28(3), 758–770. https://doi.org/10.1016/j.ymthe.2019.11.011

Shrimali, R. K., Yu, Z., Theoret, M. R., Chinnasamy, D., Restifo, N. P., & Rosenberg, S. A. (2010). Antiangiogenic Agents Can Increase Lymphocyte Infiltration into Tumor and Enhance the Effectiveness of Adoptive Immunotherapy of Cancer. Cancer Research, 70(15), 6171–6180. https://doi.org/10.1158/0008-5472.CAN-10-0153

Sidky, Y. A., & Borden, E. C. (1987). Inhibition of angiogenesis by interferons: effects on tumor- and lymphocyte-induced vascular responses. Cancer Research, 47(19), 5155–5161.

Siegel, R. L., Miller, K. D., Fuchs, H. E., & Jemal, A. (2022). Cancer statistics, 2022. CA: A Cancer Journal for Clinicians, 72(1), 7–33. https://doi.org/10.3322/caac.21708

Sivick, K. E., Desbien, A. L., Glickman, L. H., Reiner, G. L., Corrales, L., Surh, N. H., Hudson, T. E., Vu, U. T., Francica, B. J., Banda, T., Katibah, G. E., Kanne, D. B., Leong, J. J., Metchette, K., Bruml, J. R., Ndubaku, C. O., McKenna, J. M., Feng, Y., Zheng, L., … McWhirter, S. M. (2018). Magnitude of Therapeutic STING

Activation Determines CD8+ T Cell-Mediated Anti-tumor Immunity. Cell Reports, 25(11), 3074-3085.e5. https://doi.org/10.1016/j.celrep.2018.11.047

Slaney, C. Y., Kershaw, M. H., & Darcy, P. K. (2014). Trafficking of T cells into tumors. In Cancer Research. 74(24), 7168–7174. American Association for Cancer Research Inc. https://doi.org/10.1158/0008-5472.CAN-14-2458

Smith, A. J., Oertle, J., Warren, D., & Prato, D. (2016). Chimeric antigen receptor (CAR) T cell therapy for malignant cancers: Summary and perspective. Journal of Cellular Immunotherapy, 2(2), 59–68. https://doi.org/10.1016/j.jocit.2016.08.001

Srivastava, S., Furlan, S. N., Jaeger-Ruckstuhl, C. A., Sarvothama, M., Berger, C., Smythe, K. S., Garrison, S. M., Specht, J. M., Lee, S. M., Amezquita, R. A., Voillet, V., Muhunthan, V., Yechan-Gunja, S., Pillai, S. P. S., Rader, C., Houghton, A. M. G., Pierce, R. H., Gottardo, R., Maloney, D. G., & Riddell, S. R. (2021). Immunogenic Chemotherapy Enhances Recruitment of CAR-T Cells to Lung Tumors and Improves Antitumor Efficacy when Combined with Checkpoint Blockade. Cancer Cell, 39(2), 193-208.e10. https://doi.org/10.1016/j.ccell.2020.11.005

Srivastava, S., & Riddell, S. (2018). CAR T Cell Therapy: Challenges to Bench-to-Bedside Efficacy. Journal If Immunology, 200(2), 459–468. https://doi.org/doi:10.4049/jimmunol.1701155.

Stickdorn, J., Stein, L., Arnold-Schild, D., Hahlbrock, J., Medina-Montano, C., Bartneck, J., Ziß, T., Montermann, E., Kappel, C., Hobernik, D., Haist, M., Yurugi, H., Raabe, M., Best, A., Rajalingam, K., Radsak, M. P., David, S. A., Koynov, K., Bros, M., … Nuhn, L. (2022). Systemically Administered TLR7/8 Agonist and Antigen-Conjugated Nanogels Govern Immune Responses against Tumors. ACS Nano, 16(3), 4426–4443. https://doi.org/10.1021/acsnano.1c10709

Strazza, M., & Mor, A. (2020). The Complexity of Targeting Chemokines to Promote a Tumor Immune Response. Inflammation, 43(4), 1201–1208. https://doi.org/10.1007/s10753-020-01235-8

Talmadge, J. E., Singh, R. K., Fidler, I. J., & Raz, A. (2007). Murine models to evaluate novel and conventional therapeutic strategies for cancer. In American Journal of Pathology . 170(3), 793–804. American Society for Investigative Pathology Inc. https://doi.org/10.2353/ajpath.2007.060929

Tan, M. C. B., Goedegebuure, P. S., Belt, B. A., Flaherty, B., Sankpal, N., Gillanders, W. E., Eberlein, T. J., Hsieh, C.-S., & Linehan, D. C. (2009). Disruption of CCR5-Dependent Homing of Regulatory T Cells Inhibits Tumor Growth in a Murine Model of Pancreatic Cancer. The Journal of Immunology, 182(3), 1746–1755. https://doi.org/10.4049/jimmunol.182.3.1746

Taub, D. D., Turcovski-Corrales, S. M., Key, M. L., Longo, D. L., & Murphy, W. J. (1996). Chemokines and T lymphocyte activation: I. Beta chemokines costimulate human T lymphocyte activation in vitro. Journal of Immunology (Baltimore, Md.: 1950), 156(6), 2095–2103.

van Kempen, T. S., Wenink, M. H., Leijten, E. F. A., Radstake, T. R. D. J., & Boes, M. (2015). Perception of self: distinguishing autoimmunity from autoinflammation.

Nature Reviews Rheumatology, 11(8), 483–492. https://doi.org/10.1038/nrrheum.2015.60

Vonderheide, R. H., & Bear, A. S. (2020). Tumor-Derived Myeloid Cell Chemoattractants and T Cell Exclusion in Pancreatic Cancer. Frontiers in Immunology, 11. https://doi.org/10.3389/fimmu.2020.605619

Wang, Y., Chen, M., Wu, Z., Tong, C., Dai, H., Guo, Y., Liu, Y., Huang, J., Lv, H., Luo, C., Feng, K. chao, Yang, Q. ming, Li, X. lei, & Han, W. (2018). CD133-directed CAR T cells for advanced metastasis malignancies: A phase I trial. In OncoImmunology. 7(7), e1440169. https://doi.org/10.1080/2162402X.2018.1440169

Went, P. T., Lugli, A., Meier, S., Bundi, M., Mirlacher, M., Sauter, G., & Dirnhofer, S. (2004). Frequent EpCam Protein Expression in Human Carcinomas. Human Pathology, 35(1), 122–128. https://doi.org/10.1016/j.humpath.2003.08.026

Wood, L. D., & Hruban, R. H. (2012). Pathology and molecular genetics of pancreatic neoplasms. Cancer Journal (United States), 18(6), 492–501. https://doi.org/10.1097/PPO.0b013e31827459b6

Wu, J., Dobbs, N., Yang, K., & Yan, N. (2020). Interferon-Independent Activities of Mammalian STING Mediate Antiviral Response and Tumor Immune Evasion. Immunity, 53(1), 115-126.e5. https://doi.org/10.1016/j.immuni.2020.06.009

Xu, M., Wang, Y., Xia, R., Wei, Y., & Wei, X. (2021). Role of the CCL2-CCR2 signalling axis in cancer: Mechanisms and therapeutic targeting. In Cell Proliferation. 54(10), e13115. John Wiley and Sons Inc. https://doi.org/10.1111/cpr.13115

Xu, N., Palmer, D. C., Robeson, A. C., Shou, P., Bommiasamy, H., Laurie, S. J., Willis, C., Dotti, G., Vincent, B. G., Restifo, N. P., & Serody, J. S. (2021). STING agonist promotes CAR T cell trafficking and persistence in breast cancer. Journal of Experimental Medicine, 218(2). https://doi.org/10.1084/JEM.20200844

Yang, R., Yu, S., Xu, T., Zhang, J., & Wu, S. (2022). Emerging role of RNA sensors in tumor microenvironment and immunotherapy. Journal of Hematology & Oncology, 15(1), 43. https://doi.org/10.1186/s13045-022-01261-z

Yatim, K. M., & Lakkis, F. G. (2015). A Brief Journey through the Immune System. Clinical Journal of the American Society of Nephrology, 10(7), 1274–1281. https://doi.org/10.2215/CJN.10031014

Yeo, D., Giardina, C., Saxena, P., & Rasko, J. E. J. (2022). The next wave of cellular immunotherapies in pancreatic cancer. In Maintenance Olaparib for Metastatic Pancreatic Cancer (2019) N Engl J Med 381: 1491–1493.Molecular Therapy – Oncolytics. 24, 561–576). https://doi.org/10.1016/j.omto.2022.01.010

Zepeda-Cervantes, J., Ramírez-Jarquín, J. O., & Vaca, L. (2020). Interaction Between Virus-Like Particles (VLPs) and Pattern Recognition Receptors (PRRs) From Dendritic Cells (DCs): Toward Better Engineering of VLPs. In Frontiers in Immunology. 11,1100. Frontiers Media S.A. https://doi.org/10.3389/fimmu.2020.01100

Zhang, J., Li, R., & Huang, S. (2022). The immunoregulation effect of tumor microenvironment in pancreatic ductal adenocarcinoma. In Frontiers in Oncology. 12, 951019. Frontiers Media S.A. https://doi.org/10.3389/fonc.2022.951019

Zhang, Z. zheng, Wang, T., Wang, X. feng, Zhang, Y. qing, Song, S. xia, & Ma, C. qing. (2022). Improving the ability of CAR-T cells to hit solid tumors: Challenges and strategies. In Pharmacological Research. 175, 106036. Academic Press. https://doi.org/10.1016/j.phrs.2021.106036

Zhou, J., Wang, G., Chen, Y., Wang, H., Hua, Y., & Cai, Z. (2019). Immunogenic cell death in cancer therapy: Present and emerging inducers. Journal of Cellular and Molecular Medicine, 23(8), 4854–4865. https://doi.org/10.1111/jcmm.14356

Zitvogel, L., Galluzzi, L., Kepp, O., Smyth, M. J., & Kroemer, G. (2015). Type I interferons in anticancer immunity. Nature Reviews Immunology, 15(7), 405–414. https://doi.org/10.1038/nri3845

Zoglmeier, C., Bauer, H., Nörenberg, D., Wedekind, G., Bittner, P., Sandholzer, N., Rapp, M., Anz, D., Endres, S., & Bourquin, C. (2011). CpG blocks immunosuppression by myeloid-derived suppressor cells in tumor-bearing mice. Clinical Cancer Research, 17(7), 1765–1775. https://doi.org/10.1158/1078-0432.CCR-10-2672

Supplementary Figures

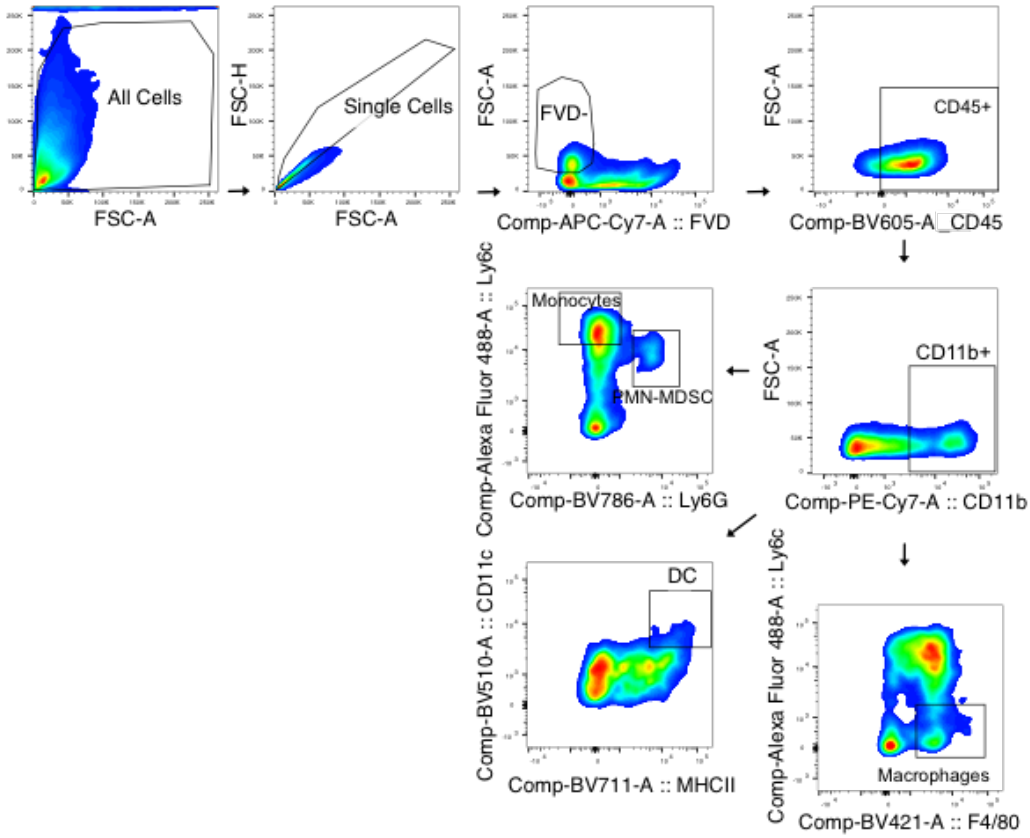

Figure S1. Gating strategy for myeloid compartment in tumor microenvironment.

Representative gating strategy for identification of myeloid populations in the single cell suspensions generated from tumors. Arrows indicate population hierarchy. Populations are labeled within the plot.

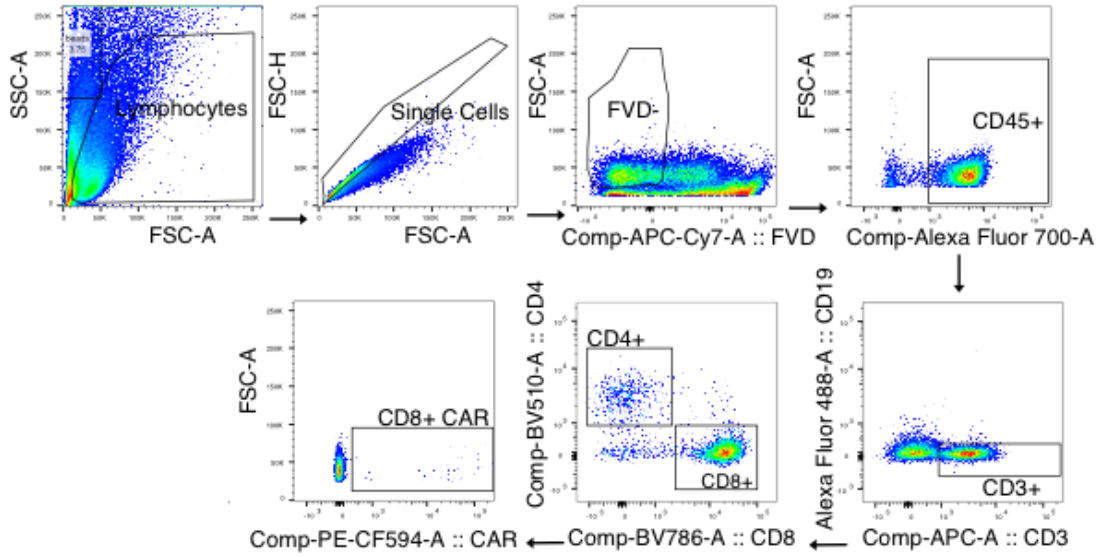

Figure S2. Gating strategy for CAR T cell infiltration in tumor microenvironment.

Representative gating strategy for identification of CAR T cells in the single cell suspensions generated from tumors. Arrows indicate population hierarchy.

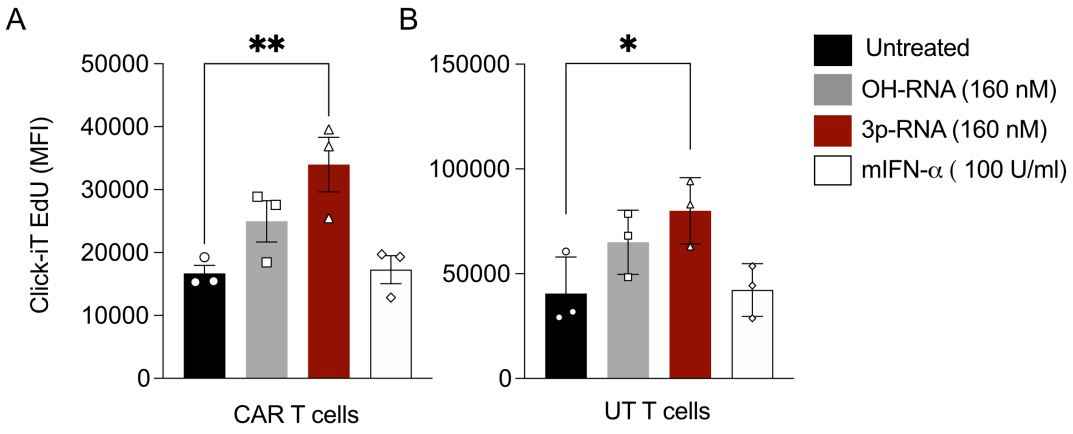

Figure S3. T cell proliferation on the Panc02-OVA-EpCAM tumor model.

Flow cytometric assessment of EdU integration into A) CAR T cells and B) UT T cells co-cultured with 3p-RNA or control transfected Panc02-OVA-EpCAM tumor cells.

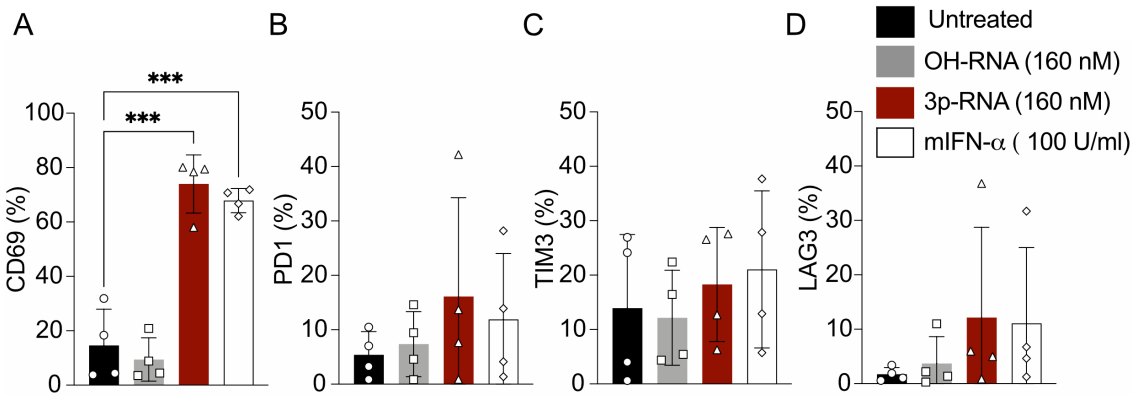

Figure S4. Activation of UT T cells when co-cultured with 3p-RNA transfected T110299- EpCAM tumor cells.

Percentage of **A)** CD69 **B)** PD1 **C)** TIM3 and **D)** LAG3 on UT T cells co-cultured for 24 hours with T110299-EpCAM tumor cells transfected with 3p-RNA or controls as indicated. Error bars show mean values ± SD of four independent experiments. Statistical analysis is based on ordinary one-way ANOVA with correction for multiple comparisons using Tukey test.

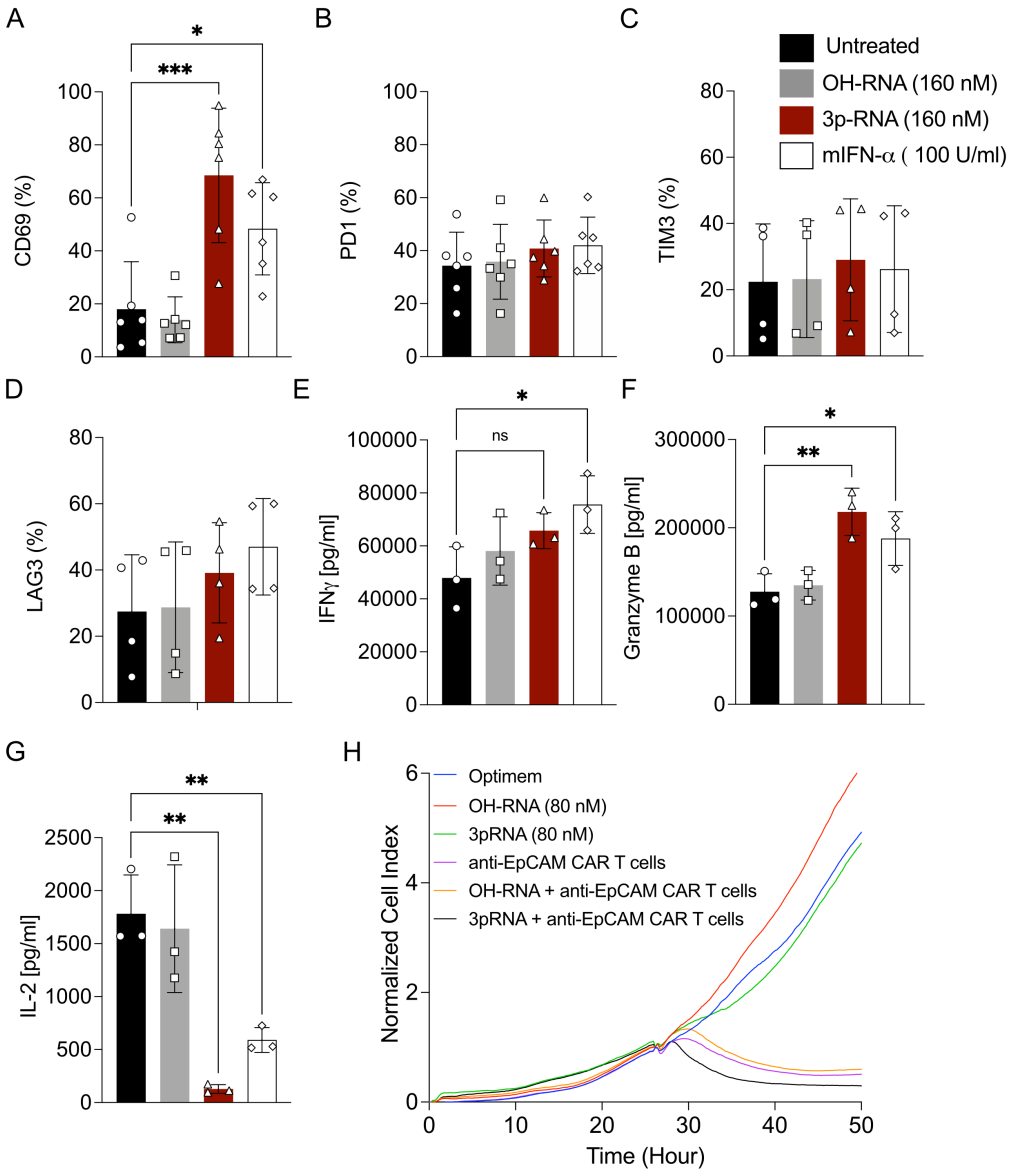

Figure S5. Activation and Cytotoxicity of CAR T cells co-cultured with 3p-RNA transfected Panc02-OVA-EpCAM.

Percentage of **A)** CD69 **B)** PD1 **C)** TIM3 and **D)** LAG3 on anti-EpCAM CAR T cells co-cultured for 24 hours with Panc02-OVA-EpCAM tumor cells transfected with 3p-RNA or controls as indicated. Error bars show mean values ± SD of four to five independent experiments. Statistical analysis is based on ordinary one-way ANOVA with correction for multiple comparisons using Tukey test. **E)** ELISA detection of IFNγ, **F)** IL-2 and **G)** granzyme B in the supernatant of Panc02-OVA-EpCAM tumor cells transfected with 3p-RNA or controls and co-cultured for 24 hours with anti-EpCAM CAR T cells. Error bars show mean values ± SEM of three biological replicates **H)** xCELLigence real-time tumor cell lysis quantification of Panc02-OVA-EpCAM tumor cells co-culture with anti-EpCAM CAR T cells in a 10:1 E:T ratio. Graph is representative of three independent experiments.

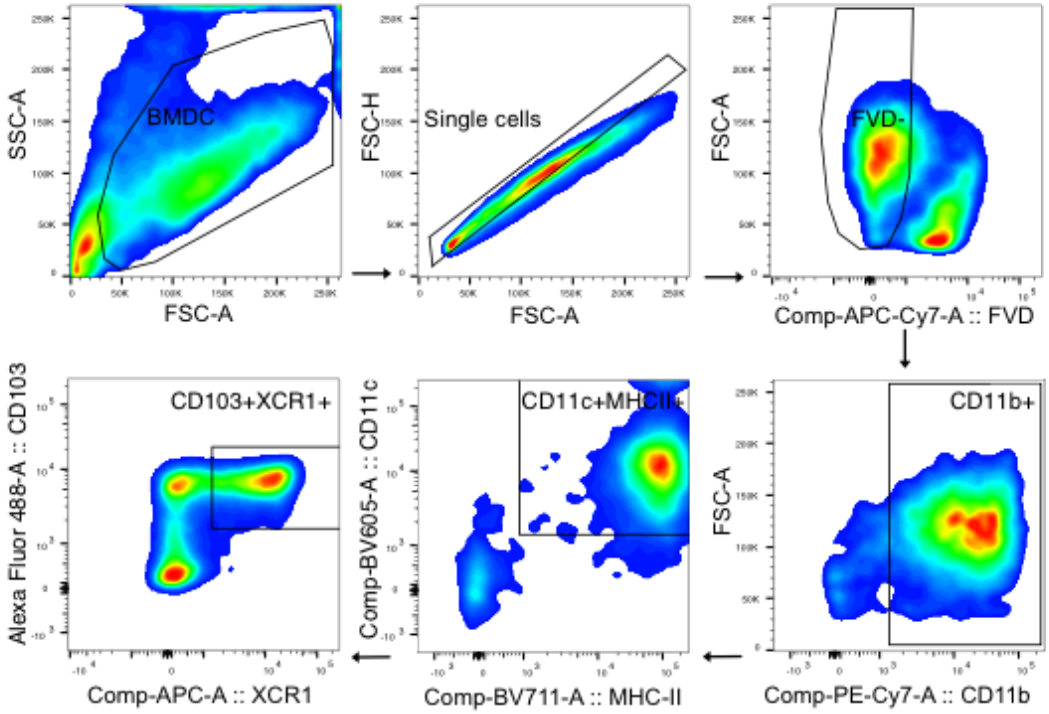

Figure S6. Gating strategy for iCD103⁺ BMDC.

Representative FACS plots of in vitro differentiated CD103⁺XCR1⁺ BMDC. Arrows indicate population hierarchy.

Acknowledgements

I would like to express my sincere gratitude to all the clinicians, scientists, laboratory staff, animal caretakers, family and friends who have actively contributed and supported me throughout the past four years.

First and foremost, I would like to thank my supervisors Prof. Dr. Max Schnurr and Dr. Lars König for taking a leap of faith with me four years ago. For giving me the chance to join them in the development of this highly interesting and challenging project and for guiding and helping me grow personally and professionally. You are knowledgeable and wise mentors, as well as strong, and kind leaders that have put together an incredible team, that in many ways feels like a small family.

I am immensely thankful to all the members of that team. Specially to Simone Formisano for setting the ground stones for this project. To Christine Hörth for all the effort and support with the mice handling and the different experiments. To Philipp Metzger and Raphael Rubens for the warm welcome and guidance upon my arrival to the lab. To Daniel Böhmer, Charlotte Marx, Carlotta Rambuscheck, Daryna Kechur, Luisa Delius, Julia Teppert and Nicolas Röhrle for their valuable input, their willingness to help in complex experiments and the overall nice working environment you all create.

I am also very grateful to Prof. Dr. Sebastian Kobold and the members of his working groups for collaborating in this project and giving valuable input and ideas on how to develop it. I would specially like to thank Bruno Cadilha for being an immense source of knowledge and wisdom. Theo Lorenzini for his big contribution on the T cell migration aspects of this project. Hannah Obeck, Stefanos Michaelides and Arman Öner thank you for your collaboration and willingness to share workload and resources.

To Prof. Dr. Stefan Endres, the heart and soul of the Division of Clinical Pharmacology. Thank you for building and nurturing such an inspiring working environment and for giving me the chance to be part of it. Moreover, a big thank you to Monika Fahrenkamp, Susanne Wenk, Patrick Layritz, and Sonja Theodoridou for their crucial role in keeping the division up and running. To the various members from AG Rothenfusser and AG Anz, thank you very much for

your help in the development of big experiments and for contributing to having a very fun working environment.

My four years as a PhD would've not been possible without the support of the elite network Bavaria and their funding of the i-Target PhD program. Thank you for supporting an integral education for international students. Above all, I want to thank Katharina Dennemarck for always being there for me, helping me sort out the bureaucracy and paperwork of a foreign country and university. I truly couldn't have done it without you. To Magda, Duc, Larsen, Jan, Arman, Philipp and my fellow i-Target PhD funded students and associates, it was a pleasure to share this time with you. I really value your friendship. You are all tremendously talented young scientist and medical doctors, and I can't wait to hear about the great things you will accomplish in the future.

To Prof. Dr. Wolfgang Zimmerman, Dr. Christian Braun, and the members of the thesis advisory committee, thank you for your scientific guidance in the development of this thesis. To Prof. Magnuss Essand and his working group in Uppsala University. Particularly to Tina Sarén, thank you very much for being an amazing first supervisor and placing the first stones of my scientific path.

To my dear "amigos", we started this journey together as master students over 4 years ago. Despite the physical distance, I've always felt like I've had you by my side. I'm incredibly proud of every single one of your scientific and personal accomplishments, and I'm even more thankful for the opportunity to share them with you. In a similar manner, I want to extend the acknowledgements to my Colombian friends, you are my chosen family and your support in every step of my life has been of paramount importance to my success. I truly cannot ask for better friends and I love you all.

A mis padres, mi hermana, tíos, tías, abuelos y abuelas. Jamás me cansaré de repetirles que son la luz y la razón de mi vida. La persona que soy es gracias a ustedes, a su constante esfuerzo y valiosas enseñanzas. Todos mis logros son igualmente suyos, pues sin su apoyo y amor incondicional simplemente no hubiesen sido posibles. Los amo infinitamente.

Titino, last but not least I want to thank you. You came into my life when I least expected it but when I most needed it. You have kept true to the words you told me when we first met and have helped me shine in every single way. You've been

my rock and shield in every storm and my confidant and best friend through every rough patch. Thank you and your family for welcoming me as one of your own. I love you and can only hope to help you shine in return.

LMU LUDWIG-MAXIMILIANS-UNIVERSITÄT MÜNCHEN

Dean's Office Medical Faculty
Faculty of Medicine

Affidavit

Senz Giusti, Anne Marie

Surname, first name

Address

I hereby declare, that the submitted thesis entitled

Exploiting RIG-I-targeted therapy as a strategy to overcome CAR T cell therapy limitations in the treatment of solid tumors

is my own work. I have only used the sources indicated and have not made unauthorised use of services of a third party. Where the work of others has been quoted or reproduced, the source is always given.

I further declare that the dissertation presented here has not been submitted in the same or similar form to any other institution for the purpose of obtaining an academic degree.

Mainz, 13th May 2024

Place, Date

Anne Marie Senz Giusti

Signature doctoral candidate

LMU LUDWIG-MAXIMILIANS-UNIVERSITÄT MÜNCHEN

Dean's Office Medical Faculty
Doctoral Office

Confirmation of congruency between printed and electronic version of the doctoral thesis

Doctoral candidate: Anne Marie Senz Giusti

Address:

I hereby declare that the electronic version of the submitted thesis, entitled

Exploiting RIG-I-targeted therapy as a strategy to overcome CAR T cell therapy limitations in the treatment of solid tumors

is congruent with the printed version both in content and format.

Mainz, 13th May 2024
Place, Date

Anne Marie Senz Giusti
Signature doctoral candidate